THE
PHYSICAL REVIEW
*A Journal of Experimental and Theoretical Physics Established by E. L. Nichols in 1893*

VOL. 49, NO. 7 APRIL 1, 1936 SECOND SERIES

# Experiments on the Variation of the Atomic Structure Factor of Potassium with X-Ray Wave-Length

SAMUEL K. ALLISON AND WILLIAM P. JESSE, *University of Chicago*
(Received February 11, 1936)

A vacuum ionization spectrometer has been constructed in which an externally controlled, motor-driven slide brings either of two powder specimens into the path of the primary x-ray beam. Comparison of the diffracted power in the Debye-Scherrer rings from NaCl, NaF, LiF, and KF powders have been made, with a FP-54 Pliotron circuit to detect the ionization currents. In the studies on KF a range of wave-lengths from 1.538A to 4.146A has been used. On the short wave-length side, the expected decrease of the crystal structure factor was observed in KF. Beyond the $K$ edge of potassium, the crystal structure factor rose again, but considerably more than predicted. Conclusions: Hönl's computations based on the wave-mechanical theory of x-ray dispersion do not correctly give the observed structure factor differences for the (200) diffraction halo from powdered potassium fluoride on the long and short wave-length sides of the potassium $K$ edge. The predicted invariance of the structure factor decrement due to $K$ electrons with scattering angle for light elements is confirmed in our experiments.

## INTRODUCTION

THE crystal structure factor $F$ is defined by the relation

$$F=\sum_j f_j \exp\left[2\pi N i(hx_j+ky_j+lz_j)\right], \qquad (1)$$

where the summation is to be carried out over all the atoms in the unit cell. $f_j$ is the atomic structure factor of the atom $j$, whose coordinates in the unit cell are $x_jy_jz_j$. $N$ is the order computed from a simple translatory lattice corresponding to the classification of the crystal under investigation and having one atom per unit cell. $hkl$ are the Miller indices of the reflecting plane. Relative values of $F$ may be obtained by comparing the powers of the diffracted Debye-Scherrer rings from powdered samples, provided suitable precautions are taken. If $F$ is a known function of the $f_j$'s, i.e., if the crystal structure is completely known, it is possible, for simple crystals, to compute $f$ values of the constituents of the crystal from a sufficiently complete set of $F$ values.

The object of the experiments reported here was to investigate the variation of $f$ with $\lambda$ in the region of the $K$ critical absorption frequency. We chose to study a light atom, because if the total number of extranuclear electrons is small, the structure factor decrements due to the anomalous $K$ electron behavior are a relatively larger fraction of the structure factor. Other considerations, such as the necessity of finding an atom having its $K$ absorption edge very near the wave-length of a strong x-ray line led to the decision to study the behavior of the potassium atom in KF. The power diffracted from powdered KF was compared with that diffracted by NaF and LiF, which should show only very minute anomalous behavior in the region around the potassium $K$ limit, and these in turn were calibrated against NaCl at wave-lengths far from

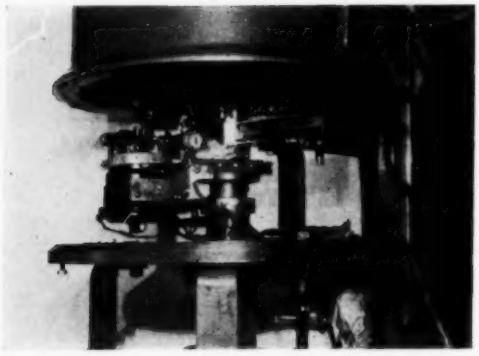

FIG. 1. Photograph of vacuum ionization spectrometer with the cover lifted.

the chlorine critical absorption edge. The potassium $K$ absorption limit in KF has been measured at 3.4277A by Stelling,[1] and this is a different value than that observed in metallic potassium by Lindh[2] (3.4310). Wave-lengths in this region are so readily absorbed in air that a vacuum spectrometer is needed.

## A. EXPERIMENTAL PART

### The vacuum ionization spectrometer

The vacuum ionization spectrometer was similar to the vacuum double spectrometer designed and constructed in this laboratory, and used by Parratt.[3] Fig. 1 shows a photograph of the spectrometer with the lid raised. The metal x-ray tube, of the type designed in this laboratory by Dershem,[4] is attached to the raised cover, upon which are mounted the diffusion pumps used in its evacuation. Thus the vacuum in the instrument itself, which is merely the lowest pressure attainable from a Megavac pump, acts as a fore-vacuum for the exhaustion of the x-ray tube. At the right of Fig. 1 are seen the slits, which were carefully machined and ground steel bars, placed side by side, and actuated by a mechanism such that the distance between them may be changed, but they are constrained to move parallel to themselves. Another slow motion device turns the entire slit assembly about a vertical axis, so that the central ray may be made to pass through the axis of rotation of the sleeves carrying the powder frames and the ionization chamber.

At the left of Fig. 1 is seen an electric motor, with speed reduction gears built in, which moves the frame carrying the powders forward and backward, so that first one sample and then the other can be brought into the path of the x-ray beam. The position of the framework carrying the powders can be read through a glass window in the top of the lid, and settings can be repeated with ease to 0.0025 cm.

The front slit of the cylindrical ionization chamber can be seen in the central background. The chamber was filled with argon gas at one atmosphere. The outer wall of the chamber is charged to 90 volts; the insulated collecting electrode leaves the chamber at the rear, and the ionization current is conducted along insulated rods which enter the central shaft of the instrument and pass down the axis of rotation. Some of the ionization current readings were taken on a Cambridge Compton electrometer, later a FP-54 Pliotron amplifying circuit was installed.

The angular positions of the ionization chamber and powder frames can be changed by rotation of sleeves which extend down the central axis, and the rotations can be read to about 2 minutes of arc on a divided circular scale. A sine screw operating on the sleeve carrying the powder frames allows angular rotations of 30 seconds of arc to be easily made. Numerical data on the spectrometer are given in Table I.

TABLE I. *Dimensions of the vacuum ionization spectrometer.*

| | |
|---|---|
| From x-ray tube target to central axis | 27 cm |
| Length, height, width, of slits | 15, 1.55, 0.041 |
| From central axis to ionization chamber window | 9.0 |
| Diameter, length, of cylindrical ionization chamber | 3.5, 6.5 |
| Width, height, of ionization chamber slit | 0.148, 1.0 |

### Experimental technique

The substances which were used, namely, NaCl, NaF, LiF, and KF were obtained from various chemical supply houses which sell analyzed chemicals. All were stated to contain only

[1] O. Stelling, Siegbahn, *Spektroskopie der Röntgenstrahlen* (J. Springer, Berlin, 1931), p. 290.
[2] A. E. Lindh, Siegbahn, *Spektroskopie der Röntgenstrahlen* (J. Springer, Berlin, 1931), p. 289.
[3] L. G. Parratt, Phys. Rev. **41**, 553 (1932).
[4] E. Dershem, Rev. Sci. Inst. **7**, 86 (1936).

traces of foreign substances. Because of the fact that the presence of chlorine as an impurity in the fluorides would have introduced serious error, tests for Cl were made on the actual samples used, insuring its absence in appreciable amounts. The powders were ground for several hours in a porcelain mortar, and in some cases finally in an agate mortar; then compressed into briquets in steel frames. These frames were rectangular pieces of steel 3 mm thick and $3.2\times4.0$ cm, with a rectangular aperture $1.6\times2.3$ cm to hold the powder. Enough powder was used so that after compression the aperture was over full. The face of the briquet from which diffraction was to occur was then eroded down to the level of the frame by rubbing on sandpaper. In this way we avoided using layers which had been immediately adjacent to a metal surface during compression and which might thus have been oriented. The normal way in which the powers diffracted into the (200), (220), and (222) rings from KF decreased, indicated lack of orientation, at least at 1.538A wave-length.

Potassium fluoride is hygroscopic, forming a hydrate, KF $2H_2O$, which melts at 41°C. Since the hydrate was supplied, dehydration was necessary. The hydrate was heated overnight on a steam-bath, thus removing all but traces of the water without danger of hydrolysis. The dried material was then heated to 600°C in a platinum crucible. The grinding operations were carried out in a mortar placed on an electric heater which maintained a temperature of over 100°C throughout the operation, and the compressing was done in a heated press. The KF was then stored in a desiccator over $P_2O_5$ pending use, and a large pan of $P_2O_5$ was always kept in the spectrometer. Air was admitted to the instrument through a drying train.

The Pliotron circuit[5] used in the latter stages of the experiment had a sensitivity of $4\times10^{-16}$ amp. per mm scale deflection. The weakest powder lines, such as the diffraction of Ti $K\alpha$ in the order (222) from KF gave deflections of 1.0 cm above the background, with the x-ray tube running at 30 kv and 3 ma. Strong lines, like Cu $K\alpha$, from (200) NaF would have given 60 cm deflection at 30 kv and 10 ma if the sensitivity of the circuit had not been reduced. Thus the measured ionization currents varied from $4\times10^{-15}$ to $2.4\times10^{-13}$ amp.

In the theory of diffraction by a powder consisting of randomly oriented particles, one calculates the power diffracted into an arc of a Debye-Scherrer ring. Two experimental methods were used to measure relative values of this power.

(1) The ionization chamber was moved in angular steps equal to the angular width of its window through the region in which a diffracted maximum appeared. The background readings were determined at positions adjacent to the diffracted beam. The sum of the differences between the readings in the beam and the background readings is proportional to the power which it is desired to measure. The method is easily seen to be equivalent to using a single position of an ionization chamber with a slit wide enough to take in the entire beam of diffracted x-rays. The angular width of the ionization chamber window (40 min.) was measured by moving the chamber past the diffracted beam from a single calcite crystal, which diffracts a beam of the same angular divergence as that leaving the slits. For the powder specimen three or four adjacent positions were always sufficient to cover the diffracted beam.

(2) The ionization chamber was moved in small steps, 5 or 10 minutes of arc, through the region of the diffracted beam, and adjacent to it until a level background was obtained. With Pliotron readings as ordinates and angles as abscissae, a smooth curve was drawn through the points obtained. The area under the peak and above the base-line is proportional to the power whose measurement is desired.

These two methods were compared many times and were shown to give the same power ratio for two diffraction rings. The technique of making a measurement was as follows: Let us suppose the relative powers of LiF (111) and KF (200) for a certain wave-length are required. The powder frame support is moved by means of the motor until LiF is in the x-ray beam. The sleeve carrying the powder frames is then rotated until the incident and diffracted beams enter and

[5] L. A. DuBridge and H. Brown Rev. Sci. Inst. **4**, 532 (1933).

TABLE II. *Sets of readings to indicate the accuracy of repetition.*
*F* values based on $\frac{1}{4}F_{NaCl}(200) = 20.80$, $\frac{1}{4}F_{NaF}(200) = 14.55$.

| POWDERS | λ(A) | ORDERS | DATE | METHOD | $[P_d]_1/[P_d]_2$ | RESULT | |
|---|---|---|---|---|---|---|---|
| LiF; NaCl | 1.934 | (111); (200) | Dec. 24, '35 | 2 | 1.66 | $\frac{1}{4}F_{LiF}(111) =$ | 4.98 |
| " | " | " | " | 2 | 1.72 | " | 5.08 |
| " | " | " | Jan. 25, '36 | 2* | 1.63 | " | 4.94 |
| | | | | | | Average | 5.00 |
| KF; NaF | 4.146 | (200); (200) | Nov. 28, '35 | 1 | 0.984 | $\frac{1}{4}F_{KF}(200) =$ | 18.50 |
| " | " | " | Nov. 29, '35 | 1 | 0.917 | " | 17.86 |
| " | " | " | Nov. 30, '35 | 1 | 0.939 | " | 18.08 |
| " | " | " | Dec. 1, '35 | 1 | 0.918 | " | 17.88 |
| " | " | " | Dec. 3, '35 | 2 | 0.914 | " | 17.84 |
| | | | | | | Average | 18.03 |

* Fresh sample of NaCl.

leave the briquet at the same angle, the so-called "reflection method" being used. The ionization chamber is moved according to method (1) or (2) above, and the Pliotron circuit readings noted. This constitutes run *A*. Run *B* is then immediately made on KF by bringing KF into the beam by means of the motor-driven slide. Going back to LiF, run *C* is made, and then a second run, *D*, on KF completes the set. The four runs could be made in about 90 minutes. In computing the power ratios KF/LiF, $B/\frac{1}{2}(A+C)$ and $\frac{1}{2}(B+D)/C$ are used. This is a rough method for correcting for a steady variation of power with time, such as might come from slow deposition of tungsten on the target, or on the cellophane window of the x-ray tube.

As an example of the accuracy attained in relative power measurement, Table II shows some determinations made with Fe $K\alpha$ and Ag $L\alpha$ wave-lengths. We estimate that our structure factors on the short wave-length side of the potassium *K* absorption edge are accurate to about 2 percent; on the long wave-length side to about 3 percent.

### Difficulties and sources of error

In the longer wave-length region, from 3 to 4A, the deposition of tungsten on the target gave some difficulty. Two effects may result from this deposition, (1) a decrease in intensity of the soft line radiation with time, (2) an appearance of higher order diffractions of the tungsten *L*-series lines superposed on truly soft x-ray diffraction haloes. It was found desirable to use a tube with a shielded filament,[4] which was very satisfactory in removing this source of error.

A curious behavior of NaF in the spectrometer was discovered in some experiments undertaken to detect an effect of particle size, if such existed. Two samples of NaF, which under a microscope showed different average sizes of particles, were placed in the spectrometer and compared. One of the specimens had been used for several weeks; the other was fresh. Contrary to expectation, the fresh specimen, of relatively small particle size, showed a smaller diffracted power in the (200) ring for the Ag $L\alpha$ wave-length. After several days standing in the spectrometer, which was essentially a vacuum desiccator, the two specimens showed equal power in the (200) diffraction haloes. This "aging effect" caused us to question all previous comparisons in which fresh specimens of NaF had been used. We repeated many of these earlier measurements with LiF as the comparison powder. No such anomalous effects were found for LiF.

Orientation of the powders was tested for by brushing the briquet with a camel's hair brush between determinations. No good evidence for such an effect was found.

Where the x-rays fell on the powder a discoloration was produced after some time. To test whether this effect was connected with a change in diffracted power, the samples were shifted slightly so that a fresh spot was selected. No change in diffracted power could be detected.

Schäfer[6] has described an effect of particle size which is equivalent to the statement that with

[6] K. Schäfer, Zeits. f. Physik **86**, 738 (1933).

very high absorption in the particles the effective absorption coefficient of the material in the briquet is no longer directly proportional to its average density, which relation is tacitly assumed in the expression for the computation of the atomic structure factors, Eq. (2). Our experiments with various particle sizes in NaF at 4.146A could not establish the presence of such an effect.

## Experimental results

It may be shown that[7]

$$\frac{F_1}{F_2}=\frac{M_2}{M_1}\left\{\frac{j_2\mu_1 \sin\theta_1}{j_1\mu_2 \sin\theta_2}\left(\frac{1+\cos^2 2\theta_1}{\sin 2\theta_1}\right)^{-1}\times\left(\frac{1+\cos^2 2\theta_2}{\sin 2\theta_2}\right)\frac{[P_d]_1}{[P_d]_2}\right\}^{\frac{1}{2}}. \quad (2)$$

In this expression the subscripts refer to two different diffraction haloes, either from the same powder or from different powders.

$F$ is the crystal structure factor, Eq. (1).
$M$ is the number of unit cells per unit volume.
$j$ is a factor showing how many orientations of the unit cell can contribute to the diffraction halo in question.
$\mu$ is the linear absorption coefficient of the particles composing the briquet.
$2\theta$ is the angle between the forward directions of the incident and diffracted beams.
$P_d$ is the power in the arc of the diffraction halo entering the ionization chamber window.

All of the crystals used were of the NaCl structure, and it can be shown[8] that $F$ can only be 0, or $4(f_a+f_b)$, or $4(f_a-f_b)$ where $f_a$ and $f_b$ are the atomic structure factors of the atoms composing the crystal. In cubic crystals the inverse ratios of the cubes of the length of the sides of the unit cells ($a_0$) can be used for $M_2/M_1$. The trigonometric factors of Eq. (2) may be grouped together to give

$$\Phi(\theta)=(1+\cos^2 2\theta)/\sin^2\theta\cos\theta \quad (3)$$

for each reflection. Pertinent data on the crystal powders used are given in Table III. The densities are those computed from x-ray data.

TABLE III. *Properties of the crystals used.*

| CRYSTAL | $a_0$ | DENSITY | $M$ |
|---|---|---|---|
| NaCl | 5.628A | 2.164 | $5.610\times10^{21}$ |
| KF | 5.328 | 2.481 | 6.612 |
| NaF | 4.62 | 2.809 | 10.14 |
| LiF | 4.01 | 2.65 | 15.51 |

Table IV gives the results obtained for atomic structure factors of KF at various wave-lengths and various values of $(\sin\theta)/\lambda$. All the structure factors in this table are based fundamentally on the value[9]

$$\tfrac{1}{4}F_{NaCl}(200)=f_{Na}+f_{Cl}=20.80$$
(1.538A, room temperature).

Based on this value are the two subsidiary standards,

$$\tfrac{1}{4}F_{NaF}(200)=f_{Na}+f_F=14.55$$
(1.538A, room temperature)

and

$$\tfrac{1}{4}F_{LiF}(111)=f_F-f_{Li}=5.00$$
(1.538A, room temperature).

Although our experiments on the comparison of LiF and NaCl were actually carried out for Fe $K\alpha$ radiation, we have assumed that the value found is valid for Cu $K\alpha$ radiation. A correction for the variation of the $f$'s of Na and F with wave-length will be discussed later.

Havighurst,[10] assuming a value of 15.75 for $\frac{1}{4}F_{NaCl}(220)$ at room temperature, obtained $\frac{1}{4}F_{NaCl}(200)=20.80$, $\frac{1}{4}F_{NaF}(200)=14.25$, $\frac{1}{4}F_{LiF}(111)=4.61$. His LiF value does not agree well with that determined by us, and we therefore made several determinations of the LiF : NaCl ratio, as shown in Table II, using different NaCl samples. There is no doubt that our results are

[7] Compton and Allison, *X-Rays in Theory and Experiment* (D. Van Nostrand, 1935). The expression is a combination of Eqs. (6.78), p. 414 and (6.85), p. 419, remembering that (effective absorption coeff.) = (coeff. for particles) [(density of powder)/(density of particles)].
[8] Compton and Allison, reference 7, pp. 354–355.
[9] R. J. Havighurst, Phys. Rev. **28**, 869 (1926).
[10] R. J. Havighurst, reference 9, Table I, lists a value of the effective linear absorption coefficient in LiF for Mo $K\alpha$ which is altogether too high according to recent tables of absorption coefficients, for instance, that due to S. J. M. Allen and quoted in Compton and Allison's *X-Rays in Theory and Experiment*. These tables give $\mu$ for solid LiF = 3.82 at 0.710A; Havighurst used $\mu=4.59$. The correction to his results seems, however, to increase rather than to decrease the discrepancy between our structure factor and his. In our experiments the iron $K$ radiation passed through a $MnO_2$ filter which removed almost all the Fe $K\beta$ line.

TABLE IV. *Observed, uncorrected, crystal structure factors.*
Based on $\frac{1}{4}F_{NaCl}(200) = 20.80$.

| POWDERS | λ(A) | LINE | ORDERS | θ's | Φ(θ) | f's | μ's | $[P_d]_1/[P_d]_2$ | RESULT |
|---|---|---|---|---|---|---|---|---|---|
| NaF : NaCl | 1.538 | Cu $K\alpha$ | (200) : (200) | 19° 25′ : 15° 53′ | 15.42 : 23.92 | 6 : 6 | 71.0 : 162.6 | 2.36 | $\frac{1}{4}F_{NaF}(200) = 14.55$ |
| LiF : NaCl | 1.934 | Fe $K\alpha$ | (111) : (200) | 24° 41′ : 20° 06′ | 9.00 : 14.28 | 8 : 6 | 69.4 : 312 | 1.67 | $\frac{1}{4}F_{LiF}(111) = 5.00$ |
| KF : NaCl | 1.538 | Cu $K\alpha$ | (200) : (200) | 16° 48′ : 15° 53′ | 21.22 : 23.92 | 6 : 6 | 243 : 162.6 | 0.688 | $\frac{1}{4}F_{KF}(200) = 19.00$ |
| KF : NaF | 1.538 | Cu $K\alpha$ | (200) : (200) | 16° 48′ : 19° 25′ | 21.22 : 15.42 | 6 : 6 | 243 : 71.0 | 0.296 | $\frac{1}{4}F_{KF}(200) = 19.14$ |
| " | 1.934 | Fe $K\alpha$ | " | 21° 18′ : 24° 44′ | 12.54 : 8.95 | " | 483 : 139 | 0.299 | 19.21 |
| " | 2.499 | Va $K\alpha$ | " | 27° 57′ : 32° 44′ | 6.77 : 4.77 | " | 960 : 287 | 0.295 | 18.56 |
| " | 2.744 | Ti $K\alpha$ | " | 31° 00′ : 36° 26′ | 5.37 : 3.83 | " | 1174 : 376 | 0.298 | 18.20 |
| " | 3.353 | Ca $K\alpha$ | " | 39° 00′ : 46° 32′ | 3.39 : 2.77 | " | 1997 : 657 | 0.181 | 14.94 |
| " | 3.432 | Sb $L\alpha$ | " | 40° 06′ : 47° 58′ | 3.24 : 2.74 | " | 358 : 705 | 0.547 | 10.80 |
| " | 3.593 | Sn $L\alpha$ | " | 42° 24′ : 51° 03′ | 3.02 : 2.75 | " | 406 : 795 | 1.18 | 16.55 |
| " | 4.146 | Ag $L\alpha$ | " | 51° 06′ : 63° 49′ | 2.75 : 3.86 | " | 602 : 1213 | 0.936 | 18.05 |
| KF : LiF | 3.593 | Sn $L\alpha$ | (200) : (111) | 42° 24′ : 50° 54′ | 3.02 : 2.74 | 6 : 8 | 406 : 416 | 1.805 | $\frac{1}{4}F_{KF}(200) = 17.22$ |
| " | 3.927 | Ag $L\beta$ | " | 47° 29′ : 58° 00′ | 2.74 : 3.13 | " | 520 : 542 | 1.44 | 17.07 |
| " | 4.146 | Ag $L\alpha$ | " | 51° 06′ : 63° 34′ | 2.75 : 3.82 | " | 602 : 638 | 1.25 | 17.46 |
| | | | | | | | $(\sin\theta)/\lambda$ | | |
| KF | 1.538 | Cu $K\alpha$ | (220) : (200) | 24° 09′ : 16° 48′ | 9.44 : 21.22 | 12 : 6 | .265 : .188 | 0.528 | $\frac{1}{4}F_{KF}(220) = 14.75$ |
| " | " | " | (222) : (200) | 30° 00′ : 16° 48′ | 5.77 : 21.22 | 8 : 6 | .325 : .188 | 0.136 | (222) = 11.70 |
| " | 2.744 | Ti $K\alpha$ | (220) : (200) | 46° 45′ : 31° 00′ | 2.75 : 5.37 | 12 : 6 | .265 : .188 | 0.597 | (220) = 13.86 |
| " | " | " | (222) : (200) | 63° 08′ : 31° 00′ | 3.75 : 5.37 | 8 : 6 | .325 : .188 | 0.260 | (222) = 9.6 |
| " | 3.353 | Ca $K\alpha$ | (220) : (200) | 62° 49′ : 39° 00′ | 3.70 : 3.39 | 12 : 6 | .265 : .188 | 1.25 | (220) = 11.33 |

TABLE V. *Correction for variation of the structure factors of the standard crystals NaF and LiF with wave-length.*

| LINE | λ(A) | $\Delta f_{Na}$ | $\Delta f_F$ | $\frac{1}{4}F_{NaF}(200)$ | $\frac{1}{4}F_{LiF}(111)$ | $\frac{1}{4}F_{KF}(200)$ | | $\frac{1}{4}F_{KF}(220)$ | $\frac{1}{4}F_{KF}(222)$ |
|---|---|---|---|---|---|---|---|---|---|
| Cu $K\alpha$ | 1.538 | −0.13 | −0.06 | 14.55 | 5.00 | 19.14 | | 14.75 | 11.70 |
| Fe $K\alpha$ | 1.934 | −0.18 | −0.09 | 14.63 | 5.03 | 19.33 | | | |
| Va $K\alpha$ | 2.499 | −0.25 | −0.13 | 14.74 | 5.07 | 18.79 | | | |
| Ti $K\alpha$ | 2.744 | −0.27 | −0.15 | 14.78 | 5.09 | 18.49 | | 14.09 | 9.7 |
| Ca $K\alpha$ | 3.353 | −0.32 | −0.19 | 14.87 | 5.13 | 15.18 | | 11.52 | |
| Sb $L\alpha$ | 3.432 | −0.33 | −0.19 | 14.88 | 5.13 | 11.04 | | | |
| Sn $L\alpha$ | 3.593 | −0.34 | −0.21 | 14.91 | 5.15 | 16.96 | 17.73* | | |
| Ag $L\beta$ | 3.927 | −0.35 | −0.23 | 14.94 | 5.17 | | 17.64* | | |
| Ag $L\alpha$ | 4.146 | −0.36 | −0.25 | 14.97 | 5.19 | 18.57 | 18.11* | | |

* LiF used as standard crystal.

uniformly higher than his. James and Firth[11] found a value of $\frac{1}{4}F_{NaCl}(200) = 20.65$ which differs from 20.80 by approximately the correction for anomalous dispersion of the $K$ electrons in chlorine at the Cu $K\alpha$ wave-length.

In spite of the fact that the $K$-absorption limits of the sodium and fluorine in our standard crystals are far from the wave-length region of the observations, the variation in their $f$'s with wave-length is appreciable and must be corrected for. We have used Hönl's theory in calculating this correction, as given in Eq. (10). The value of $\Delta$ for sodium and fluorine has been taken as 0.30. The critical absorption wave-lengths of Na and F were taken as 11 and 18A respectively. Eq. (10) leads to a set of $\Delta f$ values for Na and F. We have computed the corrected values of $\frac{1}{4}F_{NaF}(200)$ and $\frac{1}{4}F_{LiF}(111)$ as follows:

$$[\tfrac{1}{4}F_{NaF}(200)]_\lambda = 14.55 - [(\Delta f_{Na})_\lambda - (\Delta f_{Na})_{1.54}] - [(\Delta f_F)_\lambda - (\Delta f_F)_{1.54}],$$

$$[\tfrac{1}{4}F_{LiF}(111)]_\lambda = 5.00 - [(\Delta f_F - (\Delta f_F)_{1.54}].$$

Thus the crystal structure factors of our standards slowly increased with wave-length through the region investigated. The KF structure factors in the last column of Table IV were computed on the assumption of no variation of the NaF and LiF factors with wave-length; the corrected values are shown in the latter columns of Table V.

The values of $f_K + f_F$ thus obtained at room temperature were reduced to values for atoms at rest in the lattice by the general relation $f = f_0 e^{-M}$

[11] James and Firth, Proc. Roy. Soc. **A117**, 62 (1917).

where $f_0$ is the corrected structure factor and $f$ is the factor observed at absolute temperature $T$. The value of $M$ is determined by Waller's formula[12]

$$M=\frac{6h^2}{m_a k\Theta}\left(\frac{\Phi(x)}{x}+\frac{1}{4}\right)\frac{\sin^2\theta}{\lambda^2},$$

where $h$ is Planck's constant,
$m_a$ is the mass of the atom considered,
$k$ is Boltzmann's constant,
$x$ is the ratio $\Theta/T$, where $\Theta$ is the characteristic temperature of the crystal.

The function $\Phi(x)$ is the result of the evaluation of a definite integral and has been tabulated by Debye.[13] The value of the characteristic temperature for a crystalline substance may be determined approximately from the Lindemann melting point formula.[14] In this manner the characteristic temperature of KF was found to be 297°K. In reducing the $f$'s to $f_0$'s, a temperature correction was computed separately for each of the two ions in KF, by using the proper mass of each ion for $m_a$. The values of $e^{-M}$ for each ion are shown in columns 2 and 3 of Table VI. Since in the experiments no diffracted beams from planes in which $\frac{1}{4}F_{KF}=f_K-f_F$ were measured, no values of either $f_K$ or $f_F$ could be obtained directly from experiment. A value of $f_0^F$ was therefore taken from the Hartree[15] curve for the corresponding value of $(\sin\theta)/\lambda$. The $f_F$ was then computed from this Hartree value of $f_0^F$ by multiplication with the factor $e^{-M_F}$. The resulting value of $f_F$ was then subtracted from the observed value of $f_K+f_F$, leaving a value of $f_K$. This value of $f_K$ was then reduced by multiplication with $e^{M_F}$ to $f_0^K$ and the above value of $f_0^F$ added to it, giving $\frac{1}{4}F_0^{KF}=f_0^K+f_0^F$. The fifth column of Table VI therefore represents the final values of $\frac{1}{4}F_0^{FK}$ from our experiments, and thus those used to compare with theory.

It should be noted that although a theoretically calculated value of $f_0^F$ is introduced into the temperature correction, the final result, $\frac{1}{4}F_0^{KF}$, has but a negligible dependence upon the value of $f_0^F$ which is introduced. Such a value need be known only approximately, since $e^{-M_K}$ and $e^{-M_F}$ differ but little for any of the planes considered. Should another value of $f_0^K$ differing by one full electron be chosen, the effect on the final value of $\frac{1}{4}F_0^{KF}$ would be 0.1 electron for the (222) diffraction, and about 0.04 electron for the (200).

TABLE VI. *Temperature corrections applied to the values of* $\frac{1}{4}F_{KF}$ *of Table V.*

| $\frac{1}{4}F_{KF}$ Table V | $e^{-M_K}$ | $e^{-M_F}$ | $f_0^F$ Hartree | $\frac{1}{4}F_0^{KF}$ | INDICES | λ(A) |
|---|---|---|---|---|---|---|
| 19.14 | 0.964 | 0.930 | 6.90 | **20.10** | (200) | 1.538 |
| 19.33 | " | " | " | **20.30** | " | 1.934 |
| 18.79 | " | " | " | **19.74** | " | 2.499 |
| 18.49 | " | " | " | **19.43** | " | 2.744 |
| 15.18 | " | " | " | **15.98** | " | 3.353 |
| 11.04 | " | " | " | **11.69** | " | 3.432 |
| 16.96 | " | " | " | **17.84** | " | 3.593 |
| 17.73 | " | " | " | **18.64*** | " | 3.593 |
| 17.64 | " | " | " | **18.54*** | " | 3.927 |
| 18.57 | " | " | " | **19.51** | " | 4.146 |
| 18.11 | " | " | " | **19.03*** | " | 4.146 |
| 14.75 | 0.933 | 0.867 | 5.50 | **16.21** | (220) | 1.538 |
| 11.70 | 0.900 | 0.807 | 4.43 | **13.45** | (222) | 1.538 |
| 14.09 | 0.938 | 0.867 | 5.50 | **15.49** | (220) | 2.744 |
| 9.7 | 0.900 | 0.807 | 4.43 | **11.2** | (222) | 2.744 |
| 11.52 | 0.938 | 0.867 | 5.50 | **12.74** | (220) | 3.353 |

* LiF used as intermediate standard.

## B. THEORETICAL PART

### Statement of the theories

The theory of the variation of the atomic structure factor with wave-length has been developed by Coster, Knol and Prins,[16] Glocker and Schäfer,[17] and Hönl.[18] As the frequency of the primary radiation decreases and approaches the critical frequency of the $K$ electrons, the amplitude of the wave scattered by them increases, becoming much larger than that of the J. J. Thomson scattering. At the same time the phase of the scattered wave changes with respect to that of the incident wave. As a result the scattered wave from the $K$ electrons interferes destructively with the waves scattered from the remaining electrons in the atom, and reduces the resultant amplitude observed at any distant point. The atomic structure factor for an atom is the ratio of the wave scattered by the atom at

[12] I. Waller, Zeits. f. Physik **17**, 398 (1923), Diss. Uppsala (1925).
[13] P. Debye, see Compton and Allison, reference 7, p. 437.
[14] Lindemann, Zeits. f. Electrochemie **17**, 817 (1911).
[15] D. R. Hartree, see Compton and Allison, reference 7, p. 781.
[16] Coster, Knol and Prins, Zeits. f. Physik **63**, 345 (1930).
[17] Glocker and Schäfer, Zeits. f. Physik **73**, 289 (1931).
[18] Hönl, Zeits. f. Physik **84**, 1 (1933); Ann. d. Physik [5] **18**, 625 (1933).

$O$ to a distant point $P$, to the amplitude which would be scattered to $P$ by a single electron at $O$, the single electron assumed to be scattering in the J. J. Thomson manner. In order to account for the type of absorption observed in the x-ray region, it has been necessary to replace the $K$ electrons by a distribution of virtual oscillators whose natural frequencies extend from $\nu=\infty$ to the frequency of the $K$ limit. If we empirically distribute these oscillators in such a manner that the absorption coefficient increases as $\lambda^3$, and retain the rest of the framework of the Lorentz dispersion theory, we find

$$f(0)=\frac{2\pi mc^2}{e^2\lambda^2}\times\left[\left\{z_K\delta_K+(Z-z_K)\frac{e^2\lambda^2}{2\pi mc^2}\right\}^2+z^2{}_K\beta^2{}_K\right]^{\frac{1}{2}}. \quad (4)$$

In this equation, $f(0)$ is the atomic structure factor in the forward direction (scattering angle zero). $z_K$ is the oscillator strength of the $K$ electrons of the atom of atomic number $Z$. $\delta_K$ is the unit decrement of the refractive index per $K$ electron and $\beta_K$ is the index of absorption per $K$ electron. The equation assumes that only the $K$ electrons are resonating in the atom.

On the short wave-length side of the $K$ limit

$$\delta_K=\frac{e^2\lambda^2}{2\pi mc^2}\{1+x^2\ln(x^{-2}-1)-2\pi\gamma x^3\} \quad (5)$$

and on the long wave-length side

$$\delta_K=\frac{e^2\lambda^2}{2\pi mc^2}\{1+x^2\ln(1-x^{-2})\}. \quad (6)$$

In these equations, $x=\lambda/\lambda_K$, and $\gamma$ is a damping constant which we have estimated from the width of the $K$ series lines of potassium. By extrapolation of Parratt's[19] values of the $K\alpha$ line widths of V (23), Ti (22), and Ca (20), we estimate that the $K\alpha$ lines of K (19) have a full width at half-maximum of $1.67\times10^{-11}$ cm. The value of $\gamma$ is this width divided by the wave-length ($3.73\times10^{-8}$ cm) or $4.5\times10^{-4}$.

We have computed values of $\beta_K$ according to the following formula:

$$\beta_K=\frac{\lambda A}{4\pi Nz_K}\frac{r-1}{r}\mu_m. \quad (7)$$

Here $A$ is the atomic weight of potassium, $N$ is the Avogadro number, ($6.023\times10^{23}$), $r$ is the absorption jump ratio of the potassium $K$ edge, (10.2), and $\mu_m$ is the mass absorption coefficient for potassium for wave-length $\lambda<\lambda_K$. $\beta_K=0$ for $\lambda>\lambda_K$.

In the earliest form of x-ray dispersion theory, due to Kallmann and Mark,[20] the factor $z_K$ which enters the preceding equations was set equal to 2, the electron population of the $K$ shell, according to the Pauli principle. More recent development of the dispersion theory has indicated that for the $K$ electrons at least, an oscillator strength less than 2 should be observed. The reason for this has been clearly stated by Kronig and Kramers.[21] In an atom having only one extranuclear electron, for instance, hydrogen, in its normal state, the sum of the oscillator strengths for all possible transitions, including those to states of positive energy in the continuous region, is one.[22] For a two electron atom however, the second electron may remove one of the possibilities of transition for the first one, by occupying one of the levels to which it could possibly jump. This subtracts a certain oscillator strength from the original electron, and also subtracts a corresponding negative oscillator strength from the second electron, because for it a possibility of emission is removed. Thus the decrement in oscillator strength is transferred from the first to the second electron. In the case of the $K$ electrons, practically all the important discrete levels to which they might go in absorption are already full, and their oscillator strength corresponds to that calculated for transitions into the continuous region alone.

An important quantity in these considerations is $\Delta f$, which may be defined as the structure factor decrement. Since the normal value of $f(0)$ is $Z$, the decrement $\Delta f$ is $Z-f(0)$. By a

[19] L. G. Parratt, Phys. Rev. **44**, 695 (1933).

[20] Kallmann and Mark, Naturwiss. **14**, 648 (1926); Ann. d. Physik **82**, 385 (1927).

[21] R. de L. Kronig and H. A. Kramers, Zeits. f. Physik **48**, 174 (1928).

[22] W. Kuhn, Zeits. f. Physik **33**, 408 (1925); W. Thomas, Naturwiss. **13**, 627 (1925).

combination of the preceding equations, it may be shown that on the short wave-length side of the limit

$$\Delta f = Z - \left[ \{ z_K (x^2 \ln (x^{-2}-1) - 2\pi\gamma x^3) + Z \}^2 + \frac{m^2 c^4 A^2}{4\lambda^2 e^4 N^2} \frac{(r-1)^2}{r^2} \mu_m^2 \right]^{\frac{1}{2}} \quad (8)$$

and on the long wave-length side

$$\Delta f = -z_K x^2 \ln (1-x^{-2}). \quad (9)$$

These equations are often referred to as those coming from the Kramers-Kallmann-Mark treatment of dispersion theory.

Hönl has made a more fundamental theoretical investigation of the problem than those which led to Eqs. (8) and (9). He computed from theoretical grounds the variation of the absorption coefficient with wave-length, instead of arbitrarily inserting a $\lambda^3$ variation law, and computed the oscillator strengths $z_K$ from hydrogen wave functions, making approximate corrections for screening. Hönl's equation for $\Delta f$ is

$$\Delta f = -\frac{2^7 e^{-4}}{9} \left[ \frac{4x^2 \ln |1-x^{-2}|}{(1-\Delta)^2} - \frac{1}{(1-\Delta)^3} \left\{ x^3 \ln \left| \frac{1-x}{1+x} \right| + 2x^2 \right\} \right], \quad (10)$$

where $\Delta = 0.246$ and represents a correction for screening in the potassium atom. The $e$ appearing in Eq. (10) is the basis of natural logarithms.

For large values of $x$, Eq. (10) approaches the value $\Delta f = 1.43$, which is the oscillator strength of the $K$ electrons of potassium. The values of $\Delta f$ computed from Eq. (10) are very close to those computed from Eqs. (8) and (9) with $z_K = 1.43$.

Hönl has also investigated the possibility that the $\Delta f$ values may depend on scattering angle, or on $(\sin\theta)/\lambda$. He finds that although such an effect is theoretically indicated, the magnitude is so small as to be undetectable experimentally except possibly for very heavy atoms. This makes it possible to use the structure factor decrements of Eqs. (8) and (9), computed with $Z = 19$, at the actual scattering angles which can be experimentally realized.

### Comparison of theory and experiment

We shall first discuss the comparison of theory and experiment for the variation of $\frac{1}{4}F_0(200)$ with wave-length in KF. In making this comparison, we assume that our measured $\frac{1}{4}F_0(200)$ contains the $\Delta[\frac{1}{4}F_0(200)]$ calculated from Hönl's theory for potassium and fluorine at the wave-length of Cu $K\alpha$ (1.538A). We have

$$\Delta[\tfrac{1}{4}F_0(200)] = \Delta f_0^K + \Delta f_0^F. \quad (11)$$

The left-hand member of the preceding equation represents the decrement in the reduced crystal structure factor; the right-hand members represent the decrements in the reduced atomic structure factors of potassium and fluorine, and are to be computed directly from Eqs. (8), (9), or (10). The computed value of $\Delta[\frac{1}{4}F_0(200)]$ at 1.538A is $-0.38$, according to Hönl's theory. Our

TABLE VII. *Comparison of observed and theoretical values of $\Delta(\frac{1}{4}F_0)$ in the (200) diffraction of KF.*

| LINE | λ(A) | $x = \lambda/\lambda_K$ | $\mu_m$ | $\Delta f_0^K$ Eqs. (8), (9) $Z_K = 1.43$ | $\Delta f_0^K$ Hönl, Eq. (10) | $\Delta(\frac{1}{4}F_0)$# Eqs. (8), (9) | $\Delta(\frac{1}{4}F_0)$# Eq. (10) | EXPERIMENT |
|---|---|---|---|---|---|---|---|---|
| Cu $K\alpha$ | 1.538 | 0.4486 | 137 | −0.38 | −0.32 | −0.44 | −0.38 | (−0.38) |
| Fe $K\alpha$ | 1.934 | 0.5643 | 272 | −0.31 | −0.20 | −0.40 | −0.29 | −0.58 |
| Va $K\alpha$ | 2.499 | 0.7289 | 540 | −0.03 | 0.09 | −0.16 | −0.04 | −0.02 |
| Ti $K\alpha$ | 2.744 | 0.8006 | 656 | 0.36 | 0.58 | 0.21 | 0.43 | 0.29 |
| Ca $K\alpha$ | 3.353 | 0.9785 | 1128 | 3.87 | 4.15 | 3.68 | 3.96 | 3.74 |
| KK abs | 3.4277 | 1.0000 | 1183 | 11.02 | — | 10.83 | — | — |
| Sb $L\alpha$ | 3.432 | 1.0013 | (125) | 8.93 | 7.78 | 8.74 | 7.59 | 8.03 |
| Sn $L\alpha$ | 3.593 | 1.0482 | (141) | 3.80 | 3.59 | 3.59 | 3.38 | 1.88, 1.08* |
| Ag $L\beta$ | 3.927 | 1.1146 | (179) | 2.71 | 2.56 | 2.48 | 2.33 | 1.18* |
| Ag $L\alpha$ | 4.146 | 1.2096 | (204) | 2.42 | 2.33 | 2.17 | 2.08 | 0.21, 0.69* |
| — | ∞ | ∞ | — | 1.43 | 1.43 | — | — | — |

# Values of $\Delta f_0^F$ used in computing cols. 7 and 8 from col. 4, Table V.
* LiF used as intermediate standard.

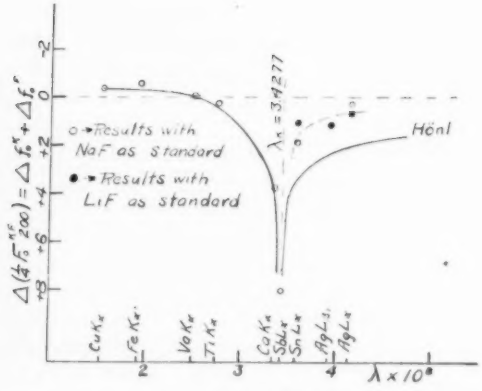


FIG. 2. The wave-length variation of the crystal structure factor for the (200) diffraction of powdered KF. Hönl's theory is the solid curve. The variation of the atomic structure factor of fluorine in this region is so small that practically the entire effect may be ascribed to the potassium $K$ electrons.

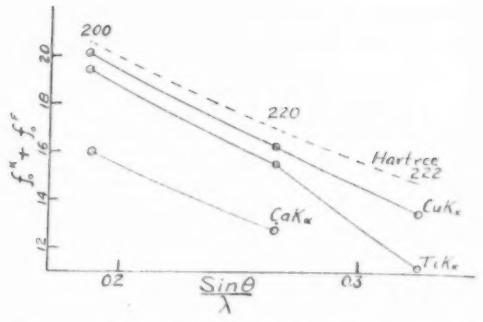


FIG. 3. Variation of the observed structure factor decrements with scattering angle. The point for Ti $K\alpha$ (222) contains a very large experimental error.

measured value of $\frac{1}{4}F_0(200)$ here is 20.10, according to Table VI; hence the value after "correction" for resonance of the $K$ electrons of potassium and fluorine would be 19.72. Thus having fitted theoretical and observed $\Delta[\frac{1}{4}F_0(200)]$ values together at this one wave-length, we can compare theory and experiment at other wave-lengths. This is shown in Table VII.

The experimental values of $\Delta(\frac{1}{4}F_0)$ shown in the last column of the table were obtained in the following way:

$$\Delta[\tfrac{1}{4}F_0(200)] = 19.72 - [\tfrac{1}{4}F_0(200)]_\lambda.$$

The crystal structure factors were taken from column 5 Table VI. The extent of the agreement between theory and experiment is shown in Fig. 2. It is seen that on the short wave-length side of the limit the agreement is within experimental error, but that large discrepancies are found on the long wave-length side. The observed decrements for Sn $L\alpha$, Ag $L\beta$, and Ag $L\alpha$ are considerably less than half those predicted. Taking only the long wave-length side of the curve into consideration, our results agree fairly well with an oscillator strength of the $K$ electrons of about 0.6. Inserting such a result into the equations, however, completely disrupts the observed agreement between theory and experiment at Ca $K\alpha$ on the short wave-length side, and also fails to predict the experimental value for Sb $L\alpha$, which is very close to the limit.

It is also interesting to note the extent of the agreement of our results on $\frac{1}{4}F_0(200)$ with the computed structure factors of Pauling and Sherman[23] and of Hartree.[24] From Table VIII it is seen that our measured factors are somewhat lower than the theoretical ones at 1.538A. In computing the theoretical factors in Table VIII, 0.38 has been added to the tabulated values in the references to allow for the resonance of the $K$ electrons of potassium and fluorine at this wave-length. In computing the structure factor for atoms according to Hartree it has been assumed that the $K$ and $K^+$ curves are indistinguishable at our values of $(\sin\theta)/\lambda$. Our (200) factor is within 0.2 electron of those computed for atoms according to Hartree, but our values fall off more rapidly with $(\sin\theta)/\lambda$ than do his.

Fig. 3 shows an experimental test of the dependence of $\Delta(\frac{1}{4}F_0)$ on $(\sin\theta)/\lambda$. The solid curves represent results taken from column 5 of Table VI. The dashed curve shows Hartree's

TABLE VIII. *Comparison of observed and theoretical atomic structure factor sums at Cu K$\alpha$, $\lambda = 1.538A$.*

| Indices | Pauling and Sherman | | Hartree | | Experiment |
|---|---|---|---|---|---|
| | Ions | Atoms | Ions | Atoms | |
| (200) | 22.0 | 21.1 | 20.9 | 20.3 | 20.10 |
| (220) | 18.0 | 17.5 | 17.4 | 17.2 | 16.21 |
| (222) | 15.5 | 15.2 | 15.1 | 14.9 | 13.45 |

[23] Pauling and Sherman, Zeits. f. Krist. **81**, 1 (1932).
[24] D. R. Hartree, see Compton and Allison, reference 7, p. 781.

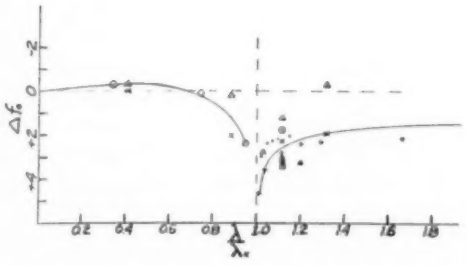


FIG. 4. Results of other observers on the wave-length variation of atomic structure factors in the region of the $K$ absorption edge. The solid curve is Hönl's predicted decrements for iron. The points are experiments on chromium, iron, nickel, and copper.

values for ions at the Cu $K\alpha$ wave-length. If the structure factor decrements are independent of $(\sin\theta)/\lambda$, the solid curves of Fig. 3 should be parallel. This is seen to be very nearly the case with the exception of the curve at the wave-length of Ti $K\alpha$ between (220) and (222). The (222) diffraction halo of Ti $K\alpha$ was the weakest measured in the entire experiment. At the maximum sensitivity of the Pliotron circuit it showed a deflection of about 1 cm above the rather high base-line. Our experimental error for this point is so great that we believe the apparent deviation from parallelism for this point is of no real significance. Our conclusion is that the structure factor decrements are independent of $(\sin\theta)/\lambda$ as predicted for light atoms by Hönl.

### C. Discussion of Results

**Résumé of previous work on this problem**

Since no previous determination has been made of the variation of the atomic structure factor with wave-length for any atom of as low an atomic number as potassium, no direct comparison of our results with those of other experiments is possible. However, some experimental data are available for atoms of somewhat higher atomic number and the agreement between such data and Hönl's calculations is shown in Fig. 4.

From Eq. (10) it may be seen that $\Delta f$ is dependent upon the variable $\lambda/\lambda_K$ and also on the parameter $\Delta$ which is a correction for screening. Since the latter is a very slowly changing function of atomic number, one might consider it almost constant throughout a very limited range of elements of adjacent atomic number. Then $\Delta f$ would depend to an extremely good approximation upon the variation in $\lambda/\lambda_K$ alone. The closeness of this approximation is shown in the table in Hönl's[25] paper. Making use of this fact, the previous experimental data for 24Cr, 26Fe, 28Ni, 29 Cu, have been condensed into a single plot in Fig. 4. The solid curve, which is actually Hönl's curve for iron, represents a very close approximation to the predictions of the theory for all these elements.

As representative of previous work covering a large range of wave-lengths, we have shown the results of Rusterholz[26] on copper (+), of Schäfer[27] on iron (×) and chromium (○), and of Bradley and Hope[28] on the intermetallic compound FeAl (Δ). All of these measurements were made by the photographic method. The values of Rusterholz are from measurements of the (220) diffraction of metallic copper for various wave-lengths, all, however, on the long wave-length side of the Cu $K$ absorption edge. They show good agreement with the calculations of Hönl in the vicinity of the limit, if we assume a value of $f_0^{Cu}(220) = 16$, as indicated by Hartree for the limiting value approached by the atomic structure factor of copper as $x$ approaches zero. At longer wave-lengths than the copper $K$ limit region, Rusterholz's experimental results fall below the Hönl curve. Schäfer's results for iron and chromium are in fairly good agreement also, but the experimental points seem a little higher than theory demands in the immediate neighborhood of the absorption edge on the long wave-length side. This discrepancy is probably within the experimental error. The values of Bradley and Hope are distinctly higher on the long wave-length side and rise to a value equal to the maximum value on the short wave-length side.

Scattered points are also given on the plot showing results for a less complete range of wave-lengths. Both Miss Armstrong[29] and

[25] Hönl, Ann. d. Physik [5] **18**, 625 (1933), p. 651.
[26] A. A. Rusterholz, Zeits. f. Physik **82**, 538 (1933).
[27] K. Schäfer, Zeits. f. Physik **86**, 738 (1933).
[28] A. J. Bradley and R. A. H. Hope, Proc. Roy. Soc. **A136**, 272 (1932).
[29] Alice H. Armstrong, Phys. Rev. **34**, 931 (1929).

Wyckoff[30] have measured the atomic structure factor for metallic copper (□, ▲) for the wave-length 1.539A using the ionization spectrometer, and Wyckoff has also made measurements with the wave-length 1.655A. Since no temperature correction was applied in either case, proper temperature corrections were made using the values of $e^M$ given by Rusterholz. Since determinations were also made in these two papers of the value of the atomic structure factor of copper using Mo $K\alpha$ (0.710A) radiation, the $\Delta f_0$ values plotted above are based upon the experimental value obtained with Mo $K\alpha$. This latter value was made to coincide with the Hönl $\Delta f$ curve just as in the treatment of our own experiments. A NaCl sample was used as a standard by Miss Armstrong and by Wyckoff throughout the range of wave-lengths which they investigated. No correction has been applied for the small change of the $F$ value of this standard due to resonance of the $K$ electrons of chlorine and sodium. A recent determination of the atomic structure factor of copper for 1.539A radiation has been made by Brindley and Spiers[31] by a photographic method. Their value, which is not plotted, would almost coincide with that of Wyckoff.

Finally there is shown on the plot a series of values of $f_0$ (●) taken from the dispersion curve obtained by Lameris and Prins[32] using the method of total reflection of the general x-radiation from a mirror of metallic nickel. These readings indicate a steeper rise of the structure factor on the long wave-length side of the absorption edge than the Hönl theory predicts. Direct measurements (not plotted) of the atomic structure factor of nickel by Wyckoff are in good agreement with the points of Lameris and Prins in this region.

Thus it may be said that taken as a whole, the experiments undoubtedly show that the behavior of an atomic structure factor at the $K$ edge is qualitatively that predicted by the modified dispersion theory that has been applied to x-rays. As to quantitative agreement, a general statement is difficult to make. Of the extended surveys, those of Rusterholz and Schäfer seem to confirm the theory in the region of atomic numbers 24 to 29, whereas those of Bradley and Hope and Lameris and Prins lie definitely above the predicted values.

[30] R. W. G. Wyckoff, Phys. Rev. **36**, 1116 (1930).
[31] G. W. Brindley and F. W. Spiers, Phil. Mag. **20**, 865 (1935).
[32] A. J. Lameris and J. A. Prins, Physica **1**, 881 (1934).

## Conclusion

Before making a definite statement of our conclusions, we wish to call attention to the manner in which we have treated our experimental data. We have endeavored to keep our values of $\Delta(\frac{1}{4}F_0)$ on as purely an experimental basis as possible. Thus we have not obtained them by subtracting our measured values from a theoretical atomic structure factor sum computed by the method of Hartree or of Pauling and Sherman. Our $\Delta(\frac{1}{4}F_0)$ values of column 9, Table VIII represent differences between an experimental value of $\frac{1}{4}F_0$ at 1.538A and our experimental values at other wave-lengths. A constant has been added in so that Hönl's computed $\Delta(\frac{1}{4}F_0)$ values are fitted to ours at one wave-length (Cu $K\alpha$).

In conclusion we may state the following:

(1) *Hönl's calculations do not correctly give the observed structure factor differences for the (200) diffraction from powdered potassium fluoride on the long and short wave-length sides of the potassium K edge.*

(2) *The predicted invariance of the structure factor decrement due to K electrons with scattering angle for light elements is confirmed in our experiments.*

The type of discrepancy between theory and experiment is such as to indicate that a revision both of the oscillator strengths and the oscillator distribution functions of the $K$ electrons of the potassium atom in solid KF is necessary.

# *K* X-Ray Absorption Spectra of Some Compounds of Bromine and Rubidium

S. T. STEPHENSON, *State College of Washington*

(Received January 17, 1936)

The *K* x-ray absorption spectrum of Br in KBr, RbBr, $CdBr_2$, and $NaBrO_3$ and of Rb in RbBr is obtained by using powder absorbing screens with a double crystal ionization spectrometer. Methyl iodide is used in the ionization chamber to eliminate the effect of Br in methyl bromide. The width of the Br edge is about 9 volts and of the Rb edge about 11 volts. The positions of secondary fine structure discontinuities are given and discussed. No discontinuity due to a possible simultaneous ejection of *K* and *L* electrons is observed.

## INTRODUCTION

THE fine structure and width of x-ray absorption edges and the secondary fine structure often found on the short wave-length side of these edges have been investigated recently by several observers. According to Kronig[1] the observed secondary fine structure is dependent upon the crystal lattice of the absorber. It was thought that it would be of interest to investigate the *K* x-ray absorption spectrum of bromine in a few bromine compounds and of both bromine and rubidium in RbBr for two reasons. First: The universal use of AgBr photographic plates when the photographic method is employed or the almost universal use of methyl bromide in ionization chambers when the ionization method is employed raises some question as to whether observed effects in the bromine absorption spectrum are due to bromine in the absorber or to bromine in the detecting plate or chamber. Second: In certain cases[2, 3, 4] two elements in the same compound do not exhibit the same secondary fine structure, making a study of both the Rb and Br absorption spectra in RbBr of importance since both edges are comparatively close together and, therefore, easy to investigate and compare.

## APPARATUS AND METHOD

The double crystal ionization spectrometer is of the type described by Ross,[5] constructed from a good Societé Génevoise optical spectroscope Crystals *A* and *B* were split from the same piece of optical quality calcite and were mounted with faces parallel to each other by the optical telescope method using a Gauss eyepiece. Crystal *B*, mounted on the prism table, is moved by a rigid lever arm run by Brown and Sharpe micrometer calipers, and the angular motions are further checked by viewing with a good telescope a millimeter scale as reflected from a mirror waxed to the top of the crystal. The angular readings can be relied upon to within 3 seconds of arc or about 0.05 X.U. in the region investigated. The ways supporting crystal *A* were taken from a micrometer microscope and fastened rigidly to the spectrometer in place of the collimator. A quadrant electrometer working at 3000 mm/volt sensitivity on a scale $1\frac{1}{2}$ meters distant measures the ionization currents in a small steel ionization chamber. It should be emphasized that here, as well as in a previous investigation of KBr,[6, 7] methyl iodide is used in the ionization chamber. Fig. 2 shows the Mo $K\alpha_1\alpha_2$ doublet in the (1,1) position, run to insure that the apparatus was working properly.

The metal x-ray tube[8] with Mo or W target was run on the pumps at about 40,000 volts peak and 30 to 40 milliamperes tube current. In view of Bearden's[9] experience with oil diffusion pumps and of their increasing popularity, it may be of interest to state that a regular General Electric X-Ray Universal broad focus filament has been used in the tube for over

[1] R. de L. Kronig, Zeits. f. Physik **70**, 317 (1931); **75**, 191 (1932).
[2] V. P. Barton and G. A. Lindsay, Phys. Rev. **46**, 362 (1934).
[3] D. Coster and G. H. Klamer, Physica **1**, 145 (1934).
[4] G. P. Brewington, Phys. Rev. **46**, 861 (1934).
[5] P. A. Ross, Rev. Sci. Inst. **3**, 253 (1932).
[6] S. T. Stephenson, Phys. Rev. **44**, 349 (1933).
[7] C. D. Cooksey and S. T. Stephenson, Phys. Rev. **43**, 670 (1933).
[8] Constructed, with some minor changes, following the design of N. S. Gingrich, Rev. Sci. Inst. **1**, 691 (1930).
[9] J. A. Bearden, Rev. Sci. Inst. **6**, 276 (1935).

200 hours and shows no signs of failure. The tube is pumped with one single stage metal diffusion pump[10] backed by a Megavac with one charcoal trap between fore pump and diffusion pump, no traps of any kind being used between diffusion pump and tube. Apiezon oil B is used and all wax joints are of Apiezon wax. Doubtless a $CO_2$ or liquid-air trap would make the vacuum conditions still better but no trouble has been experienced and faster pumping is obtained without such traps.

The absorbing screens were made by saturating cigarette papers with a solution of the salt and drying over a hot plate.[4] Seven or more papers were used in each screen to secure uniformity. Various precautions were taken to eliminate any apparent structure due to (1) nonuniform screens or (2) to crystal imperfections or (3) to variations in primary intensity by (1) moving the screens between runs, (2) taking blank runs without the absorber present; also sliding the crystals so that the same portions were not always used, and (3) removing the absorber after each reading to check the intensity without absorber on at least one run for every substance except $CdBr_2$. All readings were made with the crystals in the (1,1) position, the absorbing screens being placed between crystals *A* and *B*. Six readings were usually taken to obtain each point in a given run.

## Results and Discussion

The curves presented in Figs. 1 and 2 show the results obtained. The ionization currents in mm/sec. due to energy transmitted through the absorber are plotted as ordinates and X.U. are plotted as abscissae starting from an arbitrary zero, no attempt having been made to measure the actual wave-length position of the edge itself or any shift of the edge due to chemical combination, though this latter could not have exceeded 3 volts between the compounds studied. In Fig. 1 each of the curves following KBr is displaced an arbitrary amount downward and approximately 1 X.U. to the right of the one preceding it. A summary of the quantitative results obtained is presented in Table I, the average values from several runs being given.

The widths of the Br and Rb edges in the compounds investigated, given in volts in column 3 of Table I, were obtained from the experimental

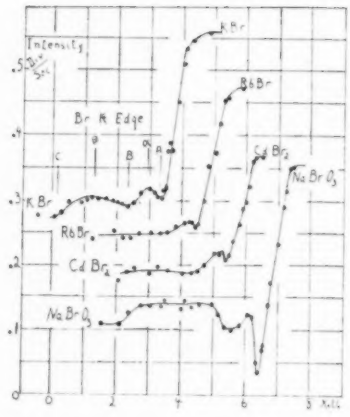


FIG. 1. The *K* absorption spectrum of Br in KBr, RbBr, $CdBr_2$ and $NaBrO_3$.

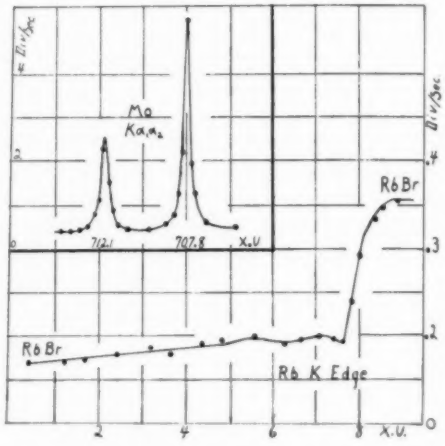


FIG. 2. The *K* absorption spectrum of Rb in RbBr. Mo $K\alpha_1\alpha_2$ doublet in inset.

TABLE I. *Widths of absorption edges and positions of secondary structure in volts.*

| Edge | Compound | Width | *A* | *α* | *B* | *β* | *C* |
|---|---|---|---|---|---|---|---|
| Br | KBr | 9±1.5 | 6.3 | 12 | 22 | 33 | 52 |
| Br | RbBr | 9±1.5 | 6.3 | 10.5 | 17 | | |
| Br | $CdBr_2$ | 9±1.5 | 6.3 | 11 | 22 | | |
| Br | $NaBrO_3$ | 9.5±1.5 | 6.5 | 11 | 19 | 48 | 77 |
| Rb | RbBr | 11±1.5 | 5.8 | 13(?) | 27(?) | | |

[10] The pump is of the type described in detail on page 80, D. H. Sloan, R. L. Thornton and F. A. Jenkins, Rev. Sci. Inst. **6**, 75 (1935).

TABLE II. *Physical constants of compounds used.*

| COMPOUND | CRYSTAL STRUCTURE | GRATING SPACE (Å) | MELTING POINT °C |
|---|---|---|---|
| KBr | Cubic | 6.57 | 730 |
| RbBr | Cubic | 6.86 | 683 |
| $CdBr_2$ | Hexagonal | 6.63 | 568 |
| $NaBrO_3$ | Cubic | 6.71 | 381 |

curves by the triangle method[11, 12] and are not corrected for the effect of the crystals. This is not the true width of the edge[13] but serves as a convenient means of recording and comparing results. The widths obtained, though slightly narrower, agree within experimental error with those quoted by Zinn.[12] No pronounced fine structure in the edges themselves of the type found by Barnes[14] for elements of lower atomic number was recorded.

The last five columns in Table I give the displacements of the secondary fine structure from the center of the main edge in volts, $A$ being the first minimum in the transmission curve, $\alpha$ the first maximum, etc. Table II gives the physical characteristics of the substances used which are pertinent to the discussion.

The most pronounced structure is shown by $NaBrO_3$, the substance of lowest melting point, in violation of the general rule that more pronounced structure is obtained for higher melting point substances. Others[12] have noted such violations. RbBr with a comparatively high melting point showed the least pronounced structure though several different screen thicknesses were tried.

The structure for KBr checks satisfactorily with the first two maxima found in a previous investigation of a KBr single crystal.[6,7] RbBr should yield a similar structure slightly closer to the main edge, because of its larger grating space according to Kronig's theory. Because of the unaccountably low intensity of the secondary structure for RbBr only the first maximum was obtained. The points $\alpha$ and $B$ for RbBr are closer to the edge by an amount in accord with the theory. The fact that $CdBr_2$ though hexagonal shows a close-in structure almost identical with that of KBr and RbBr is interesting and perhaps explainable on the same basis as that used by Coster[15] to account for similar structures exhibited by close-packed cubic and hexagonal lattices. $NaBrO_3$ is cubic and of about the same grating space as RbBr and KBr; but as 3 O atoms are associated with each Br atom in the lattice the close-in fine structure should not be similar to that of KBr and RbBr. Comparing we see that $\beta$ and $C$ differ for KBr and $NaBrO_3$ but $A$, $\alpha$, and $B$ are quite closely the same. Hanawalt[16] has obtained photographically pronounced secondary fine structure for $NaBrO_3$. $A$, $\alpha$, and $B$ obtained here agree with his data. $\beta$ and $C$ do not agree although it is possible that the large peak $\beta$ is complex, being made up of two discontinuities close together as was evidenced by some of the runs, in which case the data are in better agreement. In an ionic crystal the outer electronic shells of Br are complete and after the ejected $K$ electron reaches the outer shells the Br nucleus and incomplete $K$ shell will act on the electron much as the element of atomic number one greater, namely, krypton. Now krypton has a large ionization potential of about 14 volts and it is probable that structure within 15 volts or so of the Br edge should be governed more by the atom[17] than by the crystal lattice, particularly since Kronig's assumptions do not hold accurately close to the edge. This may be the main factor resulting in the similarity of $A$, $\alpha$, and $B$ in the cases studied.

The comparison of the secondary fine structure of Br and Rb in RbBr is inconclusive because of the meager structure found for Br and the almost complete lack of structure for Rb, $\alpha$ and $B$ here being doubtful. The structures might be expected to differ at least close to the edge.[18] The two here are similar in that both exhibit comparatively weak structure. $\alpha$ and $B$ are not the same. No very extended structure was found which would prove whether the two are in better agreement 100 or more volts from the edge.

It is of interest that a discontinuity due to the simultaneous ejection of a $K$ and an $L$ electron from a Br atom would have appeared at about 815 X.U. whereas the wave-length of

[11] P. A. Ross, Phys. Rev. **44**, 977 (1933).
[12] W. H. Zinn, Phys. Rev. **46**, 659 (1934).
[13] F. K. Richtmyer, S. K. Barnes and E. Ramberg, Phys. Rev. **46**, 843 (1934).
[14] A. H. Barnes, Phys. Rev. **44**, 141 (1933).
[15] D. Coster, Physica **2**, 606 (1935).
[16] J. D. Hanawalt, Phys. Rev. **37**, 715 (1931).
[17] W. Kossel, Zeits. f. Physik **1**, 119 (1920).
[18] D. Coster and R. Smoluchowski, Physica **2**, 1 (1935).

the Rb edge is 814 X.U. It was necessary to search for such a discontinuity due to Br to make sure that it did not affect the runs on the Rb edge in RbBr. Two runs over the region 810–820 X.U. with $NaBrO_3$ as absorber failed to show any pronounced evidence for simultaneous $K$ and $L$ ejection large enough to affect the results for the Rb edge.

The secondary fine structure obtained by others[11, 12] using polycrystalline absorbers of atomic number greater than 34 and the double crystal spectrometer is not very pronounced and is obtained only comparatively close to the main edge as in this investigation. More secondary fine structure of the Kronig type further from the edge than that obtained here undoubtedly exists for all the compounds but does not appear prominently enough to be recorded above experimental errors. It would be more pronounced if the absorption took place in a single crystal, the case of KBr[6, 7] being one example. A study of Rb and Br in a single crystal of RbBr would prove interesting if a perfect enough crystal could be prepared.

---

APRIL 1, 1936 PHYSICAL REVIEW VOLUME 49

# A Simple Method for Demonstrating and Measuring Approximately the Index of Refraction of Crystalline Substances for X-Rays

H. C. HOYT AND GEO. A. LINDSAY, *University of Michigan*

(Received January 21, 1936)

An x-ray spectrum line may be formed by reflection at the surface of a crystal even if that surface is not parallel to the atomic planes concerned in the reflection. If two faces are good very close to the line of their intersection, then, using a slit that is not too narrow, the same line may be reflected simultaneously from these two faces of a stationary crystal by turning it so that for the proper reflecting angle the rays must fall at the intersection. If the wave-length of the line is such that the reflected beam from the beveled face almost grazes the surface, then that portion will be refracted much more than the portion of the line reflected from the other face, and the two parts of the line are plainly separated. A very simple calculation gives the index of refraction from the width included between the two portions of the line. In this way $\delta/\lambda^2$ for a cerussite crystal has been found to agree fairly well with the calculated value.

IN 1922 Davis and Terrill[1, 2] suggested a method of increasing the refraction of a beam of x-rays by grinding a crystal surface at an angle with the atomic planes so that the incident or emergent beam might make a very small angle with the reflecting surface.

The present investigation retains the principle of the Davis method of unsymmetrical reflection, but introduces two important modifications. Firstly, two natural faces were used instead of a natural face and a ground surface; secondly, the same spectrum line was reflected simultaneously from two faces of the crystal by turning the crystal so that for the proper reflecting angle the rays fell at the intersection of the two faces. The crystal was stationary during the exposure. The wave-length of the line was such that the rays reflected from the beveled face, almost grazed the surface, and were therefore refracted much more than the portion of the line reflected from the Bragg face, so that the two parts of the line were plainly separated. No reference line is needed but the two reflecting surfaces selected must be good very close to their line of intersection.

## The Crystal Structure of $PbCO_3$

The crystal specimens chosen were cerussite ($PbCO_3$) which is orthorhombic in form and resembles aragonite in its structure and symmetry.[3] The density is 6.5 g/cc. Sharp x-ray emission lines were obtained by reflection from the faces used. In a number of investigations

[1] Davis and Terrill, Proc. Nat. Acad. Sci. **8**, 537 (1922).
[2] Nardoff, Phys. Rev. **24**, 143 (1924).
[3] W. L. Bragg, Proc. Roy. Soc. **A105**, 16 (1924).

the refracting medium has been used as a grating to determine the index of refraction with crystals of low density. Thus Hjalmar[4] used gypsum (specific gravity 2.3), and Larsson[5] used mica (sp. gr. 3.0), calcite (sp. gr. 2.7), and quartz (sp. gr. 2.65). Cerussite was selected in the present work because its density is more than twice the density of the heaviest of these, and hence it should give a much greater refraction.

Since the method employed requires the use of two faces of the crystal for each exposure, a knowledge of the grating spaces and of the angle between the faces used is necessary.

Measurements of the grating spaces for several faces of the crystal were made, together with two of the angles between faces. The results were as follows:

| Crystal plane | (001) | (011) | (110) | (111) | (102) |
|---|---|---|---|---|---|
| $d$ (x.u.) | 3065 | 2483 | 4416 | 3583 | 2637 |

The angle between the (100) and (110) faces was found by an optical spectrometer to be 31° 21′ 30″, and that between the faces (111) and (102), 31° 6′ 10″. From these values of $d$ and one of the angles, the axes of the crystal were calculated to be as follows:

$a=5173\pm4$ x.u.; $b=8478\pm5$; $c=6129\pm3$.

The axial ratios from the above values are

$$a : b : c = 0.6102 : 1 : 0.7229.$$

These ratios agree well with those given in crystallographic tables, the latter values varying according to the specimen used for the measurements. For example, the following are three samples of previous values.

| $a$ : | $b$ : | $c$ | Source |
|---|---|---|---|
| 0.6102 : | 1 : | 0.7232 | Kokscharow |
| 0.6100 : | 1 : | 0.7230 | Goldschmidt's Atlas |
| 0.6101 : | 1 : | 0.7230 | Artini |

Our probable errors are based on the assumption that the above values of $d$ are accurate to about 1 x.u.

The axial values given by Zachariasen[6] are:

$a=5.14$A, $b=8.45$A, $c=6.10$A.

[4] Hjalmar, Dissertation, Lund (1923).
[5] Larsson, Dissertation, Uppsala (1929).
[6] W. H. Zachariasen, Norske Videnskaps-Akad., Oslo. Mat.-Naturv. Klasse (1928).

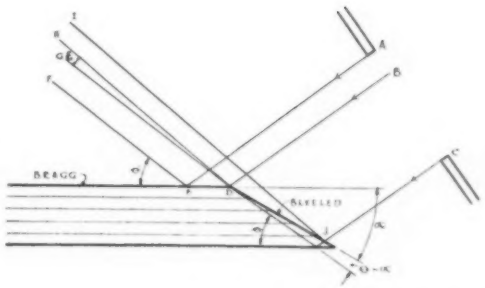


$1-\mu=\delta=\tan(\theta-\alpha)\sin\epsilon\leqq(\theta-\alpha)\epsilon$

FIG. 1. Geometrical relations involved in the derivation for the expression of the index of refraction.

These latter values were determined by the powder method.

## APPARATUS

All spectra in this investigation were obtained with a Siegbahn vacuum spectrograph. The radius of the spectrograph was 183 mm, and the width of the slit was 0.07 mm. Cellophane was used to seal the slit and visible light from the filament or other sources was intercepted by red colored gold beater's skin. The materials, for the several characteristic lines studied, were either soldered to the target or rubbed on as a powder. The crystal was mounted with the line of intersection between the two faces in the axis of rotation of the crystal table.

## GEOMETRICAL RELATIONS AND DERIVATION OF THE EXPRESSION FOR THE INDEX OF REFRACTION

In Fig. 1, $AC$ is the slit width very much magnified and $AEDJC$ is the outline of the beam directed towards the intersection of the two faces. $FG$ is the portion of the spectrum line from the Bragg face and $III$ the portion from the beveled face. $\epsilon$ represents the angle of separation, measured from the inside edges, between the two portions of the line.

The path of the incident and refracted rays $ACED$ is shown in Fig. 2.

From the definition of the index of refraction

$$\mu=\frac{\sin i}{\sin r}\frac{\cos\beta}{\cos\gamma}=1-\delta, \qquad (1)$$

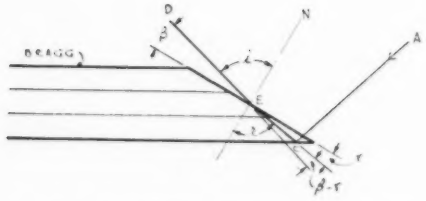


FIG. 2. Path of the incident and refracted rays.

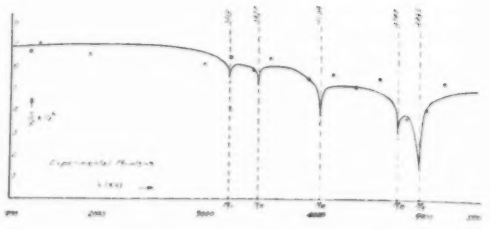

FIG. 3. Plot of $\delta/\lambda^2$ against $\lambda$.

from which

$$\delta=\frac{\cos\gamma-\cos\beta}{\cos\gamma}=\frac{2\sin\tfrac{1}{2}(\gamma+\beta)\sin\tfrac{1}{2}(\beta-\gamma)}{\cos\gamma}. \quad (2)$$

$\beta-\gamma$ is the deviation of the ray $ED$ due to refraction. $\beta$ and $\gamma$ are nearly equal, therefore $(\gamma+\beta)/2$ equals $\beta$ or $\gamma$ approximately (until $\beta$ becomes very small). The sines and tangents are approximately equal to the angles expressed in radian measure.

Therefore

$$\delta=\frac{2\sin\beta\sin\tfrac{1}{2}(\beta-\gamma)}{\cos\gamma}=\beta(\beta-\gamma)$$

very approximately. (3)

From Fig. 1, $\beta=\theta-\alpha$ and $(\beta-\gamma)=\epsilon$, (4)

so that $\delta=\epsilon(\theta-\alpha)$. (5)

Thus $\delta$ is simply the product of two angles expressed in radian measure.

Since the separation which was measured is the difference between the positions of the inside edges of the two portions of the separated spectrum line, a correction is necessary for the refraction of the portion of the line coming from the Bragg face. The deviation due to refraction of the ray reflected at the Bragg face is given by $\theta'-\theta=\delta\cot\theta$ where $\theta$ is the glancing angle within the crystal and $\theta'$ is the corresponding angle between the emergent ray and the Bragg face. Hence the amount to be added to $\epsilon$ is $\delta\cot\theta$

or $$\delta=\epsilon(\theta-\alpha)+\delta(\theta-\alpha)\cot\theta, \quad (6)$$

whence $$\delta=\frac{\epsilon(\theta-\alpha)}{1-(\theta-\alpha)\cot\theta}. \quad (7)$$

The quantum theory of dispersion as developed by Kronig, Kramers,[7] Kallman and Mark,[8] and Prins[9] gives the following relation between $\delta$ and the frequency

$$\delta=\frac{e^2}{2\pi c^2 m}\Sigma\frac{N_i}{\nu^2}\left\{1+\left(\frac{\nu_i}{\nu}\right)^2\ln\left[1-\left(\frac{\nu}{\nu_i}\right)^2\right]\right\},$$

where $N_i$ is the number of electrons of frequency $\nu_i$ per cubic centimeter, and $\nu$ is the frequency of the incident radiation. Damping is neglected.

Rewriting the equation for $\delta$, after substituting $1/\lambda$ for $\nu$ and dividing by $\lambda^2$ we have

$$\frac{\delta}{\lambda^2}=\frac{e^2N}{2\pi c^2 m}+\Sigma\frac{e^2N_i}{2\pi c^2 m}\left(\frac{\lambda}{\lambda_i}\right)^2\ln\left\{1-\left(\frac{\lambda_i}{\lambda}\right)^2\right\},$$

where $N$ is the total number of electrons of the medium per cubic centimeter.

$\delta/\lambda^2$, calculated from this equation is plotted with $\lambda$ giving the dispersion curve shown in Fig. 3.

A few comments may be made on this method of determining the index of refraction for x-rays.

(a) The slit must not be too narrow.

(b) For good lines an intense radiation should strike both faces. This is especially true of the beveled face since the radiation reflected from the beveled face traverses a considerable amount of the crystal and is therefore strongly absorbed.

(c) The direction of radiation cannot be reversed, that is, it must take the direction indicated in Fig. 1. If it were sent towards the crystal in the reverse direction, there would be no separation of the line, since, for a given wave-length, the reflected rays would emerge practically parallel from both faces.

(d) The limiting wave-length for a given crystal can be determined by substituting $\alpha$, Fig. 1, for $\theta$ in the Bragg

[7] H. A. Kramers, Nature **113**, 673 (1924).
[8] Kallman and Mark, Ann. d. Physik (4) **82**, 585 (1927).
[9] J. A. Prins, Zeits. f. Physik **47**, 479 (1928).

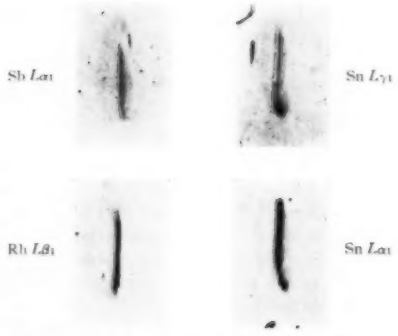


FIG. 4. Separation of a monochromatic beam due to refraction.

relation $n\lambda = 2d \sin\theta$. The minimum wave-length which may practically be employed is somewhat larger than this, since the refracted beam is nearly all absorbed if $\theta - \alpha$ is very small.

(e) As stated previously an imperfect edge between the two planes is likely to cause serious error in the readings. For one crystal the character of the intersection between the (111) and (102) planes was studied by taking photographs at shorter distances. The regular distance from the axis of the spectrograph to the photographic plate was 183 mm. One photograph was taken at 103.5 mm and another at 41.4 mm. This procedure was repeated for different lines. Since the photograph is a record of two reflected beams of rays having the same wave-length, any separation due to an imperfect edge would be the same for all distances of the plate. With these photographs the separation was proportional to the distance, indicating that the separation was due to an actual difference in direction between the two beams and that any irregularities in the surfaces close to the edge were too small to affect the readings.

A microscopic examination of the second crystal gave no indication of imperfections near the edge.

## RESULTS

The edge of the line to be measured at $G$ (Fig. 1) was in all cases quite sharp, while that at $H$ was less so, especially when the angle between the face and the emergent ray was small. Since the incident rays are concentrated into a narrower beam after reflection from the beveled face, as shown in Fig. 1, it might be expected that the refracted line would be rather intense but, as explained in (d), when $(\theta - \alpha)$ is small the refracted line is strongly absorbed.

Observations were made over a range of wave-lengths extending from 1389 x.u. to 5166 x.u. Several photographs of the separated lines are shown in Fig. 4. Table I contains a summary of the lines with their wave-lengths, the grating constants used, the angle $(\theta - \alpha)$ between the reflected ray and the beveled face, the angle $\epsilon$ due to the difference in refraction between the two portions of the beam, and the final value of $\delta/\lambda^2$ as calculated from Eq. (11). The readings for the last three wave-lengths appearing in Table I were taken with the second crystal. All observations were taken in the first order with the exception of the lines Fe $K\alpha_1$, W $L\alpha_1$ and Cu $K\beta_1$, which were taken in the second order.

TABLE I. *Summary of computed values of $\delta/\lambda^2$ for two crystals and the various wave-lengths.*

| LINE | $\lambda$(x.u.) | $d$(x.u.) | $(\theta-\alpha)$ (min.) | $S$(mm) | $\epsilon(=S/R)$ | $\delta/\lambda^2\cdot10^6$ |
|---|---|---|---|---|---|---|
| *Crystal* No. 1, $\alpha = 31°\ 7'$ | | | | | | |
| Cu $K\beta_1(2)$ | 1389 | 2637 | 41 | 0.195 | 0.001065 | 6.71 |
| W $L\alpha_1(2)$ | 1473 | 2637 | 171 | .053 | .000289 | 7.17 |
| Fe $K\alpha_1(2)$ | 1932 | 3583 | 91 | .161 | .000781 | 6.52 |
| Sn $L\gamma_1$ | 2995 | 2637 | 210 | .153 | .000836 | 6.25 |
| Sb $L\beta_1$ | 3218 | 2637 | 390 | .092 | .000503 | 6.45 |
| Sb $L\alpha_1$ | 3432 | 2637 | 570 | .067 | .000366 | 6.39 |
| Sn $L\alpha_1$ | 3592 | 2637 | 711 | .057 | .000311 | 6.42 |
| Ag $L\beta_1$ | 3927 | 3583 | 127 | .393 | .002147 | 5.45 |
| Ag $L\alpha_1$ | 4146 | 3583 | 254 | .217 | .001186 | 5.69 |
| Rh $L\beta_1$ | 4364 | 3583 | 384 | .137 | .000748 | 5.14 |
| Rh $L\alpha_1$ | 4588 | 2637 | 1764 | .029 | .000158 | 5.44 |
| *Crystal* No. 2, $\alpha = 31°\ 23.5'$ | | | | | | |
| Ru $L\alpha_1$ | 4836 | 4416 | 108.5 | 0.469 | 0.002562 | 3.63 |
| S $K\beta_1$ | 5021 | 4416 | 195.5 | .308 | .001667 | 4.14 |
| Mo $L\beta_1$ | 5166 | 4416 | 264.3 | .301 | .001644 | 5.30 |

For each line the difference $S$ is the mean of the measured separations on two or more photographic plates. Ten settings of the comparator were made on each position.

Fig. 3 contains the theoretical curve for $\delta/\lambda^2$ and also the experimental values represented by small circles.

The experimental points obtained do not show conclusively the influence of the absorption edges. However, in the region of the smallest value of $\delta/\lambda^2$, that is, near the $M_V$ absorption edge, the two points for Ru $L\alpha_1$ and S $K\beta_1$ fell to low values, and they lie nearly on the curve.

The results, though approximate (probably accurate to about ten percent), are simply and directly obtained without special apparatus.

# Excitation Potential, Relative Intensities and Wave-Lengths of the $K\alpha''$ X-Ray Satellite Line

LYMAN G. PARRATT,* *Cornell University*

(Received January 25, 1936)

With a two-crystal vacuum spectrometer, ionization curves of the $K\alpha''$ satellite line have been recorded for elements S(16) to V(23). This satellite line, on the short wave-length side of and very close to the $K\alpha_1$ line, was observed in 1922 by Dolejšek and has been until now a forgotten line. The excitation potential of this satellite has been determined: The initial atomic state for its emission appears to be one of $KM$ ionization. The $K\alpha''$ intensity relative to the $K\alpha_1$ intensity varies with atomic number, reaching a maximum of 2.3 percent at Ca(20). The $K\alpha''$ wave-length positions have also been determined for each element. The observed data are compatible with both the Wentzel-Druyvesteyn and the Richtmyer theories for the origin of this satellite line.

## I. INTRODUCTION

SATELLITES comprise a large fraction of the total number of characteristic x-ray emission lines; but as yet we do not have a generally acceptable explanation of satellite origins. The greatest need in resolving this enigma is that of a more complete and accurate experimental description of these nondiagram lines.

In another paper[1] the writer has recently reported the results of experiments on the excitation potential of the satellite lines of the $K\alpha_{3,4}$ group. This group of lines consists (for elements near titanium ($Z=22$)) of five components: $\alpha'$, $\alpha_3$, $\alpha_3'$, $\alpha_3''$ and $\alpha_4$. For these lines[2] the excitation potential was found to be in agreement with the voltage required to ionize doubly the emitting atom by ejection of a $K$ and an $L$ electron by a single cathode-ray impact. This result is in support of the Wentzel-Druyvesteyn theory which supposes that the atomic (or ionic) transition $KL \rightarrow LL$ gives rise to the $K\alpha_{3,4}$ lines. The present paper is concerned with determinations of the excitation potential, relative intensities and wave-lengths of the $K\alpha''$ satellite line. We shall conclude that this line is not of the $\alpha_{3,4}$ group but, in terms of the Wentzel-Druyvesteyn theory, is produced by a $KM \rightarrow LM$ transition.

## II. EXPERIMENTAL PART

The two-crystal vacuum spectrometer, on which were mounted calcite crystals $A$, $B_4$, was used in the present as in the previous experiments.[1] The advantages of this type of instrument over the single-crystal spectrograph are (1) in the greater practical resolving power and dispersion, and (2) in the greater accuracy with which intensities can be measured. The relative disadvantages of the ionization method of registering intensities as compared with the photographic method are (1) in the greater difficulties encountered in preparing satisfactory targets of the materials to be studied, and (2) in maintaining the higher vacuum in the x-ray tube necessary for accurate intensity measurements. These advantages and disadvantages have been mentioned elsewhere.[1, 3] The reader is referred to previous papers for discussions of the accuracy[1] with which the present ionization curves[4] were recorded and of the instrument perturbations[5] which distort the true x-ray line contours into the observed curves.

The targets used in these experiments were prepared as follows: $CaCl_2$, KCl, $SrCl_2$, $K_2PO_4$, CaO and $Sc_2O_3$ in the powdered form were pounded into a roughened copper surface. CuCl was formed by passing chlorine gas over copper. A metallic calcium target was made in the manner previously described.[6] The pure metallic titanium and vanadium targets have also been

* The author is indebted to the Carnegie Foundation for a grant-in-aid of this research.

[1] L. G. Parratt, Phys. Rev. **49**, 132 (1936).

[2] The intensity of the two strongest lines, $\alpha_3$ and $\alpha_4$, dominates the intensity of the group, and, as discussed in reference 1, whether or not all five components of the group have the same excitation potential could not be determined in these experiments.

[3] L. G. Parratt, Rev. Sci. Inst. **6**, 372 (1935).

[4] The experimental set-up in the present work was identical with that in the previous work, reference 1.

[5] L. G. Parratt, Rev. Sci. Inst. **6**, 387 (1935).

[6] L. G. Parratt, Phys. Rev. **44**, 695 (1933).

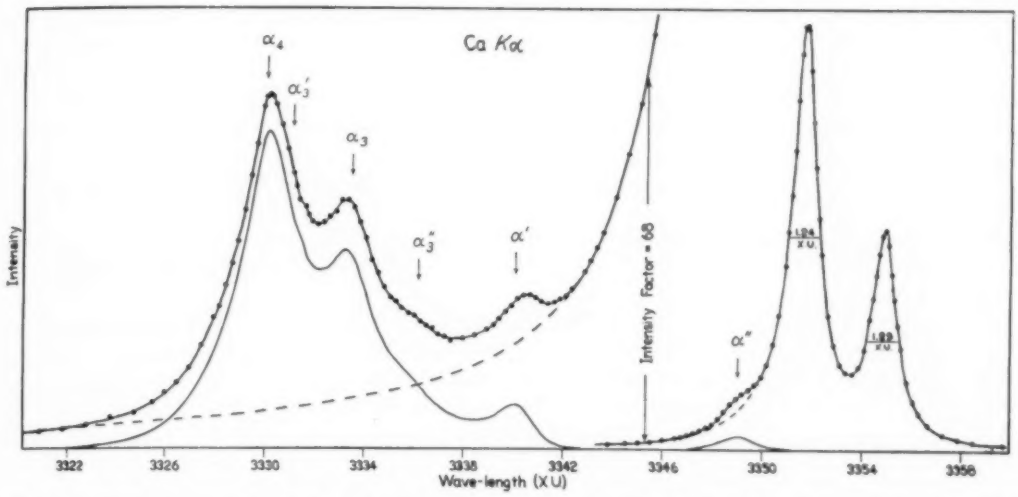


FIG. 1. Ionization curve of the Ca $K\alpha$ region. This curve was recorded with a CaO target and with a tube potential of 20 kv. The $\alpha_{3,4}$ group of satellites is plotted to an intensity scale 68 times the scale used in plotting the $\alpha''$, $\alpha_1$ and $\alpha_2$ lines. The satellite background (the side of the $\alpha_1$ line) has been sketched in and the satellite contours, corrected for this background, are also drawn in the figure.

described,[3, 6] and likewise the sulphur targets.[7] All of these targets were satisfactory in studying the $K\alpha_{1,2}$ doublet and the $K\alpha''$ lines, but only FeS, $K_2PO_4$, CaO, $Sc_2O_3$, questionably $CaCl_2$, and metallic Ca, Ti and V served satisfactorily in obtaining data on the $K\alpha_{3,4}$ lines. This latter group of targets would dissipate, with the focal spot approximately 2 mm in diameter, from 400 to 700 watts of power.

**Notation**

The term $K\alpha''$ in the present paper is used to refer to the "bump" which appears on the short wave-length side, near the base, of the $K\alpha_1$ line with elements S(16) to V(23). That the reader may gain perspective, an ionization curve of the $K\alpha$ region, $K\alpha_{1,2}$, $\alpha''$ and the $\alpha_{3,4}$ group, for calcium (20) is shown in Fig. 1. Ca $K\alpha''$ appears at the wave-length 3349.1 X. U. In Fig. 1 of the previous paper[1] the same $K\alpha$ region is reproduced for titanium (22).

The notation used to designate x-ray satellites is confused; this confusion becomes more apparent as our knowledge of these lines becomes more complete. Many faint x-ray lines known in the literature as satellite or nondiagram lines can now be accounted for easily as diagram lines for which the quadrupole, rather than the dipole, selection rules are obeyed. Another type of confusion is illustrated by the following: Hulubei recently reported[8] a triplet nature of the $K\alpha_{3,4}$ satellites in the region of elements Cu(29) to As(33). The third component of this group, the one between $\alpha_3$ and $\alpha_4$, Hulubei calls $\alpha_3'$. This is an extrapolation of the notation of Bäcklin[9, 10] from the range of elements Si(14) to Cl(17). The writer, using the two-crystal spectrometer, has been able to trace[11] the component $\alpha_3'$ from S(16) to Ge(32). Relative to the $\alpha_3$ or to the $\alpha_4$ line, $\alpha_3'$ moves progressively as the atomic number changes: In the region of low atomic numbers the $\alpha_3'$ is in the position reported by Bäcklin[9] and by Ford,[10] that is, on the *long*[12] wave-length side of

[7] L. G. Parratt, Phys. Rev. **49**, 14 (1936).

[8] M. H. Hulubei, Comptes rendus **201**, 544 (1935).

[9] E. Bäcklin, Zeits. f. Physik **33**, 547 (1925); **38**, 215 (1926).

[10] O. R. Ford, Phys. Rev. **41**, 577 (1932).

[11] Discussed in more detail in another paper in process of publication.

[12] If these trends are extrapolated to atomic numbers lower than Si(14) the $\alpha_3$ and $\alpha_3'$ lines should be coincident in wave-length at Al(13) or Mg(12): In fact, with these elements, Al and Mg, no $\alpha_3'$ has been found while the relative intensity of $\alpha_3$ has been reported as being anomalously large (reference 10). From ionization curves at S(16) the writer estimates the intensity of the resolved $\alpha_3'$ component to be approximately 80 percent of the intensity of the $\alpha_3$ component. With elements of atomic number less than 12 the $\alpha_3'$ line may be expected to appear, if one continues the extrapolation, on the long wave-length side of $\alpha_3$.

$\alpha_4$; at Ti(22) the $\alpha_3'$ and $\alpha_4$ are coincident in wave-length; and with elements of atomic number greater than 22 $\alpha_3'$ is on the *short* wave-length side of $\alpha_4$. These observations, in agreement with those of Hulubei, show that in the range of higher atomic numbers $\alpha_{3,4}$ is complex, actually a quadruplet since the $\alpha'$ line, although very faint, is still present, and also show that the terms $\alpha_3'$ and $\alpha_4$ as assigned by Hulubei should be interchanged.

A third type of confusion in notation is in regards to the present line $K\alpha''$. In 1922 Dolejšek[13] observed an "emission band" on the short wave-length side of the $K\alpha_1$ line with elements Cl, K, Ca and Sc. The short wave-length edge of this band he called $\alpha'$; the line now known as $\alpha'$ Dolejšek, following Siegbahn's lead, called $\alpha_7$. Dolejšek's "emission band" and the writer's "bump," $\alpha''$, are the same line (or group of lines). It speaks well of Dolejšek's care in his observations and of the resolving-power of his spectrograph that he was able to detect this emission band: Of the numerous investigators following him, none, so far as the writer is aware, has reported finding it.

Druyvesteyn[14] refers to Dolejšek's emission edge $\alpha'$ as the $\alpha''$ line, and reverts to Hjalmar's[15] use of the term $\alpha'$. In Fig. 1 the $\alpha'$ line is at 3340.1 X. U. Deodhar[16] has reported a possible doublet nature of the $K\alpha'$ line with elements Si(14) and P(15). The terms $\alpha'$ and $\alpha''$ were used by Deodhar to refer to this doublet. So far as the writer is aware no other observer has seen a doublet structure in $\alpha'$ for Si, P or other elements, and the writer has found no indication of such structure for S(16). Deodhar states that his $\alpha''$ may have been due to chemical combination or may have been spurious. We shall therefore adhere to the notation used by Druyvesteyn in assigning the term $\alpha''$ to the "bump."

## Relative intensities

Ionization curves of $K\alpha''$ with elements S(16) to Cr(24) are reproduced in Fig. 2. The $\alpha''$ line is most prominent at Ca(20). This may or may not mean that the intensity of $\alpha''$ relative to the intensity of $\alpha_1$ is a maximum at Ca: We do not know the shape of the $\alpha_1$ line and consequently we have considerable latitude in drawing in the background of the $\alpha''$ satellite. In Fig. 2 the side of the $\alpha_1$ line for each element has been drawn in such that the width at half-maximum intensity of the $\alpha''$ line is approximately the same as the width of the $\alpha_1$ line. There is no justification for choosing this particular resolution; in fact, satellite lines in general are wider than the associated diagram lines: The component lines of the Ca $K\alpha_{3,4}$ satellites are 1.5 to 3 times as wide as the $\alpha_1$ line. Furthermore if $\alpha''$ is in reality a group of lines the width should certainly be greater than is here assumed. This question bears not only on the shape and possible multiplet structure of $\alpha''$ but also on the asymmetry of the $\alpha_1$ lines, a subject beyond the scope of the present paper.[11] In Fig. 3 is plotted the intensity of $\alpha''$ relative to the intensity of $\alpha_1$ when the resolution is arbitrarily made as indicated in Fig. 2. These intensity ratios are listed in Table I. The uncertainty in the relative intensity due to the indefinite background is greatest for S(16) and, with this element, may be as great as a factor of two or even three. The values given in Table I are probably a minimum. A slight trace of the existence of $\alpha''$ for Cr(24) was observed but this evidence was within the observational error. The reality of the presence of $\alpha''$ for V(23) may be questioned since the "bump" with this element is close to the observational error.

TABLE I. *Relative intensities and wave-lengths of the $K\alpha''$ satellite line.* Four different chemical compounds of Cl(17), $CaCl_2$, KCl, CuCl and $SrCl_2$, and two chemical compounds of Ca(20), $CaCl_2$ and CaO, in addition to metallic Ca were used as targets. No difference in the $\alpha''$ line due to chemical binding was observed greater than the observational error. In the case of CaO and metallic Ca, however, a marked difference is observed in the widths of the $\alpha_{1,2}$ lines. See Figs. 1 and 4. The wave-lengths given by Dolejšek[13] for the short wave-length edge of his "emission band" are listed in the last column. Dolejšek did not give wave-lengths of the $K\alpha_1$ line.

| Target | Element | Relative Intensity $(\alpha''/\alpha) \times 100$ | Wave-Lengths $\alpha_1$* | $\alpha''$ | $\alpha''$ (Dolejšek) |
|---|---|---|---|---|---|
| FeS | S(16) | 1.0 | 5361.28 | 5358.6 | —— |
| $CaCl_2$ | Cl(17) | 1.4 | 4718.2 | 4714.8 | 4712 |
| $K_2PO_4$ | K(19) | 2.1 | 3733.68 | 3730.9 | 3730 |
| CaO | Ca(20) | 2.25 | 3351.69 | 3349.1 | 3349 |
| $Sc_2O_3$ | Sc(21) | 1.4 | 3025.03 | 3022.8 | 3023 |
| metal | Ti(22) | 0.9 | 2742.87 | 2740.9 | —— |
| metal | V(23) | 0.3 | 2498.42 | 2496.5 | —— |

* The wave-lengths of the $K\alpha_1$ line of vanadium and of titanium are taken from Bearden and Shaw, Phys. Rev. **48**, 18 (1935); of scandium to chlorine from Siegbahn, *Spektroskopie der Röntgenstrahlen* (1931); and of sulphur from Valasek, Phys. Rev. **43**, 612 (1933).

[13] M. V. Dolejšek, Comptes rendus **174**, 441 (1922).
[14] M. J. Druyvesteyn, Doctor's Dissertation, Groningen, 1928.
[15] E. Hjalmar, Zeits. f. Physik **1**, 439 (1920).
[16] G. B. Deodhar, Proc. Roy. Soc. **A131**, 633 (1931).

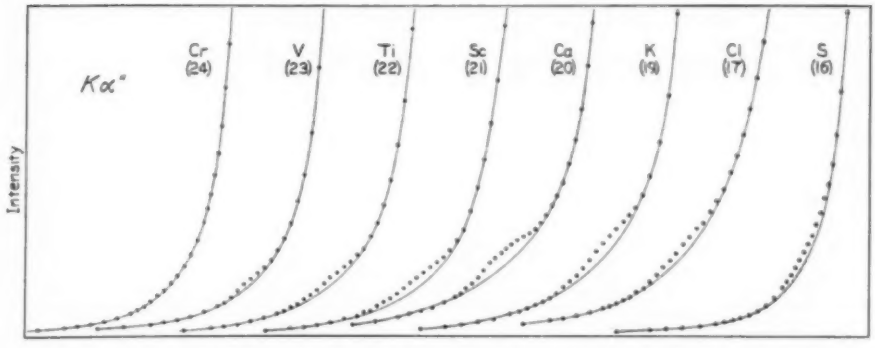


FIG. 2. Ionization curves of the $K\alpha''$ line for elements S(16) to Cr(24). The tube potential used in recording these curves was 15 to 20 kv. The abscissae and ordinate scales are arbitrary in the case of each curve.

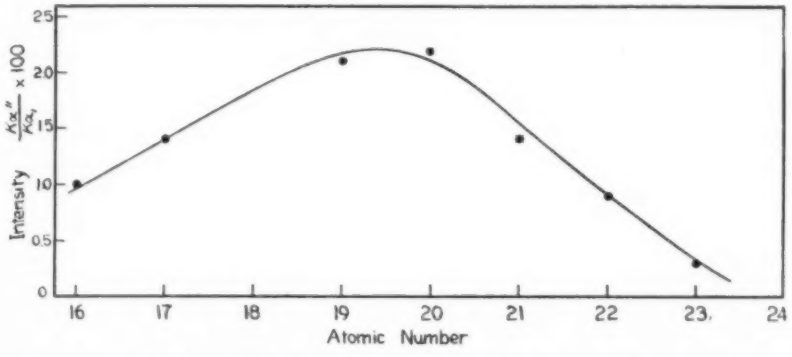


FIG. 3. Intensity of the $K\alpha''$ satellite line relative to the intensity of the $K\alpha_1$ line for elements S(16) to Cr(24). As mentioned in the text, these values are very sensitive to slight changes in the arbitrarily assumed shapes of the $\alpha_1$ lines: Whether or not this curve reaches a maximum point depends upon the shape one chooses to draw in each of the curves of Fig. 2.

### Wave-lengths

Measured from the peak of the $K\alpha_1$ line as a standard, the wave-length positions of the peaks of the $\alpha''$ lines, resolved as discussed above, are as given in Table I. Only differences in wave-length can be accurately measured with the writer's spectrometer, so the wave-lengths of the $\alpha_1$ lines used as references are included in the table. Surprisingly good agreement exists between the present $\alpha''$ wave-lengths and those given by Dolejšek for the edge of his "emission band."

### Excitation potential

As discussed in the previous paper[1] a knowledge of the minimum voltage required to produce a given satellite line is especially requisite in developing or in testing any theory of satellite origin. In the case of the $K\alpha''$ satellite, however, the two principal contemporary theories, the Wentzel-Druyvesteyn theory[14] and Richtmyer's "double-jump" theory,[17] predict the same excitation potential: The initial state of the atom emitting the $K\alpha''$ line is supposed in each case to be that of $KM$ ionization.

Fig. 4 shows ionization curves of Ca $K\alpha''$ recorded at various voltages. For these curves a consistency in the background is managed by superimposing the observed curves, matched in intensity at the $\alpha_1$ peak, on an assumed but *fixed* $\alpha_1$ shape. Consequently, the differences in the relative intensity which may be present with

[17] F. K. Richtmyer, J. Frank. Inst. **208**, 325 (1929).

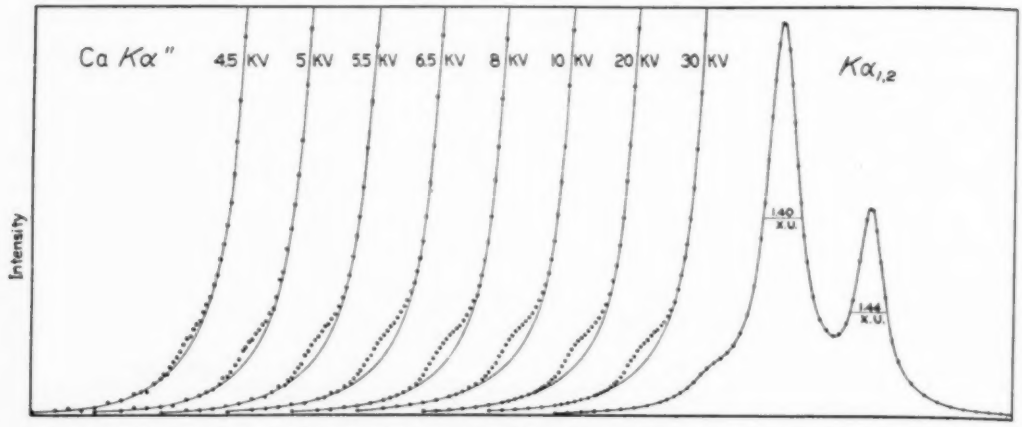


FIG. 4. Ionization curves of Ca $K\alpha''$ recorded at various tube voltages. A metallic calcium target was used. No *relative* uncertainty is present in the background of these curves as discussed in the text.

Although there is a very pronounced difference in the widths of the Ca $K\alpha_{1,2}$ lines observed from targets of metallic calcium and of CaO (Fig. 1), no difference in the $\alpha''$ satellite was observed greater than the observational error.

different tube voltages or tube currents can be measured without the background uncertainty mentioned above. In testing for a possible effect of chemical binding by using targets of calcium oxide and of metallic calcium the background uncertainty is again large because of the different $\alpha_1$ shapes. See the widths of $\alpha_1$ in Figs. 1 and 4.

The $\alpha''$ relative intensity was observed to be constant with tube current from 10 to 30 ma at 15 kv.

The $\alpha''$ relative intensity as a function of tube voltage is plotted in Fig. 5 and the data are listed in Table II. As the voltage decreases the curve of this figure definitely breaks at about twice the excitaton potential and exhibits the same general features as the voltage function for the intensity of the $K\alpha_{3,4}$ satellites, Fig. 2 of reference 1. This may be taken as evidence that $\alpha''$ is a satellite line. There can be no doubt that the excitation voltage is less than that which is required to produce a state of $KL$ ionization. This indicates, in view of the conclusions of the previous experiments,[1] that $\alpha''$ is not of the $\alpha_{3,4}$ group of satellites.

If one assumes that the curve of Fig. 5 should be similar in shape to the curve of the intensity of $\alpha_{3,4}$ *vs.* voltage,[1] one obtains, by the consequent extrapolation to zero intensity, the excitation voltage of $\alpha''$ as $4070\pm250$ volts. The energy required to remove a $K$ electron of atom $Z=20$ (calcium) is 4030 volts.[18] The energy required to

TABLE II. *The intensity of the Ca Kα'' satellite line relative to the intensity of the $K\alpha_1$ line as a function of the x-ray tube voltage.*

| VOLTAGE | CURRENT (ma) | RELATIVE INTENSITY $(\alpha''/\alpha_1)\times100$ |
|---|---|---|
| 4,500 | 115 | 0.80 |
| 5,000 | 89 | 1.50 |
| 5,500 | 88 | 1.90 |
| 6,500 | 65 | 2.15 |
| 8,000 | 57 | 2.30 |
| 10,000 | 46 | 2.18 |
| 15,000 | 22 | 2.30 |
| 20,000 | 15 | 2.20 |
| 30,000 | 12 | 2.25 |

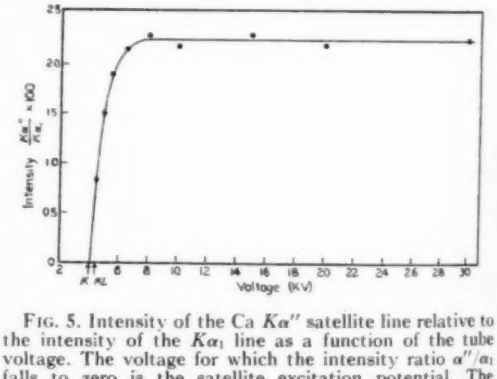


FIG. 5. Intensity of the Ca $K\alpha''$ satellite line relative to the intensity of the $K\alpha_1$ line as a function of the tube voltage. The voltage for which the intensity ratio $\alpha''/\alpha_1$ falls to zero is the satellite excitation potential. The voltage indicated by $K$, 4030 volts, is the excitation potential of the $K\alpha_{1,2}$ lines; that indicated by $KL$, 4440 volts, is the excitation potential of the $K\alpha_{3,4}$ satellites.

[18] M. Siegbahn, *Spektroskopie der Röntgenstrahlen*, second edition (Julius Springer, 1931), p. 348.

remove an $M_{II, III}$ electron of atom $Z=21$ (scandium) is approximately 37 volts. Then the energy requisite to producing a state of $KM$ ionization in the calcium atom is 4067 volts, in excellent agreement with the experimental value.

## III. Conclusions

From the excitation potential measurement we conclude that the initial state of the atom emitting the $K\alpha''$ satellite is one of $KM$ ionization, a conclusion which is in agreement with the Wentzel-Druyvesteyn theory and also with the Richtmyer theory for the origin of this satellite.

From the wave-length positions there is no choice between the theories. Druyvesteyn, using Dolejšek's wave-length measurements, has shown[14] that the $\Delta\nu$ interval between $\alpha''$ and $\alpha_1$ is of the same order of magnitude as the interval between the frequencies of the $M$ levels of atom $Z+1$ and of atom $Z$. On the basis of this evidence, Druyvesteyn ascribed, in accord with the Wentzel-Druyvesteyn theory, the origin of the $\alpha''$ line as due to the transition $KM \rightarrow LM$. In this region of atomic numbers the energy values of the $M$ shells are rather indefinite[18] and by "order of magnitude" must be meant a factor of possibly several-fold. Agreement of about the same order of magnitude is also obtained with Richtmyer's theory.

From the relative intensities, so far as theoretical predictions can be or have been made,[19, 20] there is likewise, as yet, no choice between the two theories.

### Acknowledgments

The author is indebted to Professor F. K. Richtmyer for his criticisms of the manuscript and to the University of Chicago for the loan of the double spectrometer with which the data of the present experiments were obtained.

[19] R. D. Richtmyer, Phys. Rev. **49**, 1 (1936).
[20] F. Block, Phys. Rev. **48**, 187 (1935).

---

APRIL 1, 1936 PHYSICAL REVIEW VOLUME 49

# Effect of Intense Illumination on Time Lag in Static Spark Breakdown

Harry J. White,* *University of California, Berkeley*

(Received February 5, 1936)

The time lag of spark breakdown in static uniform fields and with *intense* illumination of the cathode has been studied in air, helium and carbon dioxide. An electro-optical shutter was used to observe the time lag, while an auxiliary spark gap supplied the intense cathode illumination. In air, the time lag was about $10^{-7}$ second for overvoltages of a few percent and increased very rapidly with decreasing overvoltage. Increasing the overvoltage to above 30 or 40 percent reduced the time lag to a more or less constant value of 2 or $3\times10^{-8}$ second. This, in part, is shown to be due to the nature of the initiatory spark. The position of the midgap streamer observed in previous experiments has been found to depend on both the overvoltage and intensity of illumination. An explanation of these observations is advanced on the basis of space charge effects. The results in carbon dioxide were quite similar to those in air. In helium a much higher overvoltage was found necessary to produce a given time lag than in air. This is explained by considerations of the relative rates of gain of energy by electrons in the two gases.

## Introduction

THE time lag of spark breakdown in static fields has been studied in a thorough and systematic manner by Zuber[1] and Tilles[2] for lags from about 1 second to below $10^{-5}$ second. The effects of overvoltage and intensity of illumination of the cathode on the time lag were investigated. Time lags down to about $2\times10^{-7}$ second with low overvoltage and high illumination intensity have been observed by Snoddy.[3] Very short time lags of the order of magnitude of

* Now with Research Corporation, New York.
[1] K. Zuber, Ann. d. Physik **76**, 231 (1925).
[2] A. Tilles, Phys. Rev. **46**, 1015 (1934).
[3] L. Snoddy, Phys. Rev. **40**, 409 (1932).

$10^{-8}$ second have been observed by Pederson,[4] Tam,[5] Beams[6] and others, by using large overvoltages. None of the investigations of the very short lags has been quantitative, correlating the effects of overvoltage and intensity of illumination on the time lag. To this end the Kerr cell electro-optical shutter has been used to study these short lags and the results are being reported in this paper.

## Method and Apparatus

In the method used, the time lag of breakdown of a given gap is determined by measuring the time interval between the impulse which sets off the spark and the appearance of luminosity in the gap. The starting impulse is provided by a flash of ultraviolet radiation focused on the cathode of the gap and coming from a spark in an auxiliary gap. The elapsed time between the starting impulse and the appearance of luminosity is determined by using an electro-optical shutter which is focused on the gap being studied, but controlled by the potential across the auxiliary gap. Thus, the shutter closes at a definite time after a spark occurs in the auxiliary gap, and, by varying this open time until luminosity is just observed to appear, the time lag is determined.[7, 8, 9, 10]

A schematic diagram of the apparatus is shown in Fig. 1. $G_2$ is the gap for which the time lag is to be determined and $G_1$ is the auxiliary gap which illuminates $G_2$ and controls the closing time of the electro-optical shutter. The high voltage direct potentials are supplied by transformers with thermionic tube rectifiers and smoothing condensers of sufficient capacity to reduce the a.c. ripple voltages to negligible values. The electro-optical shutter is designated by E.O.S. and involves no unusual features.

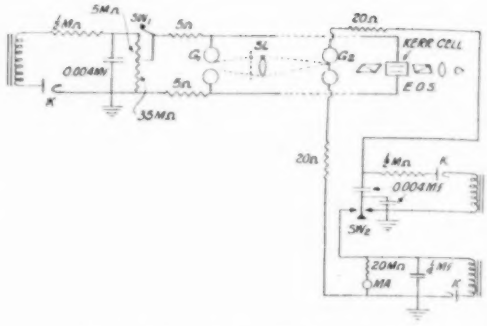


Fig. 1. Schematic diagram of apparatus.

The voltage supply for gap $G_2$ is divided into two sections for the purpose of applying an overvoltage of a definite and easily variable value. The upper section supplies a voltage approximately equal to the static sparking voltage of $G_2$, while the lower section supplies the overvoltage. The magnitude of the overvoltage is measured by means of a voltmeter consisting of an accurate 20 megohm-resistor and a milliammeter. The overvoltage is applied to $G_2$ by moving the switch SW2 from the right to the left contact. Gap $G_1$ is fired by closing switch SW1 which raises the voltage to a few percent above the sparking value. A quartz mercury arc is used to illuminate the cathode of $G_1$ in order to reduce the time lag to a small value. The switches are synchronized so that SW2 closes a few hundredths of a second ahead of SW1, thus enabling an essentially static voltage to be applied to gap $G_2$ without its sparking before being set off by gap $G_1$. To be sure that the switching operation did not affect the voltage supplied to $G_2$, tests were made for its sparking with zero overvoltage.

The procedure followed in making the measurements is as follows. The length of the leads to the Kerr cell is adjusted to a definite value and the voltage of the upper section of the supply for $G_2$ set at just the minimum sparking potential. Then gap $G_1$ is fired at intervals of about 10 seconds and the overvoltage on $G_2$ raised until luminosity is just seen to appear. Using this procedure the time lag was measured as a function of the overvoltage and intensity of illumination for

[4] P. O. Pedersen, Ann. d. Physik **71**, 317 (1923).
[5] R. Tam, Archiv. f. Elektrotechnik **19**, 235 (1928).
[6] J. W. Beams, J. Frank. Inst. **206**, 809 (1928).
[7] This assumes that the photoelectrons from the cathode are released instantaneously, and that the appearance of luminosity is simultaneous with the breakdown of the gap as marked by the rapid fall of the potential difference across it. The photoelectric effect has been shown to be instantaneous to within $3\times10^{-9}$ second by the work of Lawrence and Beams,[8] while observations by Dunnington[9] and the writer[10] show that luminosity first appears within about $2\times10^{-9}$ second after the beginning of breakdown.
[8] E. O. Lawrence and J. W. Beams, Phys. Rev. **32**, 478 (1928).
[9] F. G. Dunnington, Phys. Rev. **38**, 1535 (1931).
[10] H. J. White, Phys. Rev. **46**, 99 (1934).

several gap lengths in air at atmospheric pressure and also for helium and carbon dioxide.

## Data

The results obtained for air at atmospheric pressure and for gap lengths of 1 mm, 3 mm and 5 mm are shown in Fig. 2. The results for helium at a gap of 10 mm and for carbon dioxide at a gap of 5 mm are shown in Figs. 3 and 4, respectively. The curves for the three gap lengths in air are very similar. At overvoltages of several percent the time lags are of the order of magnitude of $10^{-7}$ second. Increasing the overvoltage causes the time lags to decrease rapidly at first, but to finally turn up sharply and approach a nearly constant value of 2 or $3\times10^{-8}$ second.

The effect of varying the cathode illumination intensity was noted by interposing wire screens between the two gaps which reduces the effective aperture of the quartz lens $L$ (Fig. 1). Decreasing the intensity resulted in increasing the time lag, the effect being much larger at low overvoltages. Thus, referring to Fig. 2 and the 3-mm gap, decreasing the intensity from 1 to 0.002 at 10 percent overvoltage increased the time lag from $68\times10^{-9}$ second to $130\times10^{-9}$ second, while at 30 percent overvoltage the corresponding increase was from $37\times10^{-9}$ second to $53\times10^{-9}$ second. Experimental difficulties prevented measurements being taken at higher values of overvoltage. However, from the trend of the curves it appears that decreasing the intensity at high overvoltages increases the time lag by a more or less constant amount.

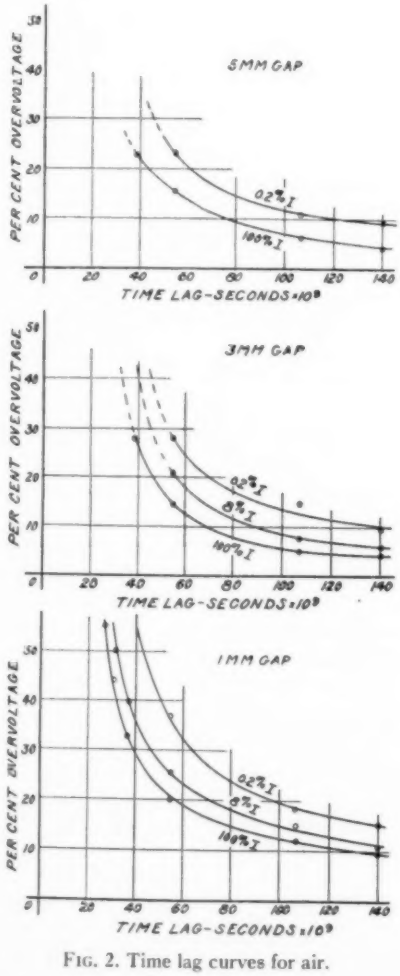


Fig. 2. Time lag curves for air.

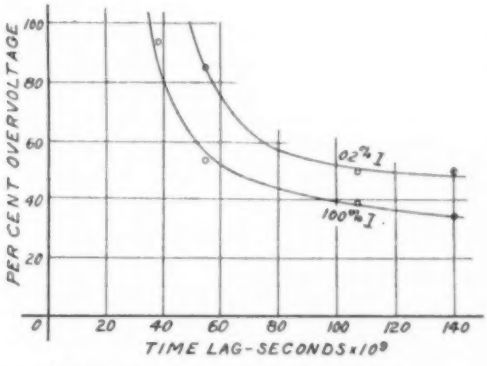


Fig. 3. Time lag curves for helium, 5-mm gap.

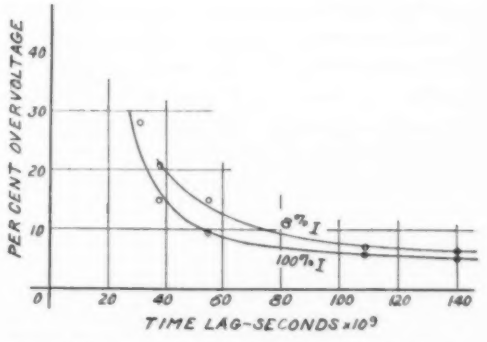


Fig. 4. Time lag curves for carbon dioxide, 5-mm gap.

The measurements show that the time lag is a function of overvoltage and intensity of illumination; also that time lags of the order of magnitude of $10^{-7}$ second occur in gaps of a few mm at low overvoltages but only provided very intense cathode illumination is used. Limitations of the apparatus prevented time lags of longer than $1.5\times10^{-7}$ second being measured, so that the curves could not be traced down to very small overvoltages. However, from the trends of the curves at low overvoltages, the time lag for voltages just above the minimum sparking potential[11] must be orders of magnitude larger than $10^{-7}$ second, and may possibly run continuously into the formative lags observed by Tilles.[2] It is of interest to extend the present measurements into the region of time lags observed by Tilles, and work in this direction is being undertaken by R. R. Wilson at the University of California.

From Fig. 3 it is seen that much higher overvoltages are required in helium than in air or carbon dioxide to produce approximately the same time lags. The significance of the curves for helium will be discussed in the theoretical interpretation of the results. No particular significance can be attached to the curves for carbon dioxide which are more or less analogous to those for air.

In the course of the present study it was found that the position of the midgap streamer[9, 10] which appears for long gaps is affected by both the overvoltage and the intensity of illumination of the cathode. Fig. 5 shows approximately how the location of this streamer varies with overvoltage for a 5-mm gap. As the gap voltage is raised above the minimum sparking potential, the streamer moves toward the anode and reaches the latter at an overvoltage of about 10 percent. Further increases in overvoltage cause the streamer to move back toward the midgap region. The position of the streamer for this latter range of overvoltage tended to be quite variable and at times even two parallel streamers would appear in the same breakdown. Increasing the intensity of illumination had the same effect on the position of the streamer as would be caused by increasing the overvoltage and *vice versa*.

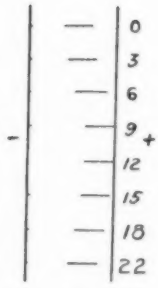


FIG. 5. Variation of the midgap streamer position with overvoltage. Percent overvoltage indicated at the right.

## DISCUSSION OF RESULTS

The short time lags observed can be explained on the basis of the theories proposed by Loeb[12] and by von Hippel and Franck[13] which were also developed by Schumann.[14, 15] According to these ideas the breakdown is precipitated by high fields being built up by space charge formation in the gap. The space charge is generated by electrons crossing the gap and producing by impact electrons, positive ions and also radiating molecules. The electrons, because of their relatively large drift velocity in the electric field, are removed from the gap before the positive ions move an appreciable distance. Thus a net positive charge is left in the gap, which, under favorable conditions, may give rise to fields large enough for positive ions to produce a sufficient number of secondary electrons at the cathode to cause breakdown to occur. The radiation from molecules excited by electron impact may also be important in releasing electrons from the cathode. In any event the elapsed time is about that required for an electron or perhaps several electrons to cross the gap, and is of the order of magnitude of $10^{-8}$ to $10^{-7}$ second for gaps of a few mm in air at atmospheric pressure.

[11] The overvoltages are calculated relative to the static sparking potential obtained with low intensity illumination, i.e., in terms of the ratio of the observed potential to the so-called normal sparking potential of the gap. Actually the real minimum sparking potential for a gap with this illumination is several percent lower than the normal sparking potential with weak light sources.

[12] L. B. Loeb, Science **69**, 509 (1929).
[13] A. von Hippel and J. Franck, Zeits. f. Physik **57**, 696 (1929).
[14] W. O. Schumann, Zeits. f. tech. Physik **11**, 131 (1930).
[15] J. J. Sämmer, Zeits. f. Physik **81**, 490 (1933).

In interpreting the results obtained, account must be taken of the nature of the flash of illumination which was used to illuminate the cathode. The distribution of its intensity with time is not definitely known. Photographs of sparks taken by Snoddy[9] with a rotating mirror under somewhat similar conditions show that the intensity rises to a large value in a few times $10^{-7}$ second and then dies out after several microseconds. Observations by Dunnington[9] and the writer[10] show that an appreciable fraction of the maximum intensity is attained in a few times $10^{-8}$ second. The photo-charge released from the cathode by a single flash of the illuminating spark at maximum intensity was measured and found to be about $10^7$ electrons. This is sufficiently large to make it probable that at least several photoelectrons were emitted during the first $10^{-8}$ second, a time equal to about 1/500 of the total duration of the flash.

The time lags measured lie in the period during which the illuminating spark intensity was rapidly increasing. Hence one must consider the rapid variation of photoemission with time in discussing the significance of the time lag-overvoltage curves. The rapidly increasing intensity of the illumination probably had a large effect on the shapes of the time lag curves. Thus, if the breakdown is due to the formation of space charge in the gap, and if the distribution of the space charge does not change appreciably, the condition for a spark to occur in a given gap is that a certain amount of charge, say $q$, be generated. Then

$$q/e = \text{No. of positive ions or electrons produced} = \sum_{1}^{N_0} \epsilon \int_0^d \alpha dx \Delta N_0,$$

where $\alpha$ = Townsend coefficient for impact ionization by electrons,
$d$ = Gap length,
$N_0$ = No. of photoelectrons effective in producing the spark.

The integral $\int_0^d \alpha dx$ is a function of the amount of space charge already generated and hence must be evaluated for each photoelectron, the latter being designated as $\Delta N_0$ in the above sum.

The space charge generated in a given gap thus depends essentially on $\alpha$ and $N_0$. Decreasing the time lag also decreases $N_0$ because of the smaller integrated light intensity of the initiatory spark. To compensate for this decrease, the value of $\alpha$, and therefore the gap voltage, must be increased somewhat. At least a part of the gap voltage increment required to reduce the time lag by a given amount is needed to compensate for the correspondingly smaller number of photoelectrons. Hence the rapidly increasing intensity of the illuminating spark doubtless accounts in a large measure for the rapid decrease in overvoltage at the longer intervals. The shortest time lags observed of 2 or $3\times10^{-8}$ second may be due to entirely inadequate illumination intensities produced by shortening the initiating spark. They may also be caused by the fact that at these time intervals the electrons are unable to cross the whole gap and therefore, in view of the shortened distance taken, the overvoltage must be increased to make the ionization more effective. The mobility of electrons in these high fields is uncertain by a factor of 3 or 4, but at least in order of magnitude the transit time of electrons across gaps of a few mm corresponds to the shortest time lags observed of 2 or $3\times10^{-8}$ second.

The space charge generated by a single electron crossing a gap under the high fields corresponding to the shortest time lags observed is significant in this connection for if, under these gap conditions, the breakdown is initiated by the first few photoelectrons, the space charge field generated by them must be large enough to cause the spark to occur. As an example consider the 3-mm gap at 50 percent overvoltage for which $X/p=73$. The value of $\alpha$ for $X/p=73$ is from Sanders'[16] data 200, and neglecting space charge distortion, $\int_0^d \alpha dx = \alpha d = 200\times0.3 = 60$. From this, the number of positive ions generated by one photoelectron in crossing the gap would be $\epsilon^{\alpha d} = \epsilon^{60}$, and the corresponding charge expressed in e.s.u., is

$$q = 4.8\times10^{-10}\times e^{60} = 4.8\times10^{-10}\times10^{26} \leqq 5\times10^{16}.$$

Such an enormous space charge could not be generated under the existing conditions and this must mean that the photoelectron traverses only a fraction of the gap before building up a large space charge. Thus, assuming that the spark is initiated by space charge effects, the breakdown

[16] F. Sanders, Phys. Rev. **44**, 1020 (1933).

under these conditions probably will start before the first photoelectron has crossed the gap. Increasing the gap voltage will reduce the time lag somewhat, but the limiting lag will be determined by the initiatory photoelectric emission.

The space charge hypothesis provides a plausible explanation for the appearance and changes in position of the central streamer as observed in Fig. 5. The point or points at which the breakdown begins in a gap will be determined by the location of the space charge in the gap. For gaps with relatively weak fields it is possible that the space charge is set up through the migration of positive ions or the passage of successive electron avalanches in such a way as to concentrate the field at the cathode for short gaps and out in the gap itself for longer gaps. As the field is increased, fewer photoelectrons will be needed to produce the intense field and the field produced becomes more a field due to the ionization by a single electron avalanche. As this process takes place with increasing field strength, the enormously enhanced ionization along a single electron path as the electron approaches the anode will tend to concentrate the positive space charge at first near the anode, and, with increased field strength, back toward the midgap region. With an intense positive space charge in the midgap region the gradient which will be most effective will be located there and while some gradient exists at the cathode, the gradient in the midgap region is sufficient to produce a beginning spark there. When visible streamers appear, they appear simultaneously at the cathode and midgap for long gaps, and within 2 or $3\times10^{-9}$ second. In short gaps the midgap streamer probably cannot be formed because the breakdown gradient will always occur first at the cathode.[17]

From the variation of overvoltage and time lag with illumination over the whole range investigated the following may be said. For time lags in the neighborhood of $10^{-7}$ second, the illuminating spark has had time to become rather bright, so that the number of photoelectrons released is large. Referring to our previous equation a very approximate condition for breakdown in a given gap is that $q$ be constant. Decreasing the illumination intensity means that the value of $\alpha$, and therefore the gap voltage, must be increased in order to keep the time lag constant. On the other hand, for very large overvoltages, the time lag is very small and only a few photoelectrons or even one are necessary to produce a breakdown. The illuminating spark intensity increases from zero at zero time lag, and an average time of several billionths of a second elapses before the several photoelectrons necessary to produce breakdown are emitted. Now decreasing the intensity will result in increasing this average time, and the time lag will be increased by just this amount. Increasing the overvoltage cannot compensate for decreasing the intensity in this region, for the condition for breakdown is that only a few, possibly one, photoelectrons appear in the gap. This is in contrast to the situation existing for the longer time lags where a decrease in the intensity can be compensated for by increasing the overvoltage.

The curves for helium are similar to those for air except that a much higher overvoltage is necessary to produce a given time lag of breakdown. The relatively large overvoltage necessary can be explained on the basis that ionization by electron impact occurs at low field strengths in helium, and at these field strengths is so inefficient that it is necessary in relatively shorter gaps to increase $\alpha$ materially in order to produce the ionization necessary for a spark. Thus, for example, Werner[18] finds that the ionizing zone in the positive corona discharge in helium comprises at least 500 free paths with a potential drop of about 200 volts, while in nitrogen about 460 volts are required and only 70 free paths. This means that the rate of gain of energy is relatively small in the low fields in helium, while in the relatively large fields in nitrogen it is large.

The writer is very much indebted to Professor L. B. Loeb for his interest in the writing of this paper and for his help in interpreting the experimental results. He also wishes to thank Dr. R. N. Varney for valuable criticism of the manuscript.

[17] The field in the neighborhood of the cathode surface is enhanced by the image of the positive space charge in the cathode. This will have a large effect in increasing the field there only if the space charge is relatively close to the cathode, as it must be in the shorter gaps.

[18] S. Werner, Zeits. f. Physik **90**, 384 (1934).

# On the Mean Lifetime of Metastable Neon Atoms*

EUGENE W. PIKE, *Scott Paper Co., Chester, Pennsylvania*

(Received February 1, 1936)

Penning has shown that illumination of the Townsend discharge in neon with red light from an auxiliary neon arc reduces the number of excited atoms in the former. The concentration of excited atoms in the Townsend discharge as a function of illumination intensity can be computed from the electronic properties of neon; a comparison with Penning's direct measurements evaluates the mean lifetimes of both the metastable and the resonance states in the gas. The numerical results for 36 mm pressure are: mean lifetime in sec. of the $^3P_2$ metastable state $=2\times10^{-3}/p$; of the $2^3P_1$ resonance state $=4\times10^{-5}/p$, where $p$ is the pressure in mm Hg. Values for the mean lifetime of the $2^3P_2$ state derived by Zemansky's method from absorption measurements at about 3 mm Hg pressure are: $9\times10^{-4}/p$ from Meissner and Graffunder's measurements, and $8\times10^{-3}/p$ from Dorgelo and Washington.

THE problem of the mean lifetimes of metastable atoms in neon, while less important fundamentally than it once was thought to be, is still of great moment in the detailed mechanism of electrical conduction in gases. Up to the present all the experimental work has been done with the absorption method,[1] most of it before the true complexity of the problem was known. For this reason it seems valuable to point out a second independent method confirming the previous results approximately, especially since the argument contributes appreciably to the mechanism of discharges.

In a Townsend discharge in neon, excited atoms in both the metastable and the resonance states are generated in numbers comparable to the number of ions formed.[2] The atoms in the resonance state rapidly radiate their energy out of the gas, but the longer-lived metastable atoms accumulate to a high concentration.[3] If the discharge is illuminated with red light from an auxiliary discharge in neon, some of these metastable atoms are raised to the 18.5-volt levels (Paschen's $p$ levels) by absorption, and a certain fraction of these latter go down to the resonance states, instead of returning to the metastable states. The resulting decrease in metastable atom concentration can be measured directly,[1a] or by using a trace of some second gas such as argon as an indicator;[4] it can also be computed from the known electronic properties of neon, using the mean lifetimes as adjustable parameters. A comparison provides a numerical value for the mean lifetimes of both the metastable and the resonance states.[5]

The equilibrium conditions for the metastable and resonance atom concentrations are simply formulated. Let the subscripts $_r$ and $_s$ refer to the resonance and metastable states, respectively; let $E$ be the total number of excited atoms generated by the discharge per cc per sec., and $n$ be the concentration of excited atoms;[6] let $\beta$ be the reciprocal of the mean lifetime $\alpha$, $L$ be the illumination intensity in arbitrary units, $2q$ be the probability that an excited atom will absorb a quantum from radiation of unit intensity in 1 sec., and $b$ the probability that this atom will return to the opposite type of lower state, i.e., *from* a metastable and *to* a resonance state, or *vice versa*. Writing the rate of generation on the left

$$aE+2b_sq_sLn_s=n_r(\beta_r+2b_rq_rL),$$
$$(1-a)E+2b_rq_rLn_r=n_s(\beta_s+2b_sq_sL). \quad (1)$$

* Presented at the Washington Meeting of the American Physical Society, April 27th, 1935. This work was done at Palmer Laboratory, Princeton, N. J. in 1934.

[1] (a) K. Meissner and W. Graffunder, Ann. d. Physik **84**, 1038 (1927); (b) H. B. Dorgelo and T. P. K. Washington, Proc. Roy. Acad. Sci. Amst. **30**, 37 (1927).

[2] Cf. J. S. Townsend and S. P. McCallum, Proc. Roy. Soc. **A124**, 543 (1929); F. M. Penning and M. C. Teves, Physica **9**, 97 (1929).

[3] Cf. W. de Groot, Naturwiss. **14**, 104 (1926).

[4] F. M. Penning, (a) Zeits. f. Physik **46**, 335 (1928); (b) ibid. **57**, 723 (1929).

[5] By *mean lifetime* is meant here the concentration divided by the rate of generation; if energy of excitation is transferred from atom to atom in the gas by radiation or by collisions of the second kind, then the mean lifetime is the lifetime of the excitation energy, equal to the sum of the lifetimes of all the atoms excited by this energy as it traverses the gas.

[6] Both $E$ and $n$ are functions of position in the discharge. At pressures sufficiently high that diffusion is small, the relation between $E$ and $n$ will be true for any volume element in the discharge; since $n$ is proportional to $E$ (*vide* Eq. (2)), the relations developed below may be summed over the discharge as a whole.

It has been shown[7] that slow electrons excite neon to the 18.5-volt levels only, rather than to the 16.5-volt levels. Because of this, $a$ can be determined from Dorgelo and de Groot's[8] photometry of the light from neon excited by a 22-volt electron beam (a sufficiently close approximation to the Townsend discharge) by a simple summation of the line intensities to the various lower states, giving $a=0.7$. The excitation was sufficiently weak that the error arising from the re-absorption of the lines is second order. Because the $^3P_0$ state disappears from the gas so rapidly, the line intensity to it was divided equally between the metastable and resonance states.

The "branching ratios" can be determined, less accurately, from Dorgelo and de Groot's[8] photometry of the light ("Rezonanzlicht") re-emitted from a Townsend discharge irradiated by a strong beam of red light from an auxiliary neon arc. To within the error of measurement, $b_r=b_s=\frac{1}{2}$. This ratio is probably dependent on the pressure and the illumination intensity, but experimentally the $\alpha$'s are insensitive to variations in $b$ or $(q_r/q_s)$.

The quantity $q$ is proportional to $\Sigma_p B_{sp} L_{ps}$,[9] where the $B$'s are the Einstein coefficients, and the $L$'s are the line intensities in emission from a positive column in neon; the sum is over all lines from the lower state in question, with the exception of the lines 5852, 6074, and 6402, whose upper states connect with only a single lower state.[10] The $L$ values are given by Dorgelo and de Groot,[8] and the $B$'s are related to the $A$ coefficients measured by Ladenburg, Kopfermann, and Levy[11] as $B_{sp}=(g_p/g_s)(\lambda_{ps}^3/8\pi h)A_{ps}$. The sums for the two resonance states $^1P_1$ and $^3P_1$ are 1655 and 1310, respectively; for the metastable $^3P_0$ and $^3P_2$ states, 790 and 680. Within the accuracy required here, $q_r=2q_s$. Implicit in this calculation is the assumption that the relation between the emission and absorption contours is the same on the average for both types of states, probably a safe assumption here.

Introducing these values into Eq. (1) and solving

$$n_r=E(q_sL+0.7\beta_s)/[\beta_s\beta_r+q_sL(\beta_r+2\beta_s)],$$
$$n_s=E(2q_sL+0.3\beta_r)/[\beta_r\beta_s+q_sL(\beta_r+2\beta_s)]. \quad (2)$$

Since the comparison with experiment is made at constant field in the discharge, $E$ is constant, and we may write $(n_r+n_s)=n_L$, $n_{L(L=0)}=n_0$, $(q_sL/\beta_s)=I$, $(\beta_r/\beta_s)=k$, and solve for

$$(n_L/n_0)=[1+3I/(0.7+0.3k)]/[1+I(2+k)/k]. \quad (3)$$

If a trace of a second gas such as argon is added to a *self-maintaining* Townsend discharge in neon, the potential $V_T$ across the discharge is greatly reduced, since the excited neon atoms ionize the argon atoms by collisions of the second kind.[4a] If the conditions are otherwise constant and the argon concentration is very small, one may safely assume that $V_T$ is a function of the product of the excited atom and argon concentrations. Penning[12] has measured $V_T$ in a neon-xenon mixture at 35.5 mm Hg pressure as a function of the illumination intensity and the xenon concentration $\nu$; for a series of points at constant $V_T$, $n_L\nu_L=n_0\nu_0$, or $(n_L/n_0)=(\nu_0/\nu_L)$. Fig. 1 shows the curve of $(n_L/n_0)$ *vs.* $L$ derived in this way.

By proper adjustment of $k$ and $q_s\alpha_s$ this curve may be fitted over its entire length by Eq. (3). The appropriate values of the constants are $k=50$, $q_s\alpha_s=0.27$. To show the sensitivity of the method, two other sets of points for nearby values of the constants are plotted. Clearly, $q_s\alpha_s$ can be determined to a few percent, while $k$ can be found to about twenty percent. Eq. (3) may also be written in terms of $q_r\alpha_r$; the best fit in this case is given by $k=50$, $q_r\alpha_r=0.01$, or $q_s\alpha_s=0.25$. If one sets $q_r=q_s$, instead of $q_r=2q_s$, then the best fit results from $k=30$, $q_s\alpha_s=0.28$.

Penning[4b] has estimated $q_s$ by an extension of the method used above to compute $(q_r/q_s)$, using the theoretical emission and absorption contours experimentally confirmed by Ladenburg and Levy,[8] and Dorgelo's measures of the efficiency of the neon positive column. His result,

[7] F. M. Penning, Zeits. f. Physik **41**, 769 (1926); M. J. Druyvesteyn, ibid. **64**, 781 (1930); **73**, 33 (1931).

[8] H. B. Dorgelo and W. de Groot, Zeits. f. Physik **36**, 897 (1926).

[9] The subscripts $_p$ and $_s$ refer to the 18.5-volt and the 16.5-volt levels, respectively.

[10] These lines were also omitted in the determination of $b$.

[11] Cf. R. Ladenburg, Rev. Mod. Phys. **5**, 248 (1933); Zeits. f. Physik **65**, 189 (1930).

[12] F. M. Penning, Physica **12**, 66 (1932).

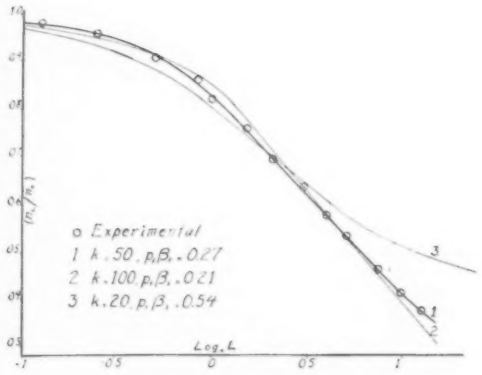


FIG. 1.

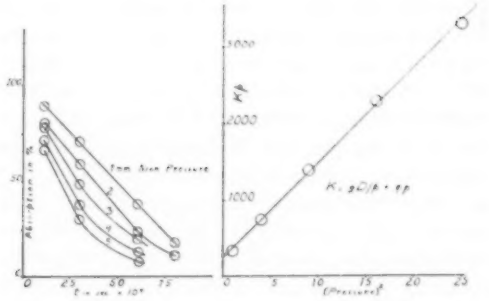

a b

FIG. 2. Reduction of absorption data from Dorgelo and Washington.

$q_s \approx 0.5 \times 10^4$ in the units of reference 12, may be in error by a factor of two; combined with our value of $q_s \alpha_s$, $\alpha_s \approx 6 \times 10^{-5}$ sec.

To complete the determinations of $\alpha$, the writer has reduced the observations of Dorgelo and Washington[11b] by the method given in detail by Zemansky.[13] Fig. 2a, plotted from their data, shows that the linear absorption *vs.* time relation predicted by Zemansky is actually fulfilled; Fig. 2b shows that $K$, the exponential decay constant for the metastable atoms in the absorption cell, is described accurately by an equation of the form $K = gD/p + \varphi p$, where $p$ is the pressure. The significance is familiar—the $gD$ term represents the loss of metastable atoms to the walls by diffusion, the $\varphi$ term arises from destruction of the metastable atoms in the gas by collision with normal atoms. The numerical values are: $\alpha = 1/\varphi p = 8 \times 10^{-3}/p$, diffusion constant $D = 220$. The values derived by Zemansky from the observations of Meissner and Graffunder[11a] are: $\alpha = 9 \times 10^{-4}/p$, $D = 470$. (The diffusion constant of normal neon is 260.)

Using these values of $D$, the loss to the walls in Penning's discharge is negligible, so that $\alpha_s$ is directly comparable with $1/\varphi$, or $\alpha = 2 \times 10^{-3}/p$, in satisfactory agreement with the absorption values. Since practically all the errors in the absorption method increase the apparent decay constant, the most probable value of $\alpha$ is in the neighborhood of $10^{-2}/p$ sec. mm$^{-1}$ Hg.

It is hoped to discuss the mechanism behind $\alpha$ in a later paper.

[13] A. C. G. Mitchell and M. W. Zemansky, *Resonance Radiation and Excited Atoms* (Cambridge Univ. Press, 1934), p. 249 ff.

APRIL 1, 1936 · PHYSICAL REVIEW VOLUME 49

# Penning's "New Photo-Effect" in Pure Neon*

EUGENE W. PIKE, *Scott Paper Company, Chester, Pennsylvania*

(Received February 1, 1936)

The maintaining voltage of a Townsend discharge in pure neon was measured as a function of the illumination of the discharge with light from a neon arc, using a more sensitive circuit than that of Penning. In contrast to the Townsend discharge in slightly impure gas, in pure gas it is almost insensitive to illumination over a wide range of pressure, current, tube geometry and cathode material. With progressive cleaning of the gas, the change in maintaining voltage due to illumination passed from a small positive value through zero to a small negative value. The general equations of the discharge are developed, but a complete identification of the active atomic processes is not yet possible.

* Abridged from a thesis presented to the Faculty of Princeton University in candidacy for the degree of Doctor of Philosophy. The work was done at Palmer Laboratory, Princeton, N. J., in 1934.

FROM experiments on the response of the Townsend discharge[1] in neon containing traces of a second gas such as argon to illumination with visible light from an intense auxiliary discharge in neon, Penning[2] has shown definitely that such illumination displaces the equilibrium between metastable atoms and resonance radiation in the discharge in favor of the latter, resulting in a net decrease in the concentration of excited atoms in the discharge.[3] One would expect such a displacement to affect the maintaining voltage of the discharge in pure gas, but extrapolation of Penning's curves to zero impurity (a matter of a few parts per million) indicates that this is not the case. The author undertook to measure the effects of this displacement in the purest possible neon, in the hope of setting upper limits to the efficiencies of various atomic processes.

## I. Experimental

A number of tubes, differing in unessential details, were used in the preliminary work. All had plane cathodes, all but one had plane parallel anodes. The odd tube had a grid of fine wire in a plane parallel to the cathode. A variety of cathode materials were used—iron, nickel, platinum, copper, Monel metal and platinum with a molecular layer of sodium. The ratio cathode diameter/electrode spacing varied from three to ten, and the pressure from 2 to 40 mm Hg.

Fig. 1 shows tube *H*, the final form with which most of the data were taken. This tube was pumped on a fast, all-Pyrex system by standard high vacuum procedure; the residual pressure after sealing off was in the order of $10^{-6}$ mm Hg. It was then reconnected to a gas-handling system through a fragile internal seal which was broken by a magnetic plunger after evacuation of the system, and pure neon introduced through a fine leak and a charcoal trap in liquid air. After again sealing off the neon was cleaned for about ten days by passing about $\frac{1}{4}$ ampere between the misch metal in *F* as cathode and *A* as anode.[4] It

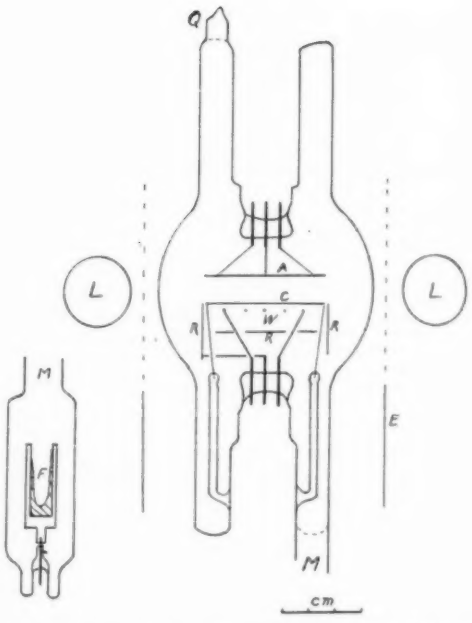


FIG. 1. Diagram of tube used in obtaining data. *A*, anode; *C*, cathode; *W*, tungsten heater filament; *R*, reflecting shields; *Q*, seal-off; *M*, side tube to misch metal; *F*, misch metal in iron cup; *L*, positive column discharge in neon; *E*, electrostatic shielding.

was not possible to measure the final residual pressure of impurity, but aside from innocuous helium it was certainly less than $10^{-6}$ mm Hg. During observations the pressure could be adjusted by withdrawing gas through a second internal seal and about 30 cm of 1 mm capillary tubing immersed in liquid air.

The electrical circuit finally adopted is shown in Fig. 2. This arrangement made it possible to follow major changes in $V_T$, the potential across the discharge, and still measure to 0.1 volt the smaller changes ($\Delta V_T$) due to illumination. Observations of $\Delta V_T$ were made with the current in *L* alternately 1 amp and 0.01 amp, using *Q* as a deflection instrument.

The experimental results may be summarized as follows:

(a) After normal cleaning, $\Delta V_T$ came to a constant value of one to two volts positive (i.e., illumination increased $V_T$). This value was quite reproducible from tube to tube, and stable against further cleaning with misch metal. After one especially thorough pumping of tube H, however, removal of residual argon and mercury by immersion of a side tube

[1] Used here to denote a space-charge-free, self-maintaining, cold-cathode discharge.
[2] F. M. Penning, Phil. Mag. **11**, 961 (1931); Zeits. f. Physik **57**, 723 (1929).
[3] Cf. E. W. Pike, Phys. Rev., this issue.
[4] Cf. C. C. Van Voorhis *et al*, Rev. Sci. Inst. **5**, 367 (1934).

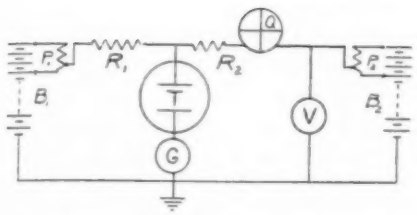


FIG. 2. Electrical circuit. $B_1$, $B_2$, 600-volt batteries; $P_1$, $P_2$, 6000-ohm potentiometers; $T$, Townsend discharge tube; $G$, galvanometer, $10^8$-ohm sensitivity; $Q$, quadrant electrometer, sensitivity 4 mm volt; $V$, 0–750-voltmeter; $R_1$, $1.2\times10^8$-ohm stabilizing resistor; $R_2$, $3\times10^7$-ohm damping resistor.

in liquid air reduced $\Delta V_T$ to zero and eventually brought it about half a volt negative. The conditions were: oxidized tungsten cathode, 28 mm Hg pressure, 25°C, electrode spacing 9 mm, electrode diameter 30 mm, $V_T$: 525v. This negative value of $\Delta V_T$ was observed earlier in one other tube, but because it was falsely ascribed to leakage currents the conditions were not recorded.

(b) $\Delta V_T$ is independent of the pressure over a wide range. Table I presents the best run on the variation of $\Delta V_T$ with pressure, made with tube H.

TABLE I. *Variation $\Delta V_T$ of the potential across the discharge produced by illumination vs. the pressure.*

| PRESSURE (mm Hg) | $V_T$ | $\Delta V_T$ | PRESSURE | $V_T$ | $\Delta V_T$ |
|---|---|---|---|---|---|
| 20 | 430 | +0.5 | 3.8 | 325 | +1.0 |
| 7.7 | 350 | +1.0 | 3.0 | 328 | +1.0 |
| 5.0 | 330 | +1.0 | 1.8 | 345 | +0.9 |

(c) $\Delta V_T$ is independent of the cathode material and the electrode geometry within the limits described above.

(d) $V_T$ is independent of the current density between at least $3\times10^{-8}$ amp./cm² and $3\times10^{-7}$ amp./cm². $\Delta V_T$ is independent of the current density over a considerably wider range.

All measurements were taken on the flat portion of the $V_T$-current curve.

## II. THEORY

The electron current passing through the neon creates by impact ions, and as well atoms excited to both the resonance and the metastable **s** states. Since all three of these are sufficiently energetic in neon to release secondary electrons from the cathode, the equation for the electron balance there must be modified to include them. Under the conditions of the experiment, all ions are drawn to the cathode. The energy represented by the atoms excited to the resonance state diffuses by rapid alternation between radiation and excited atoms; it crosses any plane in the gas primarily as radiation, and the fraction which is intercepted by the cathode releases photoelectrons. Some of the metastable atoms diffuse as such to the walls and the electrodes, but the major part are destroyed in the gas, their energy converted to radiation by impact of normal atoms in a process not yet fully understood; the cathode will intercept a fraction of both the diffusing metastables and the radiation.

Taking these processes in order the total number of secondary electrons emitted, assuming infinite parallel plane electrodes and reducing to the basis of a single isolated electron leaving the cathode,[5] is

$$\psi(e^{\alpha d}-1)+\psi'\lambda f'(e^{\alpha d}-1)+\psi'' S_0 + t\psi'[f''(e^{\alpha d}-1)-S_0-S_1]=1, \quad (1)$$

where the symbols have the following meanings:

$\psi$—Coefficient of secondary emission under ion impact, corrected for back-diffusion.[6]

$d$—Electrode separation.

$\alpha$—Townsend coefficient; the probability that an electron will form an ion by impact while moving a distance **dx** along the field is $\alpha$ **dx**. The bracket is the total number of ions formed.

$\psi'$—Photoelectric efficiency of resonance radiation, also corrected for back diffusion.

$f'\alpha$—Cognate to $\alpha$, for excitation to the resonance state.

$\lambda$—The fraction of the energy expended in excitations to the resonance state which is intercepted by the cathode.

$\psi''$—Coefficient of secondary electron emission from the cathode for metastable atom impact.

$S_0$, $S_1$—The number of metastable atoms diffusing as such to the cathode and to the anode (and walls), respectively.

$f''\alpha$—Cognate to $\alpha$, for excitation to the metastable state.

$t\psi'$—Corresponds to $\lambda\psi'$, for the radiation resulting from destruction of metastable atoms in the gas. The ratio of the photoelectric efficiencies between this radiation and true resonance radiation is absorbed in the factor **t**.

No account has been taken of ionization in the gas by ion impact, since under the conditions of the experiment the energy available from the field per ion free path is less than 0.1 volt.

[5] This reduction is possible because all processes in the discharge are linear in the current. (Cf. Paragraph d), Part I.

[6] I. Langmuir, Phys. Rev. **38**, 1656 (1931); C. Kenty, Phys. Rev. **44**, 894 (1933).

The left-hand side of (1) must necessarily equal unity if the discharge is to be stable, since each electron leaving the cathode must on the average just replace itself.

External illumination transfers some of the metastable atoms to the resonance state;[3] the energy intercepted by the cathode is similarly redistributed. In consequence, $V_T$ changes to $(V_T+\Delta V_T)$, and $\alpha$ to $(\alpha+\Delta\alpha)$. The equation for electron balance at the cathode now is

$$\psi(e^{(\alpha+\Delta\alpha)d}-1)+\psi'\lambda f'(e^{(\alpha+\Delta\alpha)d}-1)+\psi''S_0^+ +[\beta/(\beta+\beta')]t\psi'[f''(e^{(\alpha+\Delta\alpha)d}-1)-(S_0^++S_1^+)] +[\beta'/(\beta+\beta')]s\psi'[f''(e^{(\alpha+\Delta\alpha)d}-1) -(S_0^++S_1^+)]=1, \quad (2)$$

where the new symbols are:

$S_0^+$, $S_1^+$ — Correspond to $S_0$, $S_1$, corrected for the effect of the external illumination.

$\beta$, $\beta'$ — These are the relative probabilities of destruction of metastable atoms by normal atom impact and action of the external illumination, respectively; i.e., a metastable atom has a probability $\beta\mathbf{dt}$ of being transferred to the normal state by impact of a normal atom in time **dt**.

$s$ — The fraction absorbed by the cathode from the resonance radiation created by the external illumination from metastable atoms.

Subtracting (1) from (2), and setting

$$e^{\alpha}(1+\Delta\alpha)\approx e^{(\alpha+\Delta\alpha)},$$

$$[(\psi+\psi'\lambda f'+\psi' tf'')e^{\alpha d}]\Delta\alpha d +t\psi'[(S_0+S_1)-(S_0^++S_1^+)] -\psi''(S_0-S_0^+)+[\psi'(s-t)\beta'/(\beta+\beta')] \times[f''(e^{(\alpha+\Delta\alpha)d}-1)-(S_0^++S_1^+)]=0.$$

By comparison with (1), the first bracket is very nearly unity. With similar approximations,

$$\Delta\alpha d=\psi''(S_0-S_0^+)-t\psi'[(S_0+S_1)-(S_0^++S_1^+)] -[\psi'(s-t)\beta'/(\beta+\beta')][f''e^{\alpha d}-(S_0^++S_1^+)]. \quad (3)$$

## III. Discussion

The chief interest of Eq. (3) lies in the possibility which it offers of determining $\psi''$, $t$, and $(s-t)$,[7] all at present unknown. The evaluation of these quantities involves accurate values of $\psi'$ and the $S$'s, however, which are at present unobtainable. Kenty[8] has measured the photoelectric efficiency of an oxidized tungsten surface for neon resonance radiation, finding a value 0.03, but substitution of the data from Section II (a) into Eq. (1) gives an upper limit of 0.005 for $\psi'$, so that the unknown correction for back diffusion is evidently all-important. Similarly, the values of the $S$'s depend on $\beta$ and on the diffusion constant of metastable neon atoms in normal neon,[9] and the present uncertainty in these latter allows a range of over 100 to one in the former. The remainder of the constants are fairly accurately known.[10]

To obtain an upper limit of $(s-t)$ from Eq. (3) one must set a lower limit to $\psi'$; until further experimental values are obtainable this application of the theory must be deferred.

One might note in passing that the experimental work above documents an excellent method for detecting and measuring traces of impurities in neon and helium.

In conclusion, it is a pleasure to thank Professor G. P. Harnwell for his generous supervision of this work, and to acknowledge stimulating discussions with Professor R. Seeliger, of the University of Greifswald, and with Dr. C. Kenty.

---

[7] A knowledge of $(s-t)$ should throw light on the mechanism which returns metastable neon atoms to the normal state by collision with normal atoms, since $s$ is certainly based on the motion of resonance radiation in the gas, and $t$ on the motion of whatever kind of radiation it is which carries off the energy of the metastable atom. The currently accepted theory, i.e., that the metastable atoms are raised to the resonance level by collisions of the first kind with normal atoms, is in conflict with some observations of Found and Langmuir, and possibly also with the theory of molecular structure. It is hoped to discuss this fully in a later paper.

[8] C. Kenty, Phys. Rev. **44**, 891 (1934).

[9] Cf. E. W. Pike, Phys. Rev. **40**, 314 (1932).

[10] $\alpha$, J. S. Townsend and S. P. McCallum, Phil. Mag. **8**, 657 (1928); $(f'+f'')$ J. S. Townsend and S. P. McCallum, Proc. Roy. Soc. **A124**, 543 (1929); F. M. Penning and M. C. Teves, Physica **9**, 97 (1929); $f'/f''$ cf. reference 3, section on $a$. $\beta/\beta'$ F. M. Penning, Physica **12**, 66 (1932) and reference 3.

# Capture of Slow Neutrons

G. Breit and E. Wigner, *Institute for Advanced Study and Princeton University*

(Received February 15, 1936)

Current theories of the large cross sections of slow neutrons are contradicted by frequent absence of strong scattering in good absorbers as well as the existence of resonance bands. These facts can be accounted for by supposing that in addition to the usual effect there exist transitions to virtual excitation states of the nucleus in which not only the captured neutron but, in addition to this, one of the particles of the original nucleus is in an excited state. Radiation damping due to the emission of $\gamma$-rays broadens the resonance and reduces scattering in comparison with absorption by a large factor. Interaction with the nucleus is most probable through the $s$ part of the incident wave. The higher the resonance region, the smaller will be the absorption. For a resonance region at 50 volts the cross section at resonance may be as high as $10^{-19}$ cm$^2$ and $0.5\times10^{-20}$ cm$^2$ at thermal energy. The estimated probability of having a nuclear level in the low energy region is sufficiently high to make the explanation reasonable. Temperature effects and absorption of filtered radiation point to the existence of bands which fit in with the present theory.

## 1. Introduction

Bethe,[1] Fermi,[2] Perrin and Elsasser,[3] Beck and Horsley[4] gave theories of the anomalously large cross sections of nuclei for the capture of slow neutrons. These theories are essentially alike and explain the anomalously large capture cross sections as a sort of resonance of the $s$ states of the incident particle. Resonance is usually helpful in causing a large scattering as well as a large probability of capture and it has been shown [H. B. Eq. (35)] that large scattering is to be expected by nuclei showing anomalously large capture at thermal energies. This consequence of the current theories is apparently in contradiction with experiment, there being no evidence of a large scattering in good absorbers. It also follows from current theories that with very few exceptions the capture cross section should vary inversely as the velocity of the slow neutrons. Experiments on selective absorption recently performed[5] indicate that there are absorption bands characteristic of different nuclei and it appears from the experiments of Szilard[6] that these bands have fairly well-defined edges. It has been pointed out by Van Vleck[7] that it is hard and probably impossible to reconcile the difference in internal phase required by the Bethe-Fermi theory with reasonable pictures of the structure of the nucleus. The combined evidence of experimental results and theoretical expectation is thus against a literal acceptance of the current theories and it is our purpose to outline an extension which is capable of explaining the above facts by a mechanism similar to that used for the inverse of the Auger effect by Polanyi and Wigner.[8]

It will be supposed that there exist quasi-stationary (virtual) energy levels of the system nucleus+neutron which happen to fall in the region of thermal energies as well as somewhat above that region. The incident neutron will be supposed to pass from its incident state into the quasi-stationary level. The excited system formed by the nucleus and neutron will then jump into a lower level through the emission of $\gamma$-radiation or perhaps at times in some other fashion. The presence of the quasi-stationary level, $Q$, will also affect scattering because the neutron can be returned to its free condition during the mean life of $Q$. If the probability of $\gamma$-ray emission from $Q$ were negligible there would be in fact strong scattering at the resonance, the scattering cross section being then

[1] H. A. Bethe, Phys. Rev. **47**, 747 (1935). We refer to this paper as H. B. in the text.
[2] E. Amaldi, O. d'Agostino, E. Fermi, B. Pontecorvo, F. Rasetti, E. Segrè, Proc. Roy. Soc. **A149**, 522 (1935).
[3] Perrin and Elsasser, Comptes rendus **200**, 450 (1935).
[4] Beck and Horsley, Phys. Rev. **47**, 510 (1935).
[5] Moon and Tillman, Nature **135**, 904 (1935); Bjerge and Westcott, Proc. Roy. Soc. **A150**, 709 (1935); Arsimovitch, Kourtschatow, Miccovskii and Palibin, Comptes rendus **200**, 2159 (1935); Ridenour and Yost, Phys. Rev. **48**, 383 (1935); Pontecorvo, Ricerca scientifica **6-7**, 145 (1935).
[6] L. Szilard, Nature **136**, 950 (1935).
[7] J. H. Van Vleck, Phys. Rev. **48**, 367 (1935).
[8] O. K. Rice, Phys. Rev. **33**, 748 (1929); **35**, 1551 (1930); **38**, 1943 (1931); J. Chem. Phys. **1**, 375 (1933). A similar process was used by M. Polanyi and E. Wigner, Zeits. f. Physik **33**, 429 (1925).

of the order of the square of the wave-length. Estimates of order of magnitude show that it is reasonable to assign 12 volts to the "half-value breadth" of $Q$ due to radiation damping and that the "half-value breadth" due to passing back into the free state is about one-fortieth of the above amount. This means that when the system passes into the state $Q$ it radiates practically immediately and the neutron has no time to be rescattered. It will, in fact, be seen from the calculations that follow that the ratio of scattering to absorption is essentially the ratio of the corresponding half value breadths. The hardness of the emitted $\gamma$-rays is of primary importance for the small ratio of scattering to absorption because it makes the probability of $\gamma$-ray emission sufficiently high. Inasmuch as the interesting phenomena occur for low energies we may suppose that in most cases the coupling of the incident state occurs through its $s$ state, i.e., in virtue of head on collisions. It will be seen, however, that the possibility of obtaining observable effects by means of $p$ states is not excluded even though it is less probable and leads to smaller cross sections. Calculation shows that with resonances of the type considered here one may obtain appreciable probability of capture at energies of the order of 1000 volts. It is possible to have at such energies cross sections of roughly $10^{-22}$ cm$^2$ with a half-value breadth of about 20 volts. It is therefore not necessary to ascribe all large cross sections to neutrons of thermal velocities and the probability of finding a quasi-stationary level in a suitable region is not so small as to make the process improbable.

We are presenting below the theory of capture on this basis in some detail not because we believe it to be a final theory but because further development may be helped by having the preparatory structure well cemented.

## 2. Theory of Damping

The process of absorption from the continuum into a quasi-stationary level and a subsequent reemission of a photon is related to the phenomena of predissociation discussed by O. K. Rice[8] who made the first application of quantum mechanics to this type of process since Dirac's first approach.[9] It is essential for us to consider two continua and in this respect the present problem is more general. It resembles closely the problem of absorption of light from a level $a$ to a level $c$ which is strongly damped by radiation in jumps to a third level $b$. The absorption from $a$ to $c$ corresponds to the transition of the neutron into the quasi-stationary level and the jumps from $c$ to $b$ correspond to the emission of $\gamma$-rays in a transition to a more stable level of the nucleus. The absorption probabilities can be obtained by using the principle of detailed balance from the solution which represents emission[10] from the level $c$ to the levels $a$, $b$ or else by a direct application of the theory of absorption.[11] The usual theory as developed for either process is not accurate enough to represent the effect of the variation of matrix elements with velocity which is essential for our purpose, inasmuch as it is responsible for the existence of two regions of large absorption. The usual type of calculation will now be generalized so as to take the variation into account.

### (a) Calculation of the absorption and scattering process

Let $a_s$ denote the probability amplitudes of states in which the neutron is free and in a state $s$. Similarly let $b_r$ stand for the probability amplitude of a state in which the neutron is captured and there is a photon $r$ emitted and let $c$ be the probability amplitude of the quasi-stationary state having energy $h\nu$. The states $r$, $s$ are here considered to be discrete but very closely spaced in energy. The average spacing of the levels $r$, $s$ are written $\Delta E_r = h\Delta\nu_r$, $\Delta E_s = h\Delta\nu_s$ so that the number of levels $s$ per unit energy range is $1/\Delta E_s$. The matrix element of the interaction energy responsible for transitions from $a_s$ to $c$, $c$ to $b_r$ will be written, respectively,

$$M_s = hA_s, \quad M_r = hB_r. \tag{1}$$

The damping constants for $c$ due, respectively, to the possibility of emitting $a_s$ or $b_r$ are then[12]

[9] P. A. M. Dirac, Zeits. f. Physik **44**, 594 (1927).
[10] V. Weisskopf and E. Wigner, Zeits. f. Physik **63**, 54 (1930).
[11] V. Weisskopf, Ann. d. Physik **9**, 23 (1931).
[12] G. Breit, Rev. Mod. Phys. **5**, 91, 104, 117 (1933).

$$(4\pi\tau_a)^{-1}=\Gamma_a=[\pi\overline{|A_s|^2}/\Delta\nu_s]_{\nu_s=\nu_0}; \quad (2)$$

$$(4\pi\tau_b)^{-1}=\Gamma_r=[\pi\overline{|B_r|^2}/\Delta\nu_r]_{\nu_r=\nu_0}; \quad \Gamma=\Gamma_a+\Gamma_r,$$

where $\tau_a$, $\tau_b$ are respective mean lives of $c$ due to emission of $a_s$ and $b_r$. The quantities $\Gamma$ represent one-half of the "half-value breadth" measured in frequency. In discussing line emission and absorption [10, 11] the directional averages of $|A_s|^2$ and $|B_r|^2$ can be taken for any energy within the breadth of the line because the line can be usually considered to be sharp. In the present case it will be necessary to distinguish among directional averages of $|A_s|^2$ for different energies.

The states $s$ will be thought of as plane waves modified by a central field due to the nucleus and satisfying boundary conditions at the surface of a fundamental cube of volume $V$. The equations satisfied by $a_s$, $b_r$, $c$ are

$$\left(\frac{d}{2\pi i dt}+\nu_s\right)a_s=A_s c; \quad \left(\frac{d}{2\pi i dt}+\nu_r\right)b_r=B_r c, \quad (3)$$

$$\left(\frac{d}{2\pi i dt}+\nu\right)c=\sum A_s^* c_s+\sum B_r^* b_r.$$

In these equations the influence of only one quasi-stationary level is taken into account and for this reason they are not quite accurate. They are sufficiently good for the present purpose because it will be supposed that different quasi-stationary levels do not fall closely together. At $t=0$ it will be supposed that

$$a_s=\delta_{ss_0}, \quad b_r=0, \quad c=0, \quad (t=0). \quad (4)$$

An approximate solution of (3) satisfying this initial condition can be obtained by forming a linear combination of

$$c=e^{-2\pi i(\nu-i\Gamma')t};$$

$$a_s=A_s[e^{-2\pi i(\nu-i\Gamma')t}-e^{-2\pi i\nu_s t}]/(\nu_s-\nu+i\Gamma'), \quad (5)$$

$$b_r=B_r[e^{-2\pi i(\nu-i\Gamma')t}-e^{-2\pi i\nu_r t}]/(\nu_r-\nu+i\Gamma'),$$

with

$$\Gamma'=[\pi\overline{|A_s|^2}/\Delta\nu_s+\pi\overline{|B_r|^2}/\Delta\nu_r]_{\text{resonance region}}, \quad (5')$$

and

$$\begin{aligned}
&a_{s_0}=e^{-2\pi i(\nu_0-i\gamma)t}; \quad c=A_{s_0}^* e^{-2\pi i(\nu_0-i\gamma)t}/(\nu-\nu_0-i\Gamma),\\
&a_s=A_s A_{s_0}^*[e^{-2\pi i(\nu_0-i\gamma)t}-e^{-2\pi i\nu_s t}]/(\nu_s-\nu_0+i\gamma)(\nu-\nu_0-i\Gamma),\\
&b_r=B_r A_{s_0}^*[e^{-2\pi i(\nu_0-i\gamma)t}-e^{-2\pi i\nu_r t}]/(\nu_r-\nu_0+i\gamma)(\nu-\nu_0-i\Gamma),\\
&\Gamma=[\pi\overline{|A_s|^2}/\Delta\nu_s+\pi\overline{|B_r|^2}/\Delta\nu_r]_{\nu_s=\nu_0}.
\end{aligned} \quad (6)$$

In Eq. (6) $s\neq s_0$. The quantities $\gamma$ and $\nu_0-\nu_{s_0}$ are small compared with $\Gamma$; they will go to zero with increasing volume. From (3), one finds for them the equation:

$$(\nu_{s_0}-\nu_0+i\gamma)(\nu-\nu_0-i\Gamma)=|A_{s_0}|^2, \quad (7)$$

so that

$$\gamma=|A_{s_0}|^2\Gamma/[(\nu-\nu_0)^2+\Gamma^2];$$

$$\nu_0=\nu_{s_0}+(\nu_0-\nu)(\gamma/\Gamma). \quad (8)$$

In obtaining Eq (7) the approximations

$$\sum_s{}' |A_s|^2\frac{1-e^{2\pi i(\nu_0-\nu_s-i\gamma)t}}{\nu_s-\nu_0+i\gamma}=\pi i\overline{|A_s|^2}/\Delta\nu_s \quad (9)$$

are made. These correspond to replacing the sums by integrals and extending the range of integration from $\nu_s=-\infty$ to $\nu_s=+\infty$ and similarly for $\nu_r$. In addition it is supposed that $\overline{|A_s|^2}$, $\overline{|B_r|^2}$ vary so slowly through the region in which the integrand is large that they may be taken outside the integral sign. These approximations are, therefore, valid only if the contributions to the sums (9a), (9b) are localized in a sharp maximum. Such a maximum exists for $\nu_s\leqq\nu_0$ because: (1) $\gamma$ vanishes as the fundamental volume is increased and therefore one may consider $\gamma t\ll 1$ and (2) for any $\nu_s-\nu_0$ it is possible to choose $t$ sufficiently large to make $|\nu_s-\nu_0|t\gg 1$. For such times the most important part of the integrand oscillates rapidly with $\nu_s$. However for $|\nu_s-\nu_0|\sim\gamma$, the values of $t$ which satisfy $\gamma t\ll 1$

are always such that $|\nu_s-\nu_0|t\ll 1$. The integrand is thus not oscillatory for $\nu_s=\nu_0\pm\gamma$ and the values of $\overline{|A_s|^2}$, $\overline{|B_r|^2}$ on the right side of (9) are to be understood as corresponding to $\nu_s=\nu_0$ with an uncertainty of the order $\gamma$. It can be verified by calculation that the contribution to (9) due to a finite region at a distance $|\nu_s-\nu_0|\gg\gamma$ contributes imaginary quantities decreasing exponentially with $2\pi|\nu_s-\nu_0|t$ and real quantities which contribute to a frequency shift[9] of $\nu$. For the present this shift will be neglected. Eqs. (6) are thus approximate solutions which become increasingly better as $t$ increases, provided $\gamma t\ll 1$. In our application $\Gamma$ is mostly due to the radiation damping $\Gamma_r$. The directional averages of $|B_r|^2$ vary smoothly since the energy of the $\gamma$-ray is of the order of several million volts and is large compared to $\Gamma$.

The quantity $\Gamma'$ which enters (5) is not determined accurately by the present method because $\overline{|A_s|^2}$ which enters in this case is some sort of average over the resonance width. This complication causes no trouble because: (a) for times $t\gg 1/4\pi\Gamma'$ the rates of emission of states $a_s$, $b_r$ are, respectively, $4\pi\gamma\Gamma_s/\Gamma$, $4\pi\gamma\Gamma_r/\Gamma$ and depend[13] only on $\Gamma$ and not on $\Gamma'$; (b) the largeness of $\Gamma_r$ in comparison with $\Gamma_s$ makes $|\Gamma'-\Gamma|\ll\Gamma$. Thus $\Gamma'$ is of importance only in determining the initial transients but not the steady rate of absorption. This can be expected from the fact that the solutions (6) represent a condition in which $s_0$ is absorbed at the rate $4\pi\gamma$. The addition of the "emission solution" (5) is only needed to enforce the condition $c=0$ at $t=0$; it modifies the emission of states $b_r$, $a_s$ during times comparable with the mean life of the nucleus but leaves them unchanged over longer periods very similarly to the way in which analogous transient conditions are of no importance in the absorption of monochromatic radiation by classical vibrating systems.

The total cross section $\sigma$ which corresponds to the disappearance of the incident states $s_0$ is given by

$$\sigma=4\pi\gamma\Gamma/v, \tag{10}$$

where $v$ is the neutron velocity because the modified plane waves denoted by $s$ were normalized in the volume $\Gamma$ and thus represent states of density $1/\Gamma$.

The number of possible plane waves in $\Gamma$ per unit frequency range is

$$1/\Delta\nu_s=4\pi\Gamma/v\lambda^2, \tag{11}$$

where $\lambda$ is the de Broglie wave-length. From (2), (10), (11) we have

$$\sigma=\gamma\lambda^2/\Delta\nu_s=\frac{\lambda^2}{\pi}S\frac{\Gamma_s\Gamma}{(\nu-\nu_0)^2+\Gamma^2}. \tag{12}$$

Here the statistical factor $S$ takes account of the fact that the state $s_0$ may be more or less effective in its coupling to the quasi-stationary level than the average modified plane wave in the same energy region. If the quasi-stationary level has an orbital angular momentum $Lh$ and if there is no spin orbit interaction then $|A_{s_0}|^2=(2L+1)\overline{|A_s|^2}$ because coupling to $c$ can take place only through $1/(2L+1)$ of the total number of states. Thus.

$$S=2L+1 \tag{13}$$

in these special circumstances. For $s$ terms $S=1$. The total cross section

$$\sigma=\sigma_c+\sigma_s,$$

where $\sigma_s$ is the cross section due to scattering and $\sigma_c$ is the cross section due to capture. We have

$$\sigma_c=\frac{\lambda^2}{\pi}S\frac{\Gamma_s\Gamma_r}{(\nu-\nu_0)^2+\Gamma^2};\quad \sigma_s=\frac{\lambda^2}{\pi}S\frac{\Gamma_s^2}{(\nu-\nu_0)^2+\Gamma^2}. \tag{14}$$

The above value of $\sigma_s$ corresponds to the value $\Sigma|a_s|^2$ and does not take into account the fact that there is scattering in the abscence of the quasi-stationary level. If this is strong one must correct $\sigma_s$ for interference of the states $s$ with the spherical wave present in $s_0$. In the applications made below the scattering effect due to either cause will be small and the correction need not be considered. According to (14) the extra scattering can be expected to be of the order $\Gamma_s/\Gamma_r$ times the capture and is quite small for small $\Gamma_s$.

It should be noted that the order of magnitude of $\sigma_c$ at resonance is changed by taking into account the radiation damping. If this were

[13] Appendix I.

neglected and if one were to calculate simply by using Einstein's emission probability for the stationary states of matter then one would obtain an incorrect value,

$$\sigma_c' = \frac{\Lambda^2}{\pi} S \frac{\Gamma_s \Gamma_r}{(\nu-\nu_0)^2+\Gamma_s^2}. \qquad (14')$$

For resonance $\sigma_c/\sigma_c' = \Gamma_s^2/\Gamma^2$ and approximately $\int \sigma_c dE / \int \sigma_c' dE$ is $\Gamma_s/\Gamma_r$. No paradox is involved here because it is not legitimate to apply Einstein's emission probability formula to levels separated by less than their breadth due to radiation damping. Eq. (14′) gives too high values to the cross section. If $\nu-\nu_0 \gg \Gamma$ there is no difference between $\sigma_c'$ and $\sigma_c$. For sufficiently large values of $\nu-\nu_0$ the discussion which led to Eqs. (13), (14) will break down because Dirac's frequency shift[9] is neglected in these formulas. A more complete formal discussion including the frequency shift is given in Appendix I. The calculation shows that one should change the frequency of the quasi-stationary level $\nu$ by

$$\nu \longrightarrow \nu - \int \frac{|A_s|^2}{\Delta\nu_s} \frac{d\nu_s}{\nu_s-\nu_0} - \int \frac{|B_r|^2}{\Delta\nu_r} \frac{d\nu_r}{\nu_r-\nu_0} \qquad (15)$$

where the integrations are extended over the complete range of states $s$, $r$ and where the principal values of the integrals are to be taken. The last part of (15) represents the frequency shift due to electromagnetic radiation and can be incorporated in $\nu$ as a constant because $\nu_0$ need be varied only in a range small in comparison with the frequency of the $\gamma$-ray. It is dangerous to take this shift into account on account of the well known inconsistency of quantum electrodynamics. The second term on the right side of Eq. (15) is due to interactions between free neutron states and the quasi-stationary state. It is physically correct and it is necessary in order to bring about agreement between (14) and calculations away from resonance by means of the Einstein emission probabilities. The shift is large in the applications. Nevertheless changes in it are small in the relatively small range of values which need be considered and its effect is therefore primarily that of displacing the resonance frequency by a constant amount.

**(b) Resonance of one-body systems**

The above discussion cannot be applied directly to cases in which resonance consists simply in a sharp increase of the wave function of one neutron to a maximum inside the nucleus because there is no intermediate state $c$ under such conditions in the same sense as in the previous section. For low velocity neutrons such resonance can be sharp for states with $L \geqq 1$. Formally one could try to apply the discussion already given by starting with wave functions which are solutions of the wave equation for an infinitely high barrier somewhat outside the nucleus. The difference between the actual height of the barrier and $\infty$ can be then treated as a perturbation essentially responsible for the matrix elements $\hbar A_s$. Such a procedure leads apparently to correct results which can be verified by other methods. It is troublesome to justify it completely because the region where the infinite barrier must be erected should be such that the wave functions within are small for all energies. It is preferable to use a more direct calculation for such a case. We consider a plane wave of neutrons incident on the nucleus. Resonance takes place to the wave functions of angular momentum $L\hbar$. We surround the nucleus by a large perfectly reflecting sphere of radius $R$ and we calculate the rate at which states of angular momentum $L\hbar$ disappear by radiation. There is no essential restriction on the possibility of forming wave packets out of the plane waves if we admit only those states $L$ which satisfy the boundary conditions on the sphere. The radius will be made finally infinitely large and the spacing between the levels infinitely small. This provides the necessary flexibility for the formation of the wave packets.

The spacing between successive possible neutron levels is given by

$$\Delta\nu = v/2R. \qquad (16)$$

The radial function will be expressed as $F/r$ where $F$ will be by definition a sine wave with unit amplitude at a large distance from the nucleus. The normalized wave function is then $Y_L(F/r)(2/R)^{\frac{1}{2}}$ where $Y_L$ is a spherical harmonic normalized so as to have $\int |Y_L|^2 d\Omega = 1$. The wave function for the bound state will be written

$$Y_{L\pm 1} f/r; \quad \int_0^\infty f^2 dr = 1. \qquad (17)$$

The damping constant which corresponds to the emission of radiation from the state $F$ is obtained by using the formula for Einstein's emission probability and is

$$\gamma_E = (C/R) \left| \int_0^\infty F f r dr \right|^2, \qquad (18)$$

where

$$C = \frac{32\pi^3 e'^2 \nu^3}{3hc^3} \frac{L+\frac{1}{2}\pm\frac{1}{2}}{2L+1}, \qquad (18')$$

the upper sign applying to jumps $L \rightarrow L+1$ and $e' \sim e/2$ is the effective charge of the neutron nucleus system. As $R \rightarrow \infty$, both $\Delta\nu$ and $\gamma_E$ decrease towards zero but their ratio remains constant. The cross section due to capture computed directly from the emission probability is

$$\sigma_C' = (2L+1)\Lambda^2 \gamma_E/\Delta\nu. \qquad (19)$$

If this expression approaches $\Lambda^2$ then $\gamma_E/\Delta\nu$ becomes com-

parable with unity and the levels are close enough together to make Eq. (19) meaningless. It is then necessary to take into account the mutual influence of neighboring levels. This can be done by means of the damping matrix.[14] The successive states of angular momentum $Lh$ will be denoted by indices $j$, $l$ and their probability amplitudes by $a_j$. These satisfy

$$\left(\frac{d}{2\pi i dt}+\nu_j\right)a_j=i\Sigma\gamma^{jl}a_l, \tag{20}$$

where

$$\gamma^{jl}=CJ_j^*J_l/R; \quad J_j=\int F_j f r dr. \tag{20'}$$

In our case only states with the same magnetic quantum number can interact so that a complete specification of the states is obtained through their energy. Solutions of (20) in which all quantities vary as $\exp\{-2\pi i(\nu_0-i\gamma)t\}$ correspond as closely as possible to the notion of a stationary state decaying under influence of radiation damping. From (20) one obtains

$$(\nu_j-\nu_0+i\gamma)a_j=i\Sigma\gamma^{jl}a_l. \tag{20''}$$

These equations with the complex eigenwert $\nu_0-i\gamma$ can be reduced making use of the fact that $\gamma^{jl}$ is a matrix of rank 1. Thus eliminating the $a_l$ one finds

$$1=\frac{iC}{R}\Sigma\frac{|J_j|^2}{\nu_j-\nu_0+i\gamma} \tag{21}$$

for the secular equation which determines $\nu_0$ and $\gamma$. This equation will be solved approximately for the case of sharp resonance. The resonance will be supposed to take place at an energy $h\nu_F$ and to have a "half-value breadth" $2h\Gamma_F$. Close to resonance

$$|J_j|^2=\frac{\Gamma_F^2|I|^2}{(\nu_j-\nu_F)^2+\Gamma_F^2}, \tag{22}$$

where $|I|^2$ is the maximum value of $|J|^2$. This approximation will usually apply only in a region of a few $\Gamma_F$. The value of $\Gamma_F$ can be estimated using [15]

$$4\pi\Gamma_F=v_r/\int\bar{G}^2dr, \tag{23}$$

where $\bar{G}$ is $F$ for resonance, $v_r$ is the velocity at resonance, and the integration is to be carried through the range of large values of $\bar{G}$. The quantity $\Gamma_F$ is analogous to $\Gamma_r$ of section (a). The state represented by $\bar{G}$ is analogous to the quasi-stationary state of section (a). In order to bring out the analogy we introduce a damping constant similar to the previous $\Gamma_r$

$$\Gamma_R=C|I|^2/2\int\bar{G}^2dr=2\pi C|I|^2\Gamma_F/v_r, \tag{23'}$$

which is the damping constant of the state represented by $\bar{G}$ when that state is normalized within the nucleus and its immediate vicinity. Substituting (23') into (21), replacing the sum by an integral everywhere except in the vicinity of $\nu_0$ and performing the summation in that region on the assumption that the $\Delta\nu$ can be considered as equal to each other in that region gives

$$1=i\{a\cot\left[\frac{\pi(\nu_{j0}-\nu_0+i\gamma)}{\Delta\nu_{j0}}\right]+ia + \int_0^\infty\frac{v_r|J_j|^2\Gamma_R d\nu_j}{\pi v_j|I|^2\Gamma_F(\nu_j-\nu_0+i\gamma)} \tag{24}$$

$$a=\left[\frac{v_r|J_j|^2\Gamma_R}{v_j|I|^2\Gamma_F}\right]_{\nu_0},$$

where the integral must be extended over all $\nu_j$ and the region around $\nu_0$ is integrated over the real axis. The quantity $\nu_{j0}$ is any one of the $\nu_j$ located so close to $\nu_0$ that the variation in $\Delta\nu$ in between can be neglected. In the approximation of Eq. (22) the integration over the resonance region $\Gamma_F$ leads to an equation which to within a sufficient approximation reduces to

$$1+itTh=(Th+it)(a+ib); \quad b=\frac{v_{j0}|I|^2q}{v_r|J_{j0}|^2(1+q^2)} \tag{25}$$

with

$$\nu_0-\nu_F=q\Gamma_F; \quad Th=\tanh\frac{\pi\gamma}{\Delta\nu_{j0}}; \quad t=\tan\frac{\pi(\nu_0-\nu_{j0})}{\Delta\nu_{j0}}. \tag{25'}$$

By eliminating $t$

$$Th+1/Th=a+1/a+b^2/a, \tag{25''}$$

which has the approximate solution

$$1/Th=a+1/a+b^2/a. \tag{26}$$

For values of $\nu_0$ which lie in the region where Eq. (22) applies and where $\Delta\nu_{j0}\sim\Delta\nu_r$ we have approximately

$$\frac{\pi\gamma}{\Delta\nu}=\frac{\Gamma_R\Gamma_F}{\Gamma_R^2+\Gamma_F^2(1+q^2)}, \tag{26'}$$

where it is supposed that $\Gamma_R\gg\Gamma_F$. If, however, $\Gamma_F\gg\Gamma_R$ then

$$\frac{\pi\gamma}{\Delta\nu}=\frac{\Gamma_R}{\Gamma_F(1+q^2)}, \tag{26''}$$

which is equivalent to using the $\gamma_E$ of Eq. (18), (19); in this case one may compute using emission probabilities. If one is so far away from resonance that $b^2/a<a$, $1/a$ Eq. (25'') gives

$$\gamma=\gamma^{j0j0}, \tag{26'''}$$

provided the right side is $\ll 1$. Here again the simple emission point of view applies. For $\Gamma_R\gg\Gamma_F$ all regions are approximated by

$$\frac{\pi\gamma}{\Delta\nu_{j0}}=\frac{v_r|J_{j0}|^2\Gamma_R\Gamma_F(1+q^2)}{v_{j0}|I|^2[\Gamma_R^2+\Gamma_F^2(1+q^2)]} \tag{27}$$

The treatment of scattering by means of the damping matrix is somewhat involved and will not be reproduced here. The phase shift due to $\nu_0-\nu_{j0}$ when added to the phase shift already present in $F_{j0}$ gives the phase shift required. The scattering is diminished by $\Gamma_R$ in much the same way as it was diminished by it in section (a). By comparing (27) with (19)

$$\sigma_C=(2L+1)\frac{\lambda^2v_r|J_{j0}|^2\Gamma_R\Gamma_F(1+q^2)}{\pi v_{j0}|I|^2[\Gamma_R^2+\Gamma_F^2(1+q^2)]}, \tag{28}$$

which is similar to Eq. (14), close to resonance. The factors $|J|^2/|I|^2$ and $v_r/v_{j0}$ take into account the deviations from the dependence of $|J|^2$ on $\nu$ given by (22). In (14) this is

[14] G. Breit, Rev. Mod. Phys. **5**, 117 (1933); G. Breit and I. S. Lowen, Phys. Rev. **46**, 590 (1934).

[15] G. Breit and F. L. Yost, Phys. Rev. **48**, 203 (1935). See also Eq. (32').

analogous to the dependence of $\Gamma_s$ on $\nu_{-0}$ combined with Dirac's frequency shift.

**(c) Sharpness of resonance for single-body problem**

The upper limit of integration in Eq. (23) has been left indefinite. By Green's theorem

$$\frac{d}{dr}\left[F_1\frac{dF_2}{dr}-F_2\frac{dF_1}{dr}\right]+\frac{2\mu}{\hbar^2}(E_2-E_1)F_1F_2=0,$$

where $F_1$, $F_2$ correspond to energies $E_1$, $E_2$ and need not be regular at $r=0$. Hence [16]

$$\frac{\partial}{\partial r}\left[F^2\frac{\partial}{\partial E}\frac{\partial F}{F\partial r}\right]+\frac{2\mu}{\hbar^2}F^2=0. \tag{29}$$

In this section let $F_i$ be the function inside the nucleus, and let $F$ stand for the regular solution of the wave equation for $r\times$radial function on the absence of the nuclear field. The normalization of $F$ is such as to make it a sine wave $\sin(kr+\varphi)$ of unit amplitude at $\infty$. Similarly $G$ is defined as satisfying the same differential equation as $F$ but it is to be 90° out of phase with $F$ at $\infty$ i.e. $\cos(kr+\varphi)$. The regular solution of the differential equation in the presence of the nuclear field, normalized in the same way as $F$ and $G$, will be called $\bar{F}$. At the nuclear radius $r_0$

$$\bar{F}^2=G^2\Big/\left\{\left[G^2\left(\frac{G'}{G}-\frac{F_i'}{F_i}\right)\right]^2+\left[FG\left(\frac{F'}{F}-\frac{F_i'}{F_i}\right)\right]^2\right\}. \tag{30}$$

Here the accent stands for differentiation with respect to $kr$. At resonance $F_i'/F_i=G'/G$ and the second term in the curly bracket is then 1, while the first term is zero. As $E$ changes to either side of the resonance value $E_r$ the first term may become 1 for $E=E_r\pm\Delta E$ where $\Delta E$ is properly chosen. The half-value breadth is then $2\Delta E$ and $\Delta E=\hbar\Gamma_F$. The value of $\Delta E$ can be estimated by

$$\Delta E\frac{\partial}{\partial E}\left[G^2\left(\frac{G'}{G}-\frac{F_i'}{F_i}\right)\right]_{r_0}=1. \tag{31}$$

Using Eq. (29) and calculation the $\partial/\partial E$ for $E=E_r$ one obtains a result which can be expressed in terms of integrals up to $R$ where $R$ is any value of $r$ which is greater than $r_0$. The function which is $G$ for $r>r_0$ and $F_i(G/F_i)_{r_0}$ for $r<r_0$ is continuous at $r_0$ and at resonance its derivative with respect to $r$ is also continuous. The function will be called $\bar{G}$ for $0<r<\infty$. We have then [17]

$$\frac{E}{\Delta E}=k\int_0^R\bar{G}^2dr+\left[\frac{G^2E\partial}{k\partial E}\frac{\partial G}{G\partial r}\right]_{r=k};\quad \Delta E=\hbar\Gamma_F. \tag{32}$$

The right side of this result is independent of $R$ and is finite. The term outisde the integral should be included in Eq. (23) changing

$$\int G^2dr\to\int_0^R\bar{G}^2dr+\left[\frac{G^2E\partial}{k^2\partial E}\frac{\partial G}{G\partial r}\right]_{r=k}. \tag{32'}$$

Eq. (32) has a well-defined meaning only if resonance is sharp. Otherwise the $\partial/\partial E$ entering in Eq. (31) cannot be supposed to be sufficiently constant through the half-breadth $2\hbar\Gamma_F$. It cannot be expected to hold for the broad $S$ resonance discussed by Bethe.

**(d) Capture by $p$ states**

For a potential well of constant depth

$$F_i=\sin z/z-\cos z;\qquad F=\sin\rho/\rho-\cos\rho;$$

$$G=\cos\rho/\rho+\sin\rho, \tag{33}$$

where

$$z=Kr;\quad \rho=kr;\quad K=\mu v_i/\hbar;\quad k=\mu v/\hbar \tag{33'}$$

$v_i$, $v$ being, respectively, the velocities inside and outside the nucleus. The resonance condition is

$$z\sin z/[\sin z/z-\cos z]=\rho\cos\rho/[\cos\rho/\rho+\sin\rho].$$

For slow neutrons $\rho\ll1$ the right side is $\ll\rho^2$ and therefore very small. The first resonance point is obtained for $z=\pi-\epsilon$, $\epsilon\sim\rho^2/\pi$. It will suffice to take $z=\pi$. By substituting into Eq. (32) it follows that

$$\Delta E/E=2\rho/3=4\pi r_0/3\Lambda. \tag{33''}$$

For $E=(1/40)$ volt, $\Lambda=1.8\times10^{-8}$ cm, $\hbar\Gamma_F=5.8\times10^{-6}$ volt. For 3-MEV $\gamma$-rays a reasonable value of $\hbar\Gamma_R$ is 5.8 volts. The cross section at resonance is by Eq. (28) $3\Lambda^2\Gamma_F/\pi\Gamma_R=300\times10^{-24}$ cm². Since scattering is of the order $\Gamma_F/\Gamma_R$ times capture the scattering cross section is small. According to Eq. (33'') the cross section at resonance for $p$ terms with $\Gamma_R\gg\Gamma_F$ can be expected to vary as $v$ and $\hbar\Gamma_F$ as $v^2$. The range in which $p$ terms can be expected to give large capture cross sections and small scattering is therefore roughly from 1/40 volt to 1 volt. At higher velocities $\hbar\Gamma_F$ is likely to be higher than $\hbar\Gamma_R$. In the absence of an apparent reason for nuclear $p$ levels to fall in this narrow velocity range, an explanation in terms of $p$ terms although possible is improbable on account of the small range of neutron velocities required.

## 3. Capture Through $s$ Wave

**(a)**

This section will contain the calculation of the $A_s$ used in 2a. It is supposed that the system

---

[16] J. A. Wheeler. We are indebted to Dr. Wheeler for communicating to us other applications of this relation.

[17] Cf. Eq. (22) reference 15. In calculations with Coulombian fields it is sometimes convenient to transform Eq. (32) of the text into

$$\frac{E}{\Delta E}=G^2\left[\frac{k}{F_i^2}\int_0^{r_0}F_i^2dr-\frac{k}{F^2}\int^{r_0}F^2dr-\frac{EG^2\partial}{kr\partial E}\left(\frac{kr}{FG}\right)\right]$$

all quantities outside the integrals being taken for $r=r_0$.

"nucleus+neutron" can be treated in first approximation by means of an effective central field acting on the neutron. The difference between the Hamiltonian of the system and the Hamiltonian corresponding to the central field will be called $H'$. On account of this difference there exist transitions from the $s$ wave of the incident state to quasi-stationary excited states of the "nucleus +neutron" system. Normalizing the $s$ waves within a sphere of radius $R$ the wave function inside the nucleus is

$$C \sin Kr/r; \qquad C^{-2}=[1+(U/E)\cos^2 Kr_0]2\pi R,$$

where $$K^2/k^2=(U+E)/E$$

and $U$ is the depth of the potential hole. The interaction energy $H'$ involves besides $r$ also internal coordinates $x$. The wave function of the whole system in the incident state may be written $C\psi_0(x)\sin Kr/r$ and in the quasi-stationary state $\psi_Q(r, x)$. The matrix element $M_s$ of Eq. (1) is then

$$M_s=\int \psi_Q(r, x)H'C \sin Kr\psi_0(x)dv/r, \quad (34)$$

where $dv$ is the volume element of the whole system. The state $Q$ is by definition such that the integral of $|\psi_Q|^2$ through nuclear dimensions is unity. The order of magnitude of $M_s$ is therefore

$$M_s=C\bar{H}r_0^{\frac{1}{2}}, \quad (34')$$

where $\bar{H}$ is an average of $H'$ through the nucleus and may have reasonably a value of 0.5 MEV. It cannot be specified further without detailed calculation which would probably be unsatisfactory in the present state of nuclear theory. Since $\Delta E=h\nu/2R$,

$$h\Gamma_s \leqq \frac{\bar{H}^2 r_0}{2\Lambda U\cos^2 Kr_0}. \quad (34'')$$

According to Eq. (14)

$$\sigma_c=\frac{\Lambda r_0}{2\pi}\,\frac{\bar{H}}{U\cos^2 Kr_0}\,\frac{\bar{H}h\Gamma_r}{h^2(\Gamma_r+\Gamma_s)^2+(E-E_r)^2}, \quad (35)$$

where $E_r$ is the value of $E$ for resonance. According to this formula there are two maxima for $\sigma_c$, one for $E=E_r$ and one for $E=0$. The expected cross sections are given in Table I to about ten percent accuracy. The numbers correspond to $\Lambda(kT)=1.8\times10^{-8}$ cm; $\Lambda(1\text{ volt})=2.9\times10^{-9}$ cm; $r_0=3\times10^{-13}$ cm; $U\cos^2 Kr_0=10^7$ volts. For $E_r=1/40$, 1 volt the table shows large cross sections at thermal energies and above. The condition is similar to Bethe's except for a relatively sharper resonance determined by $h\Gamma_r$. For 50 volts one sees the development of two maxima one at resonance and one at thermal energies. For $E_r=1000$ and 10,000 volts the maximum at thermal energies decreases as $E_r^{-2}$ and the maximum at resonance roughly as $E_r^{-\frac{1}{2}}$. For such high values of $E_r$ scattering has a chance of becoming comparable with absorption or even greater than the absorption at resonance. In the thermal energy region the $1/v$ law is obeyed for high values of $E_r$; for low $E_r$ the maximum at $E_r$ interferes with the $1/v$ law and the region of its validity is displaced below thermal energies.

TABLE I. *Calculated cross sections for neutron capture.*

| Position of Resonance (volts) | $\bar{H}$ (MEV) | $h\Gamma_r$ (volts) | $h\Gamma_s$ at resonance (volts) | $10^{24}\sigma$ (cm²) Resonance | Thermal Energies |
|---|---|---|---|---|---|
| 1/40 | 0.1 | 10 | 0.01 | 90 000 | |
| | .1 | 1 | .01 | 900 000 | |
| 1 | .1 | 10 | .05 | 14 000 | |
| | .1 | 1 | .05 | 140 000 | |
| 50 | .1 | 10 | .37 | 2 000 | 3500 |
| | .5 | 10 | 9 | 13 400 | 80000 |
| | .1 | 1 | 0.37 | 11 000 | 350 |
| | .5 | 1 | 9 | 4 800 | 9000 |
| 1000 | .1 | 10 | 1.6 | 320 | 9 |
| | .5 | 10 | 40 | 420 | 200 |
| 10000 | .1 | 10 | 5 | 60 | 0.09 |
| | .5 | 10 | 125 | 18 | 2 |

In Table I only the effect of a quasi-stationary level at $E_r$ is considered. In addition there may be effects of other levels as well as radiation jumps of the kind considered by Bethe and Fermi which do not depend on the existence of virtual levels. It is thus probable that in most cases there is a region with a $1/v$ dependence although it may be at times masked by a resonance region.

### (b) Dirac's frequency shift

In the above estimates the effect of Dirac's frequency shift was neglected. This is given by

$$(h\Delta\nu)_D=\int_0^\infty \frac{h\Gamma_s}{\pi}\frac{dE}{E-E_0}$$

$$=\frac{\bar{H}^2 r_0}{\pi\Lambda_0 x_0^4}\int_0^\infty \frac{x^2dx}{(x^2-x_0^2)(x^2+a^2)},$$

where $x=E^{\frac{1}{2}}$, $a^2=U\cos^2 Kr_0$ and the value of $h\Gamma_s$ was substituted by means of Eq. (34''). Here the subscript 0 refers to the neutron energy $E_0$ and the principal value of the integral is understood. Evaluating the expression

$$(h\Delta\nu)_D=\frac{\bar{H}^2 r_0 U^{\frac{1}{2}}\cos Kr_0}{2\Lambda_0(E_0+U\cos^2 Kr_0)E_0^{\frac{1}{2}}}. \quad (36)$$

The shift is seen to be of the order of 3000 times $h\Gamma_s$ for $E_0=1$ volt. The shift is nearly independent of the velocity. In the approximation of Eq. (36)

$$\frac{d(h\Delta\nu)_D}{dE_0}=\frac{h\Gamma_s}{E_0}\frac{E_0^{\frac{1}{2}}}{U^{\frac{1}{2}}|\cos Kr_0|}, \quad (36')$$

which shows that the variation in the shift is small and of the order of $2\times10^{-3}(E-E_r)$ for $\bar{H}=0.1$ MEV.

## 4. Discussion

### (a) Absence of scattering

According to Dunning, Pegram, Fink and Mitchell[18] the elastic scattering of slow neutrons by Cd is less than one percent of the number captured. According to A. C. G. Mitchell and E. J. Murphy[19] scattering as detected by silver is about the same as absorption for Fe, Pb, Cu, Zn, Sn while for Hg scattering is about 1/80 of the absorption. In the later communication of Mitchell and Murphy[19] it is also found that Ag, Hg, Cd are poor scatterers of slow neutrons detected by silver. It is interesting that Ag shows small scattering in these experiments because the detection took place by means of silver and that Hg and Cd show small scattering because they have large absorption cross sections.[18] The observation of scattering by a material having large absorption is difficult because the neutrons entering the material are absorbed before they can be scattered and it is possible that to some extent the failure to observe scattering in good absorbers is due to this cause. The absence of observed scattering in the region of strong absorption is therefore not a surprise, particularly in view of the relatively small numbers of neutrons available for experimentation. It seems more significant, however, that strong absorbers do not show, so far, strong scattering in any velocity region because, according to the Fermi-Bethe theory, the scattering cross section should be large in a wide range of energies. The experimental evidence says little about the ratio of scattering to absorption near resonance. It indicates that this ratio is less than 1/10 in most cases. It is impossible, therefore, to ascertain definitely the ratio $\Gamma_s/\Gamma_r$ until more detailed experimental data are available. According to Table I the condition $\Gamma_s/\Gamma_r<1/10$ can be satisfied in many ways up to velocities of over 1000 ev.

### (b) Magnitude of interaction with internal states and probability of internal state in required region

In Table I arbitrary assignments of values of $\Gamma_s$, $\Gamma_r$ were made. It will be noted that at low neutron velocities the desired large capture cross sections are easily obtained through relatively wide bands having a half-value breadth $2\Gamma_r$. Keeping $\Gamma_r$ fixed one can decrease the interaction energy $\bar{H}$ to 10,000 ev for $h\Gamma_r=1$ volt, $E_r=1$ volt and still have a cross section of $1000\times10^{-24}$ cm$^2$ in an energy range up to 2 volts. In some cases relatively weak radiative transitions will come into consideration leading to smaller $\Gamma_r$. For such transitions $\bar{H}$ need not be as large as 10,000 ev in order to have cross sections of $1000\times10^{-24}$ cm$^2$ in the resonance region. For the large energies involved in nuclear structure it is reasonable to expect interaction energies of the order of 10,000 volts between practically any pair of levels not isolated by a selection rule and interaction energies of the order 100,000 volts between a great many levels.

There are about ten elements among 72 observed that show cross sections of more than

[18] J. R. Dunning, G. B. Pegram, G. A. Fink and D. P. Mitchell, Phys. Rev. **48**, 265 (1935).
[19] A. C. G. Mitchell and E. J. Murphy, Phys. Rev. **48**, 653 (1935). Cf. also Bull. Am. Phys. Soc. **11**, paper 27, Feb. 4, 1936.

$500\times10^{-24}$ cm². Allowing for the fact that there are more isotopes than elements it appears fair to say that the chance of such an anomalous cross section is about 1/20. One can try to account for these solely by the low velocity regions which exist for any resonance level, thus probably overestimating the necessary number of levels. In order that $\sigma_c > 500\times10^{-24}$ cm² at 1/40 volt for a nucleus having $r_0=10^{-12}$ cm and $h\Gamma_r=10$ volts the resonance region must be not farther than at $|E_r|=\overline{H}/420$ from thermal energies by Eq. (35). We do not wish $h\Gamma_a$ at thermal energies to be greater than 0.1 volt so as not to have too much scattering and therefore $\overline{H}$ should be below $2\times10^5$ ev at the higher $E_r$. Thus $E_r$ should be kept below about 460 volts in order to give the large capture cross sections for $E=1/40$ volt together with small scattering. A level below ionization will also be effective in producing an increased absorption. The observed number of large absorptions corresponds in this way to one level in 900 volts for 1/20 of nuclei or one level every 18,000 volts for a single nucleus. In addition some cross sections will be caused by direct resonance. Just how many is uncertain but it is clear that such effects exist in Cd, Ag, Au, Rh, In.

The average spacing between the $\gamma$ ray levels of Th C″ as given in Gamow's book is about 100,000 volts and this is apparently the order of magnitude usual for $\gamma$-ray levels of radioactive nuclei. There appears to be no reason why the energy levels found through the analysis of $\gamma$-ray spectra should include all the nuclear levels and there may be as many as one level in 20,000 of a kind that may be responsible for coupling to incident neutrons. It should be remembered here that some of the levels may be active even though the coupling is weak so that more possibilities are likely to matter than for the $\gamma$-rays of radioactive nuclei.

For a complicated configuration of particles it seems reasonable to consider a total number of 100 possible levels per configuration because protons and neutrons can be combined separately to give different states. On this basis we deal with an average spacing between configurations of about 2 MEV which is not excessively small. It is, of course, impossible to prove anything definitely without calculating the levels; this appears to be premature at present on account of uncertainties in nuclear theories.

### (c) Existence of two maxima

According to the calculation given above it is expected that there will be in general two maxima one of which should be at resonance and another at $v=0$. According to the experiments of Rasetti, Segrè, Fink, Dunning and Pegram[20] the $1/v$ law is not obeyed by Cd but is obeyed by Ag. Cadmium has therefore a resonance region close to thermal velocities. In the classification of Fermi and Amaldi[21] this region must be affected by the $C$ group since absorption measurements by the Li ionization chamber which was used in these experiments agree for most elements with the measurements of Fermi and Amaldi on the $C$ group.[22] The verification of the $1/v$ law for Ag by the rotating wheel indicates that in Ag the resonance band is located above thermal energies. This conclusion is in agreement with the smallness of the temperature effect for the $A$ neutrons detected by silver which was recently established by Rasetti and Fink.[23] Since Rh behaves similarly to Ag in these temperature experiments Rh also has a resonance region above thermal velocities. Fermi and Amaldi have evidence that $D$ neutrons, which affect Rh, are different from $A$ neutrons which affect Ag. It is very probable that both of these groups lie above the thermal region and they may reasonably cover a range of 30 volts inasmuch as the $B$ group overlaps weakly with both $A$ and $D$.

According to Szilard[6] In shows strong selective effects outside the $C$ group and according to Fermi and Amaldi[21] the same period of In (54 min.) detects the $D$ group. The number of neutrons in the groups is presumably in the ratios $C/80=B/20=D/15=A/1$. One could try to conclude that the order of increasing energies is $C$, $B$, $D$, $A$ on the assumption that the number of neutrons increases towards low energies. Such a conclusion is dangerous because little is known about the velocity distribution, because within

[20] F. Rasetti, E. Segrè, G. Fink, J. R. Dunning and G. B. Pegram, Phys. Rev. **49**, 103 (1936).
[21] E. Amaldi and E. Fermi, Ricerca scientifica **2**, 9 (1936); E. Fermi and E. Amaldi, Recerca scientifica **2**, 1 (1936).
[22] Unpublished results of F. Rasetti. We are very grateful to Professor Rasetti for informing us of these results.
[23] F. Rasetti and George A. Fink, Bull. Am. Phys. Soc. **11**, Paper 28, Feb. 4, 1936.

each group there may be several bands at different velocities, and also because the number of expected neutrons in a group should depend on its width. Temperature effects show that practically all captures increase as the energy is lowered. The effects are strongest[24] for Cu, V are smaller for Ag, Dy weaker for Rh and weakest for I. The absorption coefficient for $C$ neutrons is, however, larger for Rh than for Ag indicating that the smaller temperature effect in Rh is due to a relatively greater importance in it of a band above thermal energies. All temperature effects agree in indicating the presence of a region in which the $1/v$ law is followed approximately but again no definite conclusion about the order of bands is possible. The low temperature effect in I would tend to indicate that its absorption region is high and detection-absorption experiments on I and Br tend to indicate that their bands are isolated from the others discussed here; perhaps these isotopes have resonance bands at higher energies. A new band was recently discovered in Au by Frisch, Hevesy and McKay[25] which represents strong absorption on a weaker background. The large number of selective effects observed makes the present explanation reasonable and the existence of a region of low energies in which the absorption decreases with energy is seen to fit in well with expectation.

### (d) Other possibilities

One may consider weak long range forces as a possible explanation of the same phenomenon. Potentials of the order of neutron energies in a region comparable with the neutron wave-length would produce strong effects on absorption and scattering. For thermal energies the wave-length is of atomic dimensions and one would therefore expect the binding energy of deuterium compounds to be different from that of hydrogen compounds by an amount comparable to 1/40 volt if such potentials were present. Such energy differences do not exist. It would be possible to devise potentials which fall off sufficiently rapidly with distance to make the interaction potential negligible for chemical binding and which would cover a total region appreciably larger than the nucleus. Such hypotheses seem improbable without additional argument. Besides special relations between the phase integrals through the nuclear interior and the part of the range of force outside the nucleus would have to be set up in order to make absorption large and scattering small. It is improbable that the large number of bands could be accounted for by any single particle picture.

Forces between electrons and neutrons even though they may exist are not likely to have much to do with the bands Thus it has been shown by Condon[26] that electron neutron interactions would give rise to scattering cross sections varying roughly as the square of the atomic number $Z$ on the assumption that the electron-neutron forces alone are responsible for the scattering. Forces inside the nucleus must also be supposed to contribute to the phase shifts responsible for scattering. Since these forces also vary with $Z$ one could obtain a more complicated dependence of the scattering cross section by suitably adjusting the nucleus-neutron and electron-neutron potentials. On such a picture one could try to account for sharp resonances by making the electron neutron interaction repulsive. However, Condon's calculation shows that isotope shifts would be also produced by these interactions. It is improbable that the isotope shift is due solely to neutron-electron interaction because the deviation from the inverse square law inside the nucleus due to smearing out of protons produces a considerably larger effect than the observed shift. But it would also be unreasonable to try to combine the proton and neutron effects in the nucleus so as to have each large but their difference small. It is therefore probable that the electron-neutron interaction is not much larger than that which corresponds to the observed isotope shift. Since the density of the Fermi-Thomas distribution varies for small $r$ as $r^{-\frac{1}{2}}$ the effective potential acting on the neutron will become high for small $r$. However, calculation shows that it is not high in a wide enough region to account for sharp resonances if the limitation due to the isotope shift is considered.

[24] P. B. Moon and R. R. Tillman, Proc. Roy. Soc. **A153**, 476 (1936).
[25] O. R. Frisch, G. Hevesy and H. A. C. McKay, Nature **137**, 149 (1936).
[26] E. U. Condon, in press. We are indebted to Professor Condon for showing us his manuscript before publication.

Bombardment of light nuclei with charged particles has also shown the existence of resonances. Thus there are resonances[27] for the emission of $\gamma$-rays in proton bombardment of Li, C, F and similarly there are the well known resonances in disintegrations produced by $\alpha$ particles. Experimental methods have not been very suitable so far for the detection of resonance regions on account of the scarcity of monochromatic sources and the necessity of using thin films. In Li protons are apparently able to produce $\gamma$-rays in two ways; by resonance at 450 kv and by another process at higher energies. In fluorine there are several peaks. In carbon there was an indication of the main resonance peak being double. It appears possible that many more levels will be detected inasmuch as neutron experiments indicate a high density of levels. Calculations on the radiative capture of carbon under proton bombardment[15] lead to a higher yield than is observed by a factor of several thousand. In these calculations the capture was supposed to occur by a jump from the $p$ state of the incident wave to an $s$ state of the $N^{13}$ nucleus. The calculated half-value breadth due to proton escape from the quasi-stationary $p$ level was of the order $\hbar\Gamma_P \sim 10{,}000$ ev and thus much larger than the width due to radiation damping. The yield in thick targets under these conditions is nearly independent of the special value of $\hbar\Gamma_P$. It is clear from the formulas given here for neutron capture that one can decrease the theoretically expected yield either by ascribing the capture to a transition having a small probability of radiation (small $\Gamma_\gamma$) such as would correspond to quadruple or other forbidden transitions or else by using an intermediate state of excitation of the nucleus with a small transition probability to the incident state of the proton (small $\Gamma_s$). In the latter case this transition probability would have to be made so small as to have $\Gamma_s < \Gamma_\gamma$ and the observed width of resonance would have to be ascribed to experimental effects. If $\Gamma_s < \Gamma_\gamma$ the thick target yield depends on $\Gamma_s$ and is proportional to it for small $\Gamma_s$. The apparent disagreement between theory and experiment previously found for carbon is thus not alarming from the many-body point of view and supports the belief that excitation states of the nucleus have often to do with the simultaneous excitation of more than one particle.

The excitation states responsible for the neutron absorption bands make it possible for a fast neutron to lose energy by inelastic impact with the nucleus. Estimates show that the cross sections for such processes are likely to be small when energy losses are high. The cross section is estimated to be

$$\frac{\Lambda_1}{4\pi\Lambda_2}\,\frac{\bar{H}^2 r_0^2}{U^2\cos^4 Kr_0},$$

where $\Lambda_1$, $\Lambda_2$ are, respectively, neutron wavelengths in the incident and final states. For large energy losses $\Lambda_2 \gg \Lambda_1$ and only a small effect need be expected. The excitation levels responsible for neutron capture will give small values $\Lambda_1/\Lambda_2$. Excitation levels located lower are more favorable and probably the excitation of Pb to about 1.5 MEV has to do with such a possibility.[28]

We are very grateful to Professors R. Ladenburg and F. Rasetti for interesting discussions of the experimental material.

## Appendix I

**Variation of damping constant with energy and Dirac's frequency shift**

Eq. (6) of the text lead to [cf. Eqs. (126′) to (129′) of reference in footnote (12)]

$$(\nu_{s0}-\nu_0+i\gamma)(\nu-\nu_0+i\gamma)=|A_{s0}|^2 + (\nu_{s0}-\nu_0+i\gamma)\Big[\Sigma'|A_s|^2\,\frac{1-e^{2\pi i(\nu_0-\nu_{s0}-i\gamma)t}}{\nu_s-\nu_0+i\gamma} + \Sigma|B_r|^2\,\frac{1-e^{2\pi i(\nu_0-\nu_r-i\gamma)t}}{\nu_r-\nu_0+i\gamma}\Big] \qquad (38)$$

which determines $\Gamma$ by comparison with (7) [$\Gamma \gg \gamma$].

It is by no means natural that this equation can be satisfied because the right side depends on $t$. If the $A_s$ as well as the $B_r$ were all essentially equal and if $\gamma$ were great in comparison with the frequency differences of consecutive levels the sums could be transformed into integrals in the well-known way[10-12] so that (9) as well as (6) would follow. We shall attempt here a more exact procedure.

Consider the $\Sigma_s'$ in the square brackets. It is natural to divide the range of $\nu_s$ into two parts: one for which $|\nu_s-\nu_0| > a \gg \gamma$ and one for which $|\nu_s-\nu_0| \leqq a$. Since

[27] L. R. Hafstad and M. A. Tuve, Phys. Rev. **48**, 306 (1935); P. Savel, Comptes rendus **198**, 1404 (1934), Ann. de physique **4**, 88 (1935).

[28] J. Chadwick and M. Goldhaber, Proc. Roy. Soc. **A151**, 479 (1935).

$\overline{|A_s|^2}/\Delta\nu_s$ changes slowly this quantity will be replaced by a constant in $|\nu_s-\nu_0|\leqq a$ and its value may be taken to be that at $\nu_0$ for the evaluation of the contribution of this region. We have then to consider

$$(\overline{|A_s|^2})_{\nu_0}\sum_{\nu_0-a}^{\nu_0+a}{}'\frac{1-e^{2\pi i(\nu_0-\nu_s-i\gamma)t}}{\nu_s-\nu_0+i\gamma}. \tag{39a}$$

An exact evaluation of this sum is not simple because $\gamma$ and $\Delta\nu$ are of the same order of magnitude and the replacement of (39a) by an integral is somewhat objectionable. This point has never been completely cleared up and we have only qualitative arguments in favor of the correctness of the replacement of (39a) by an integral. For $\nu_s-\nu_0$ of the order of a few $\gamma$ such a replacement is indeed meaningless but fortunately this region is not vital for $t\ll 1/\gamma$ since the numerator of (39a) is then small. For larger $|\nu_s-\nu_0|$ the terms of (39a) vary more smoothly and finally they become rapidly oscillating for $|\nu_s-\nu_0|t\gg 1$ which can be satisfied simultaneously with $t\ll 1/\gamma$ provided $a\gg\gamma$. The smallness of $\gamma$ is thus not as serious as might appear from the fact that $\gamma/\Delta\nu\sim 1$. It should also be observed that the treatment of Rice[8] using real eigenwerte for a single one-dimensional continuum is in agreement with replacing (39a) by an integral. The result of doing so is given by (9).

In addition one has the contribution of $|\nu_s-\nu_0|>a$. This integral can be treated neglecting $\gamma$ because it is of interest to evaluate $\gamma$ only to quantities of order $\gamma/(\nu-\nu_0)$ and because the discussion is supposed to apply only to $\gamma t\ll 1$. This integration gives

$$\left(\int_0^{\nu_0-a}+\int_{\nu_0+a}^{\infty}\right)\frac{\overline{|A_s|^2}}{\Delta\nu_s}\frac{d\nu_s}{\nu_s-\nu_0} \tag{39b}$$

which means that the principal value of the $\int$ is understood. Similarly one obtains a contribution due to $|B_r|^2$. These two integrals give the Dirac frequency shift which is included in Eq. (15).

As stated in the text the difference between $\Gamma''$ and $\Gamma'$ does not affect the absorption for $t\gg 1/\Gamma$. Thus for the initial condition given by Eq. (4)

$$|b_r|^2=\frac{|B_r|^2|A_{s0}|^2}{(\nu-\nu_0)^2+\Gamma^2}\left\{\frac{1+e^{-4\pi\gamma t}-2e^{-2\pi\gamma t}\cos 2\pi(\nu_r-\nu_0)t}{(\nu_r-\nu_0)^2+\gamma^2}\right.$$
$$\left.+\frac{1+e^{-4\pi\Gamma' t}-2e^{-2\pi\Gamma' t}\cos 2\pi(\nu_r-\nu_0)t}{(\nu_r-\nu)^2+\Gamma'^2}+\text{cross product term}\right\}.$$

Only the first fraction in the curly brackets contributes to the steady increase of $\Sigma|b_r|^2$ in times $\gg 1/\Gamma$. Its contribution is

$$\frac{\pi|A_{s0}|^2\overline{|B_r|^2}}{\gamma[(\nu-\nu_0)^2+\Gamma^2]\Delta\nu_r}(1-e^{-4\pi\gamma t}).$$

The last factor is for practical purposes $4\pi\gamma t$. The second and third terms in the curly bracket give terms $\exp(-4\pi\Gamma' t)$, $\exp(-2\pi\Gamma' t)$ and constants. The first two kinds die off and the last kind represents the effect of transients which do not matter in the long run, so that for times not too large as compared with $1/\gamma$ and yet great as compared with $1/\Gamma$ one may consider the rates of change of $\Sigma|b_r|^2$ and of $\Sigma'|a_s|^2$ to be $4\pi\gamma\Gamma_r/\Gamma$ and $4\pi\gamma\Gamma_s/\Gamma$. These are the results used in the text.

---

APRIL 1, 1936 PHYSICAL REVIEW VOLUME 49

# The Theoretical Cross Section for $K$ Electron Ionization by Electron Impact

W. W. WETZEL, *Colgate University*

(Received February 11, 1936)

Born's approximation is applied to the general problem of single $K$ shell ionization without excitation. Slater's wave functions are used and a formula is derived which expresses the cross section as a function of the atomic number, the ionization potential of the $K$ shell and the energy of the colliding electron. By comparison with experimental measurements the theory is shown to give good qualitative results for collision energies above about three times the ionization energy.

THE Born approximation leads, in the case of single ionization by electron impact, to a value of the collision cross section given by the relationship

$$\sigma(k,z,I)=(m^2/2\pi h^4k)\int k'|U|^2k''^2dk''d\Omega''d\Omega', \tag{1}$$

where $$U=\int\Psi_a e^{i\mathbf{k}\cdot\mathbf{r}_0}\bar{V}\Psi_i^* e^{-i\mathbf{k}'\cdot\mathbf{r}_0}e^{-i\mathbf{k}''\cdot\mathbf{r}_1}dv. \tag{2}$$

Here $m$ is the mass of the electron, $k$, $k'$ and $k''$ are equal respectively to $2\pi m/h$ times the velocity of the colliding, deflected and ejected electrons. $\Psi_a$ is the wave function of the normal atom and $\Psi_i$ that for the ionized atom. $r_0$ and $r_1$ are, respectively, the radial coordinates of the colliding and ejected electrons. $d\Omega'=\sin\theta' d\theta' d\phi'$ and $d\Omega''=\sin\theta'' d\theta'' d\phi''$ where the angular coordinates are those of the vectors $\mathbf{k}'$ and $\mathbf{k}''$. The origin of the coordinate systems is chosen

at the atomic nucleus leaving the polar axis to be designated later. The integral in Eq. (2) is extended over the space coordinates of all the electrons.

The perturbation energy is

$$V=e^2(z/r_0-\sum_{n=1}^{z}1/r_{n0}),$$

where $r_{n0}=|\mathbf{r}_n-\mathbf{r}_0|$.

Let us build the functions representing the normal and the ionized atom from which a $1s$ electron has been removed by a product of functions representing individual electrons.

$$\Psi_a=\prod_{l=1}^{z}\psi_l \quad \text{and} \quad \Psi_i=\prod_{m=2}^{z}\psi_{m'}.$$

The $\psi$'s will be selected from the appropriate functions of Slater.[1] The primed functions will be identical with the unprimed in the angular factors but their radial factors will differ from those of the unprimed by a suitable increase in the effective nuclear charge.

Following Bethe's procedure[2] we may integrate Eq. (2) over the coordinates of the colliding electron. Thus

$$\int\frac{e^{i\mathbf{q}\cdot\mathbf{r}_0}}{r_{n0}}dv_0=\frac{4\pi}{q^2}e^{i\mathbf{q}\cdot\mathbf{r}_n},$$

where $\mathbf{q}=\mathbf{k}-\mathbf{k}'$ gives

$$U=(4\pi e^2/q^2)\int\Psi_a\Psi_i^*e^{-i\mathbf{k}''\cdot\mathbf{r}_1}(z-\sum_{n=1}^{z}e^{i\mathbf{q}\cdot\mathbf{r}_n})dv'. \quad (3)$$

Since $\mathbf{q}$ is not a function of the electron coordinates we may select it as their polar axis. Then $\mathbf{q}\cdot\mathbf{r}_n=qr_n\cos\theta_n$ and we may expand the exponential as

$$e^{iqr_n\cos\theta_n}=1+iqr_n\cos\theta_n-\cdots. \quad (4)$$

The important contribution to the matrix element occurs when the scattering angle is small, i.e., $\mathbf{q}$ near its minimum value, and when $r_n$ is not much greater than the radius of the Bohr orbit occupied by the $n$th electron. Under these conditions $qr_n$ is less than unity and we may as a first approximation neglect terms of the expansion beyond the second. This approximation becomes more exact with increase of collision energy.

Combining Eqs. (3) and (4) gives

$$U=-\frac{4\pi ie^2}{q}\sum_{n=1}^{z}\int\Psi_a\Psi_ie^{-i\mathbf{k}''\cdot\mathbf{r}_1}r_n\cos\theta_n dv'. \quad (5)$$

Because Slater's functions are of the hydrogenic type and because ionization does not affect the angular factors there will arise in the integrals of Eq. (5) for all values of $n$ other than unity a factor of the form

$$\int\cos\theta_n|P_s^t(\cos\theta_n)|^2\sin\theta_n d\theta_n.$$

It is possible to show by repeated application of a reduction formula in a process too lengthy to be of interest here that the above integral is equal to zero for all values of $s$ and $t$.

Eq. (5) is therefore reduced to one term of the sum, that is where $n=1$.

$$U=-\frac{4\pi ie^2}{q}\int\Psi_a\Psi_i^*e^{-i\mathbf{k}''\cdot\mathbf{r}_1}r_1\cos\theta_1 dv'.$$

It may be shown that changing the effective nuclear charge by unity does not affect greatly the normality of the $\psi$-functions we are using. That is

$$\int\psi_2\psi_2^{*\prime}dv_2\approx 1.$$

Making this assumption and integrating over all coordinates except those of the ejected electron gives

$$U=-\frac{4\pi ie^2}{q}\int\psi_1e^{-i\mathbf{k}''\cdot\mathbf{r}_1}\cos\theta_1\times\sin\theta_1r_1^3dr_1d\theta_1d\phi_1, \quad (6)$$

where $\psi_1=(\alpha^3/\pi)^{\frac{1}{2}}e^{-\alpha r_1}$, $\alpha=[(z-0.30)/a_0]$,

$a_0$ is the radius of the first Bohr orbit in hydrogen and $z$ is the atomic number.

Let $\epsilon$ be the angle between $\mathbf{q}$ the polar axis and $\mathbf{k}''$. Then, neglecting subscripts since the remaining coordinates are all those of the ejected electron, we have

[1] J. C. Slater, Phys. Rev. **42**, 33 (1932).
[2] H. Bethe, Ann. d. Physik **5**, 325 (1930)

$$\mathbf{r}\cdot\mathbf{k}''=rk''(\cos\theta\cos\epsilon+\sin\theta\cos\phi\sin\epsilon),$$

where $\phi$ is measured from the plane containing $\mathbf{q}$ and $\mathbf{k}''$. Eq. (6) may now be integrated over $\phi$[3]

$$\int_0^{2\pi} e^{-ik''r\sin\epsilon\sin\theta\cos\phi}d\phi = 2\pi J_0(-k''r\sin\epsilon\sin\theta).$$

The $\theta$ integration becomes

$$2\pi\int_0^{\pi} e^{-ik''r\cos\epsilon\cos\theta}J_0(-k''r\sin\epsilon\sin\theta) \times\cos\theta\sin\theta d\theta,$$

which is a form of Gegenbauer's integral having the value

$$(2\pi)\frac{\cos\epsilon}{k''r}J_{3/2}(-k''r).$$

The Bessel function may be expressed in trigonometric form and the final integration is

$$-(4\pi i\cos\epsilon/k'')\int_0^{\infty} r^2e^{-\alpha r}\left(\frac{\sin k''r}{k''r}-\cos k''r\right)dr.$$

This may be integrated by parts to give

$$-32\pi k''i\alpha\cos\epsilon/(\alpha^2+k''^2)^3.$$

We have finally

$$U=A\frac{k''}{q}\frac{\cos\epsilon}{(\alpha^2+k''^2)^3},\quad\text{where}\quad A=-2^7\pi^{3/2}\alpha^{5/2}e^2.$$

Substituting this value of $U$ in Eq. (1) and expressing $\sin\theta' d\theta'=qdq/kk'$ from the relationship $q^2=k^2+k'^2-2kk'\cos\theta'$ we obtain

$$\sigma(k,z,I)=\frac{m^2A^2}{2\pi h^4k^2}\int\frac{k''^4}{q}\frac{\cos^2\epsilon}{(\alpha^2+k''^2)^6} \times\sin\theta''d\theta''d\phi''d\phi'dqdk''.$$

Since $\mathbf{k}$ and $\mathbf{k}'$ remain fixed during integration over $\theta''$ we are at liberty to choose $\mathbf{q}$ as the polar axis from which $\theta''$ is measured. Thus $\theta''=\epsilon$.

Integrating over $\theta''$, $\phi'$ and $\phi''$ gives

$$\sigma(k,z,I)=\frac{4\pi m^2A^2}{3h^4k^2}\int_0^{k''_{\max.}}\int_{q_{\min.}}^{q_{\max.}} \times\frac{dq}{q}\frac{k''^4}{(\alpha^2+k''^2)^6}dk''.$$

Performing the integration over $q$ and making the substitution of $V$ and $V''$ for $k$ and $k''$ from the equations

$$k^2=8\pi^2meV/300h^2,$$
$$k''^2=8\pi^2meV''/300h^2,$$

we have

$$\sigma(V,z,V_i)=\frac{2^{11}\alpha^5}{3a_0^2V_i}\int_0^{V''_{\max.}}\log\frac{k+k'}{k-k'} \times\frac{k''^3}{(\alpha^2+k''^2)^6}dV'', \quad (7)$$

where $V_i$ is the ionization potential in volts of the $1s$ electron, $V$ the potential through which the colliding electron has dropped before encountering the atom and $V''$ is the potential drop necessary to stop the ejected electron. The energy relationship are $V=V'+V''+V_i$ and $k^2=k'^2+k''^2+I^2$. $I^2=8\pi^2meV_i/300h^2$.

Eq. (7) gives the ionization cross section for collisions in which the $1s$ electron is ejected from the atom. The cross section is seen to depend only upon the energy of the colliding electron and two constants of the atom, the ionization potential and the atomic number. The final integration must be performed numerically.

## Comparison with Experiment

Experimental cross sections for the ionization of $K$ shell electrons have been measured for only the two atoms helium and silver. Smith[4] and Liska[5] have done the last work on helium and their absolute values are used in this comparison.

Fig. 1 shows the measured[4] and calculated values (from Eq. (7)) for low energy collisions in helium. For values of $V>4V_i$ the qualitative agreement is good. It will be noticed particularly that the maxima of the two curves agree well.

[3] H. S. W. Massey and C. B. O. Mohr, Proc. Roy. Soc. **A132**, 612 (1931).

[4] P. T. Smith, Phys. Rev. **36**, 1293 (1930).

[5] John W. Liska, Phys. Rev. **46**, 169 (1934).

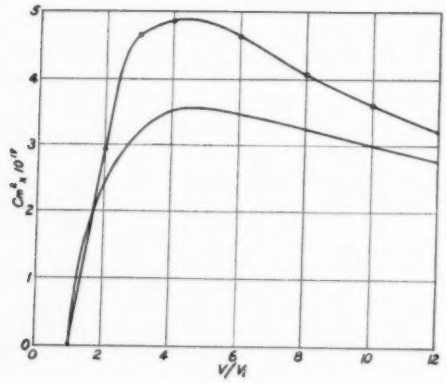


Fig. 1. The cross section for ionization of helium by electron impact. The circles are calculated values and the solid curve represents the experimental values determined by P. T. Smith.

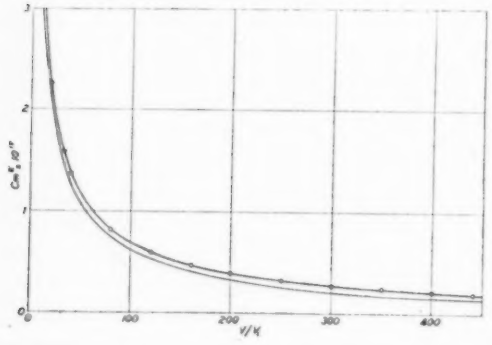


FIG. 2. The cross section for ionization of helium by electron impact. The circles are calculated values and the solid curve represents experimental values determined by John W. Liska.

Quantitatively, however, the error is rather large and agreement at these low energies is not as good as that obtained in an earlier calculation[6] where the expansion of Eq. (4) was not used. This is to be expected from the nature of the assumption made in neglecting terms of Eq. (4).

Fig. 2 shows a comparison for large collision energies in helium. Again good qualitative agreement is obtained but the calculated results are

[6] W. W. Wetzel, Phys. Rev. **44**, 25 (1933).

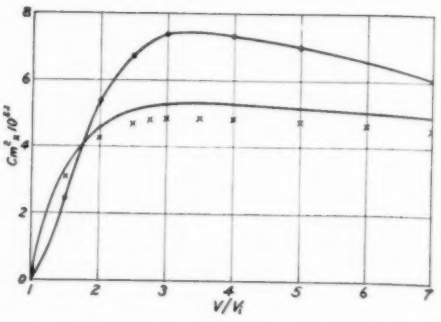


FIG. 3. The cross section for $K$ shell ionization of silver by electron impact. The circles are calculated values, the solid curve represents a prediction of what the absolute value of Webster's measurements should be and the crosses represent the absolute value as fixed experimentally by Clark.

too high by varying percentages of the total cross section.

Fig. 3 shows the values for the cross section for 1$s$ ionization of silver. Again the calculated and experimental maxima check and the theory seems to be approaching the experimental values at high collision energies.

The predicted curve was determined by correcting the relative experimental values given by Webster and his associates.[7] Since this correction involved an unjustified assumption, namely, that the percent error between the calculated and observed curves at a point near their maxima should be the same in the case of helium and silver, the publication of this paper was delayed. Recently Clark[8] has made a determination of the absolute values of the cross section. The results of adjusting the experimental points according to his data are shown as crosses on Fig. 3. The predicted curve agrees with Clark's measurements within the limits of his probable error. This gives some justification for using Eq. (7) corrected in this fashion to determine absolute values of 1$s$ ionization for atoms intermediate between helium and silver.

[7] D. L. Webster, W. W. Hansen and F. B. Duveneck, Phys. Rev. **43**, 839 (1933).

[8] J. C. Clark, Phys. Rev. **48**, 30 (1935). References are given in this paper to other theoretical treatments of the problem.

# Vibrations of Tetrahedral Pentatomic Molecules

## Part V. General Criteria for Potential Functions

JENNY E. ROSENTHAL,* *Chemistry Department, Columbia University*

(Received February 17, 1936)

The requirement that the forces along the bonds of the $YX_4$ molecule be fairly large as compared with "interaction forces" is shown to be sufficient to remove the ambiguity in the values of the constants in the potential energy function; no further special assumptions as to the types of forces involved are necessary. The ratio of the masses of the Y and X atoms determines in practically every case which set of force constants is the chemically acceptable one. Limiting values are given for the constant of the YX bond for $CH_4$, $CCl_4$, $TiCl_4$, $SO_4^=$, and other molecules. Wherever possible comparison is made between the limiting and the actual values.

IT has been pointed out in the earlier papers[1] of this series that the four fundamental frequencies of the tetrahedral molecule $YX_4$ enable us to calculate directly two of the five constants in the potential energy function and to express two of the others as functions of the third one considered as a variable parameter. While the values of some of the constants are thus undetermined, certain limits are imposed on them by the requirement that they should all be real. If the rotational structure is known, the absolute value of the parameter $D$ may be found from the vibration-rotation interaction.[2] However, even in the latter case there remains an ambiguity, for corresponding to every value of the parameter there are two possible sets of values for the other constants. This is due to the fact that the constants $A$ and $B$, or rather $A/4\mu$ and $8B$ are obtained as the roots of a quadratic equation. ($\mu = M/(4m+M)$ and $M$ and $m$ are, respectively, the masses of the Y and X atoms.) There are no mathematical grounds for deciding which of the two quantities corresponds to the larger root, so that both possibilities have to be taken into account. Since only the square of the parameter $D$ may be obtained, the one linear and two quadratic empirically known functions of the three constants $A$, $B$, and $D$ give four different sets of solutions. These again lead to four different sets of vibration frequencies for the isotopic molecules. If we introduce some simplifying assumption, for example, the Urey-Bradley field,[3] we can discard all but one set of constants for chemical reasons. However, the validity of such an assumption may be questioned, in particular since it involves a smaller number of constants than are permitted by symmetry considerations.[4] A method will now be discussed which makes it possible to set up a very general criterion for discarding certain sets of constants.

If we write the potential function in the same form as has been done for the $XYZ_2$ type molecules,[5] we can ascribe a physical meaning to the constants involved and make definite predictions as to the relative orders of magnitude. Since this particular form of the potential energy has been given before, only the terms essential for the further discussion will be repeated here. Let $\delta r_i$ as before denote the displacement between the Y and the $i$th X atom and let $\delta q_{ij}$ be a similar quantity for two X atoms. The potential energy is[6]

---

* Sarah Berliner Research Fellow of the American Association of University Women.

[1] Parts I, II, Phys. Rev. **45**, 538 (1934) and Parts III, IV, Phys. Rev. **46**, 730 (1934). The notation in the present paper conforms to the one introduced there.

[2] M. Johnston and D. M. Dennison, Phys. Rev. **48**, 868 (1935). Cf. also D. M. Dennison and M. Johnston, Phys. Rev. **47**, 93 (1935).

[3] H. C. Urey and C. A. Bradley, Jr., Phys. Rev. **38**, 1969 (1931).

[4] The only way to check this assumption would be to compare the values of the constants $A$, $B$, and $D$ calculated by means of it with those obtained with the use of additional experimental data, e.g., isotopic shifts, vibration-rotation interaction, or the spectra of certain derivatives of $YX_4$ like $XYZ_3$ and $ZYX_3$. This comparison has so far been possible for two molecules. For $CH_4$ the agreement is very good, as a matter of fact the potential function of $CH_4$ is of an even more special type, namely the valence force type. For $CCl_4$ the force field does not appear to be of the Urey-Bradley type.

[5] H. H. Voge and J. E. Rosenthal, J. Chem. Phys. **4**, 137 (1936).

[6] It should be pointed out that while the constants $G_{11}$, etc., are susceptible of a simpler physical interpretation than $A$, $B$, etc., the latter correspond to geometrical symmetry coordinates. As written in Eq. (1) the potential energy function would prove very cumbersome for any actual calculations.

$$2V = G_{11}(\delta r_1+\delta r_2+\delta r_3)^2+G_{22}\delta r_4^2 +2G_{12}\delta r_4(\delta r_1+\delta r_2+\delta r_3) +2G_{23}\delta r_4(\delta q_{12}+\delta q_{13}+\delta q_{23})+\cdots, \quad (1)$$

where $G_{11}$, $G_{22}$, $G_{12}$, $G_{23}$ are related to the usual constants $A$, $B$, $D$ and $E$ by:

$$\begin{aligned} G_{11} &= \tfrac{9}{16}A+4B+4E-3D, \\ G_{22} &= \tfrac{1}{16}A+4B+4E+D, \\ G_{12} &= 4B+4E-\tfrac{3}{16}A-D, \\ G_{23} &= (\tfrac{1}{8}A-4B+\tfrac{1}{2}D)\sqrt{\tfrac{2}{3}}. \end{aligned} \quad (2)$$

Solving for $A$, $B$, and $D$ we get:

$$\begin{aligned} A &= G_{11}+G_{22}-2G_{12}, \\ B &= \tfrac{1}{8}(\tfrac{5}{8}G_{22}+\tfrac{1}{8}G_{11}-\tfrac{3}{4}G_{12})-\tfrac{1}{2}G_{23}\sqrt{\tfrac{3}{8}}, \\ D &= \tfrac{3}{8}G_{22}-\tfrac{1}{8}G_{11}-\tfrac{1}{4}G_{12}. \end{aligned} \quad (3)$$

$G_{22}$ is the constant of the YX bond, and $G_{11}$ is a quantity of a similar nature, while $G_{12}$ and $G_{23}$ are interaction constants. Simple ideas concerning chemical structure lead us to expect $G_{11}$ and $G_{22}$ to be positive and of the same order of magnitude with $G_{12}$ and $G_{23}$ comparatively small in absolute value, particularly $G_{23}$. This assumption which has been verified for the two molecules $CH_4$ and $CCl_4$ where the calculation was possible[7] seems to be a very reasonable one. We cannot, of course, predict, how close the values of $G_{11}$ and $G_{22}$ should be for any given molecule, or how small the interaction constants. The last question could not be answered anyway, for while $G_{22}$ is quite insensitive to small changes in the frequencies, $G_{12}$ and $G_{23}$ are very much affected. Thus for $CH_4$ the constants $A$, $B$, and $D$ obtained from the observed $CH_3D$ frequency 2205 lead to $G_{12}=0.043\times10^5$ dynes/cm and $G_{23}=0.002$ as compared with $G_{12}=0.442$ and $G_{23}=-0.250$ obtained with the use of the vibration-rotation interaction data.

On the basis of this assumption concerning the relative orders of magnitude of the various constants $G$ we may conclude from Eqs. (3) that $D>0$. To find out, whether $A/4\mu$ is smaller or larger than $8B$, we compare their values expressed in terms of the $G$'s. If $A/4\mu>8B$, then:

$$G_{11}(1+M/8m)+G_{22}(1-3M/8m) -2G_{12}(1-M/8m)>(M/m)G_{23}\sqrt{6}. \quad (4)$$

This inequality should certainly be satisfied if $3M/8m<1$, but not if $3M/8m>2$. No conclusions can be made at present for the intermediate region, i.e., for $1<3M/8m<2$. However, with the exception of $SnCl_4$ for which $3M/8m=1.255$, there are no molecules with known vibrations for which the mass ratio has this intermediate value. Thus we conclude that for practically all molecules except the hydrogen compounds, the larger root of the quadratic equation represents $A/4\mu$. This result differs markedly from the one obtained on the basis of the Urey-Bradley field, where the smaller root has always to be chosen for $A/4\mu$. It might be interesting to point out in this connection that in those cases where the valency assumption holds, we have to select the roots so that $A/16>B$, i.e., $A/4\mu>8B$ if $2\mu<1$, or $3M/8m<3/2$. We shall now apply these results to find the limiting value for the bond constant $G_{22}$.

Consider first the case $3M/8m<1$. If we make use of the formulas giving $A$ and $B$ in terms of the parameter $D$[8] and substitute in Eq. (2) for $G_{22}$, we get:

$$G_{22}/m=\tfrac{1}{8}(2+\mu)(\lambda_3+\lambda_4)-\tfrac{1}{8}(2-\mu)[(\lambda_3-\lambda_4)^2 -8D^2/\mu m^2]^{\frac{1}{2}}+\tfrac{1}{4}\lambda_1+D/m. \quad (5)$$

Here $\lambda=4\pi^2\omega^2$. Since $D$ can only vary from 0 to $\frac{1}{2}m(\lambda_3-\lambda_4)\sqrt{(\mu/2)}$ (the last condition being imposed by the reality requirement), we have:

$$\tfrac{1}{4}\lambda_1+\tfrac{1}{4}\mu\lambda_3+\tfrac{1}{2}\lambda_4<G_{22}/m\leqslant\tfrac{1}{4}\lambda_1 +\tfrac{1}{4}[1+\sqrt{(\mu/2)}]^2\lambda_3+\tfrac{1}{4}[1-\sqrt{(\mu/2)}]^2\lambda_4. \quad (6)$$

Eq. (3) does not lead us to expect $D$ to be actually zero, so probably $G_{22}$ is not too close to the lower limit.

TABLE I. *Limiting values of the bond constant of various $YX_4$-type molecules.*

| | $G_{22}$ MINIMUM | $G_{22}$ MAXIMUM | ACTUAL VALUE |
|---|---|---|---|
| $CCl_4$ | $2.640\times10^5$ | $6.238\times10^5$ | $3.611\times10^5$ |
| $SiCl_4$ | 1.745 | 4.237 | |
| $TiCl_4$ | 1.292 | 3.085 | |
| $SnBr_4$ | .996 | 2.311 | |
| $CH_4$ | 4.127 | 4.944 | 4.916 |
| $SO_4^=$ | 5.023 | 8.328 | |
| $ClO_4^-$ | 4.986 | 7.081 | |

All values given in dynes/cm.

[7] See Table II in reference 5.

[8] Cf. Part III of reference 1.

In the case of the hydrogen compounds, the formulas for $G_{22}$ are:

$$G_{22}/m=\tfrac{1}{8}(2+\mu)(\lambda_3+\lambda_4)+\tfrac{1}{8}(2-\mu)[(\lambda_3-\lambda_4)^2-8D^2/\mu m^2]^{\frac{1}{2}}+\tfrac{1}{4}\lambda_1+D/m \quad (7)$$

and

$$\tfrac{1}{4}\lambda_1+\tfrac{1}{2}\lambda_2+\tfrac{1}{4}\mu\lambda_1<G_{22}/m\leqslant\tfrac{1}{4}\lambda_1+\tfrac{1}{2}\lambda_3+\tfrac{1}{4}\mu\lambda_3, \quad (8)$$

the minimum occurring for $D=0$ and the maximum for $D=m\mu(\lambda_0-\lambda_4)/(2+\mu)$. Here again we would not expect $G_{22}$ to be very close to the lower limit.

The numerical values of the bond constant calculated for various molecules are given in Table I.

APRIL 1, 1936 PHYSICAL REVIEW VOLUME 49

# The Ferromagnetism of Nickel

J. C. SLATER, *Massachusetts Institute of Technology*

(Received February 11, 1936)

By using metallic energy levels extrapolated from copper to nickel, the energy difference between a nonmagnetic and a ferromagnetic state with permanent magnetic moment is calculated for nickel, and it is shown that the ferromagnetic state is the stable one. Both saturation magnetic moment and Curie point are calculated, in agreement with experiment within the limits of error of the calculation. Extrapolation further into the iron group, though less justified than to nickel, indicates that ferromagnetism should persist in that group down approximately to iron. The criterion for ferromagnetism previously suggested by the author, the existence of inner unfilled electron shells (the 3*d*), small in proportion to their distance apart, is justified. The calculation is not made according to Heisenberg's method, which is considered to be unsuitable for application to ferromagnetism, except in its general principle of explaining the energy of orientation of elementary magnets in terms of exchange energy.

TWO different approaches have been made to the theory of ferromagnetism, that of Heisenberg[1] and that of Bloch.[2] The former operates with wave functions of the Heitler and London type, localized around the atoms of the crystal, while the latter uses plane waves traveling through the whole crystal. Neither theory has met with great success, except in the fundamental point of explaining the large energy of orientation of the elementary magnets, or magnetic spins, within a ferromagnetic crystal in terms of exchange energy rather than magnetic energy. This fundamental principle is surely correct, but Heisenberg's theory postulates the existence of a positive sign for certain exchange integrals which, in every case where they have been calculated, have negative sign, and Bloch's theory does not permit ferromagnetism except for lattice spacings much larger than those observed in the ferromagnetic metals. Neither theory has been applied specifically to the metals which are known to be ferromagnetic, and neither one gives any suggestion of why just iron, cobalt, and nickel should have these properties.

Several years ago the writer[3] pointed out that a necessary condition for ferromagnetism appeared to be the possession by the atoms in question of an incompleted inner shell of electrons, capable therefore of taking on a magnetic moment by proper orientation of the spins, and small enough so that the shells of neighboring atoms overlapped very little, so that these shells did not take part in the cohesion. The reason is that the theory of valence and cohesion demands, in agreement with experiment, that the stable state be that in which the spins are neutralized, so as to produce no net magnetic moment. The electrons responsible for ferromagnetism cannot then be those engaged in cohesion, but must be much more like those in free atoms, in which the condition of stability is known to be just the opposite: the stable state is in general that of highest multiplicity, or that with the maximum magnetic moment. It was at that time pointed out that the incom-

[1] W. Heisenberg, Zeits. f. Physik **49**, 619 (1928). See also Van Vleck, *Electric and Magnetic Susceptibilities*, Oxford, 1932.

[2] F. Bloch, Zeits. f. Physik **57**, 545 (1929). For discussion of both theories, see A. Sommerfeld and H. Bethe, *Handbuch der Physik*, Vol. 24, second edition.

[3] J. C. Slater, Phys. Rev. **36**, 57 (1930).

pleted groups of $d$ electrons in the transition groups were appropriate for ferromagnetism, and it was found that of all the elements of these groups, those with the greatest distance between the $d$ shells in proportion to their size, and therefore the least overlapping, were just iron, cobalt and nickel. The recent discovery of the ferromagnetism of gadolinium, in which the $4f$ group is presumably effective, fits in with this rule, as Bethe[4] has pointed out.

Recent advances in the theory of electronic energy levels within a metallic crystal[5] have made it possible to carry Bloch's type of theory much further than before. In the reference just mentioned, it was shown to be possible to understand ferromagnetism in terms of this type of theory, and to see why those elements with non-overlapping unfilled shells should be likely to show it. Until the present time, however, energy levels for a ferromagnetic crystal have not been calculated, and consequently no detailed comparison of the theory with experiment could be made. Such computations have still not been carried out, but the calculations of Krutter[6] on energy bands in copper makes possible an extrapolation to the next element, nickel, which has the same face-centered cubic crystal structure, with a good deal of assurance. Similar computations are now being made by Dr. Manning for iron, and when they are completed an interpolation for the whole iron group will be possible. In the meantime, however, it was thought worth while in the present paper to develop the method of calculation, and apply it to the ferromagnetism of nickel, using the extrapolated energy bands. The result is to show definitely that nickel should be ferromagnetic, and to calculate saturation magnetic moment and Curie point in good agreement with experiment. Thus for the first time the theory of ferromagnetism has advanced far enough to make one fairly sure of its correctness. At the same time, with much less justification, the calculations have been extrapolated all the way to iron. The extrapolation indicates definitely that only a few metals preceding nickel in the periodic table should be ferromagnetic; as a matter of fact, it would predict the limit of the ferromagnetic elements to lie about at iron rather than between iron and manganese, but the calculation depends on the small difference between large quantities, and a small error in the extrapolation could shift the limit to its correct position. It is hoped to remedy this when the calculations for iron are completed. It is worth noticing that while the present calculations are made by the general method of electrons traversing the whole crystal, there seem to be good reasons to doubt whether any calculations of Heisenberg's type, depending on wave functions surrounding the individual atoms, could lead to the correct result in any simple way.

The writer is indebted to Mr. R. H. Fowler, Professor J. H. Van Vleck and Professor Francis Bitter for illuminating discussions regarding the question of ferromagnetism.

## Unfilled Energy Bands and Ferromagnetism

The wave functions of an electron in a periodic potential field representing a crystal are modulated waves, behaving around each nucleus like an atomic wave function, but changing phase from one atom to another. In the case of rather tightly bound electrons like the $3d$ electrons concerned in ferromagnetism, the wave function is very much like an atomic one, falling to a rather low value in the region midway between atoms. The energy level is no longer a sharp one, as in an atom, but is spread out into a band, the spreading being greater and greater as the overlapping gets greater. Thus in the $3d$ functions the spreading is not very great. In copper, it amounts to about 0.4 atomic unit, or about 5.5 volts. Since there are five types of $d$ electrons (corresponding in the atomic case to the five degenerate states given by $m=2, 1, 0, -1, -2$), there will be five bands in the crystal, but these overlap in a complicated way. For our present purposes we need only the distribution in energy of the levels. This is given in Fig. 1, where $f(E)$, the number of states between $E$ and $E+dE$, divided by $dE$, is plotted as a function of $E$, for the five $3d$ bands combined. The total area under the curve then gives the total number of electrons which can be accommodated in the band; this is $10N$, where $N$ is

[4] See article in *Handbuch der Physik*, Vol. 24, see p. 596.
[5] J. C. Slater, Rev. Mod. Phys. **6**, 209 (1934).
[6] H. Krutter, Phys. Rev. **48**, 664 (1935).

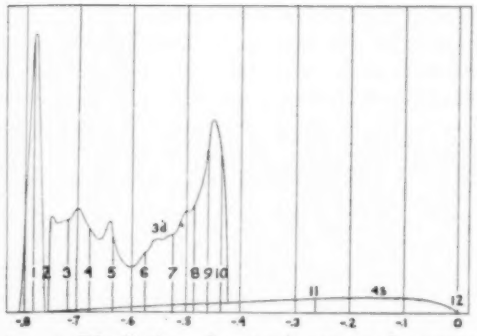


FIG. 1. Distribution of states in energy, for copper. $f(E)$, number of levels per unit energy range, plotted against $E$, in atomic units, lowest energies to the left. $3d$ and $4s$ bands shown separately. Vertical lines indicate the portion of bands filled by 1, 2, . . . 12 electrons, respectively.

the number of atoms in the crystal, since each band can hold one of each spin per atom. The values of Fig. 1 were found by starting with Krutter's calculations, extending them from the particular directions of propagation for which he found them to all directions of propagation by a method of interpolation, and tabulating the number of states for each range of energy of 0.01 atomic unit. The method will be described in a forthcoming paper. The fluctuations noted in the curve of Fig. 1 are partly of significance, partly a result of the approximate method of calculation used.

Overlapping the band of $3d$ electrons is another band, also shown in Fig. 1, arising from the $4s$ level of the atom, with interaction with the $4p$ and other higher levels. This band, capable of holding 2 electrons per atom, has wave functions of a very different character, large in the regions between atoms, and acting there very much like plane waves. Electrons in this band act like free electrons, and possess high electrical conductivity, in contrast to the $3d$'s. At the same time they contribute strongly to the cohesion, as in Wigner and Seitz's[7] calculation of cohesion in sodium, and in Fuchs's[8] calculation of the cohesion in copper, where wave functions very similar to the present ones were used.

As a first approximation to the structure of the metal, we may suppose that levels are filled, beginning with the lowest energies, high enough up so that all the electrons of the crystal are accommodated. There will be two electrons per state up to a certain energy, none above. In Fig. 1, lines are drawn indicating the maximum energy if there are 1, 2, 3 · · · 12 electrons in the $3d$ and $4s$ bands combined. The case of 11 corresponds to copper, whose atom has 10 $3d$ and 1 $4s$ electrons. It is seen that the metallic $3d$ band is filled, and that the $4s$ contains one electron per atom. If now the energy levels remained the same for the preceding elements, the case of 10 electrons would represent nickel, 9 cobalt, and 8 iron, respectively. We shall not try to estimate the changes in the energy levels, but shall wait until the case of iron is actually calculated. We see that the ferromagnetic elements contain less than one $4s$ electron per atom (explaining partly the poorer conductivity of these metals compared with copper, as Mott[9] has pointed out), but that nickel contains only about 9.5 electrons in the $3d$ band, cobalt about 8.5 and iron about 7.5. These missing electrons in the $3d$ band are necessary for ferromagnetism. But as long as the electron arrangement is as we have described, with each state either occupied by two electrons of opposite spins or empty, there will be no net magnetic moment, and the metal cannot show ferromagnetism.

We must, then, go to a higher approximation to find any net magnetic moment. A similar situation arises in the structure of atoms. As a first approximation, we assign to each electron a set of quantum numbers, $n$, $l$, $m$, and a spin quantum number, and assume that, as in a central field of force, the energy of each depends on $n$ and $l$. We then assume that the energy levels in the central field are filled far enough up to accommodate all the electrons, deducing in this way which of the quantum states are occupied in the normal state of the atom. As a next step, however, we consider the vectorial interaction of electrons, resulting in the multiplet structure. The electrostatic interaction is already taken into account if we set our central field up properly, and the same is true in the metal if the periodic field is chosen properly. But we must consider the changes of energy resulting from orientations of the orbits (change in $m$) and from orientations of spins. The energy

[7] E. Wigner and F. Seitz, Phys. Rev. **43**, 804 (1933).
[8] K. Fuchs, Proc. Roy. Soc. **A151**, 585 (1935).
[9] N. F. Mott, Proc. Phys. Soc. **47**, 571 (1935).

of a state proves to be, to the first order of perturbation theory, given by the energy neglecting orientations, minus the sum of certain exchange integrals over all pairs of electrons having parallel spins.[10] The integral is positive; with the result that the energy depends on the arrangement of spins, and that the minimum energy corresponds to the state where as many electrons as possible have spins parallel to each other. Now suppose there are $(10-n)$ electrons per atom in the $3d$ shells, $(10-n)N$ in the whole crystal. If these are divided, as we have assumed, into equal groups of each spin, there will be $(5-n/2)N$ of each spin. With each spin there will then be $\frac{1}{2}\{(5-n/2)N\}\{(5-n/2)N-1\}$ pairs, or, neglecting 1 compared with $N$, the total number of exchange integrals will be $\{(5-n/2)N\}^2$. Suppose on the other hand that there are only $(5-n/2-\mu/2)N$ electrons with negative spin, but $(5-n/2+\mu/2)N$ of positive spin, leaving the same number of electrons as before, but with a net positive spin of $(\mu/2+\mu/2)=\mu$ electrons per atom. Then there will be approximately

$$\tfrac{1}{2}\{[(5-n/2+\mu/2)N]^2+[(5-n/2-\mu/2)N]^2\} = [(5-n/2)N]^2+[\mu N/2]^2$$

exchange integrals, an increase of $(\mu N/2)^2$ integrals. Since these terms are to be subtracted, there will be a decrease of energy, and a tightness of binding, if the spins set themselves parallel, resulting in a magnetic moment. The maximum possible moment is determined by the condition that the number of electrons of either spin in the $3d$ bands must be between zero and five. The second limiting condition is the significant one in the ferromagnetic case, and as a result we see that the maximum value of $\mu$ equals $n$. In this case, all states of positive spin are filled, but there are $nN$ electrons missing from the states of negative spin. The exchange energy in this case is less than that in the case of zero spin by $(nN/2)^2$ times the average exchange integral between two electrons.

We have just seen that the total energy of the crystal is decreased, on account of exchange effects, if as many spins as possible set themselves parallel, resulting in a permanent magnetic moment. There is, however, a compensating effect, which may be less or greater than the exchange effect depending on circumstances. If we go from the state of balanced spins to that of unbalanced spins, we remove $\mu N/2$ electrons from states of minus spin, and add them to the states of plus spin. In the balanced state, the lowest $(5-n/2)N$ levels of each spin were occupied, up to a certain definite energy level. In the process of unbalancing, the $\mu N/2$ electrons of negative spin are removed from energies lower than this maximum value, and are raised in energy so as to occupy levels of positive spin above this maximum value. Thus there is a net increase of energy. This increase is likewise approximately proportional to $\mu^2$; for the number of shifted electrons is proportional to $\mu$, and the energy difference through which they must be raised is, at any rate for small $\mu$, approximately proportional to $\mu$. The net effect of this energy increase and the energy decrease due to exchange will then be positive or negative depending on the relative magnitude of the effects, but in any case it will generally remain of the same sign independent of the magnitude of $\mu$, so that either the state of balanced spins will be the most stable, or it will be the least stable and the unbalancing will go the whole way, resulting in an unbalanced spin of $n$ electrons per atom. This latter case is that for ferromagnetism.

The magnitude of the exchange integral is not very different for different atoms, and for most atoms the increase in energy on account of shifting the electrons to higher levels, increasing the binding energy, is far greater than the decrease of exchange energy when going into a magnetic state. (Algebraic rather than absolute values of the energies are here referred to.) Thus most metals are nonmagnetic. For the ferromagnetic elements we must seek those whose unfilled energy bands are as little split up as possible, so that as little energy change as possible will result from a rearrangement of electrons within the band. Thus we are led back to our former criterion of nonoverlapping unfilled shells, for it is just here that the splitting will be small. Furthermore, the whole calculation, based on the top part of the band being unfilled, the bottom part filled, is one for which the method of periodic wave functions is particularly suited, but for which Heisenberg's method

[10] J. C. Slater, Phys. Rev. **34**, 1293 (1929).

of atomic wave functions could be adapted only with great difficulty.

### Calculation of Exchange Integral

To get the exchange effect, we need only find the average value of the exchange integral between two $3d$ electrons in the lattice. Such an exchange integral between two wave functions $a_i$ and $a_j$ is by definition

$$\int a_i^*(1)a_j^*(2)(e^2/r_{12})a_j(1)a_i(2)dv_{12}, \qquad (1)$$

where 1 and 2 represent the coordinates of two electrons. We divide the volume into $N$ polyhedral cells, each surrounding an atom, and integrate separately over each pair of cells. Thus the integral is the sum, as $p$ and $q$ range from 1 to $N$, of the integral in which $dv_1$ ranges over the interior of the $p$th cell, $dv_2$ over the $q$th cell. Within the $p$th cell, according to the modulation of the wave function described by Bloch, the function $a_i$ is equal to its value at the corresponding point of the central cell, multiplied by the factor $\exp(i\mathbf{k}_i\cdot\mathbf{R}_p)$, where $\mathbf{k}_i$ is the vector wave number describing this stationary state, $\mathbf{R}_p$ is the vector from the center of the central cell to the corresponding point of the $p$th cell. Similar relations hold for the other functions. Thus our integral becomes

$$\sum_{p=1}^{N}\sum_{q=1}^{N}\exp\left(i(\mathbf{k}_j-\mathbf{k}_i)\cdot(\mathbf{R}_p-\mathbf{R}_q)\right)$$

times the integral in which $dv_1$ ranges over the $p$th cell, $dv_2$ over the $q$th, and where we replace $a_i$ and $a_j$ by their values at corresponding points of the central cell. Let these values in the central cell be $u_i$, $u_j$; then the exchange integral becomes

$$I=\sum_{p=1}^{N}\sum_{q=1}^{N}\exp\left(i(\mathbf{k}_j-\mathbf{k}_i)\cdot(\mathbf{R}_p-\mathbf{R}_q)\right)\int_p\int_q u_i^*(1)u_j^*(2)(e^2/r_{12})u_j(1)u_i(2)dv_{12}. \qquad (2)$$

A single term is the potential of a charge density $eu_i^*(1)u_j(1)$ in the $p$th cell, on a charge of density $eu_j^*(2)u_i(2)$ in the $q$th cell, times the appropriate exponential. First we shall consider the terms $p=q$, which prove to be the leading terms. For this case, $\mathbf{R}_p-\mathbf{R}_q=0$, so that the exponential reduces to unity, and the integral becomes simply $N\int u_i^*(1)u_j^*(2)(e^2/r_{12})u_j(1)u_i(2)dv_{12}$, integrated through the central cell only. Now within this cell, the functions $u_i$ and $u_j$ are very much like atomic $d$ functions, on account of the relatively small perturbations of the $d$ electrons of different atoms on each other. The normalization, however, is different, each function being approximately $1/N^{\frac{1}{2}}$ times the corresponding atomic function, so that the square of the function, integrated over the $N$ cells, can equal unity. Thus the exchange integral finally is seen to be approximately $1/N$ times the corresponding atomic integral, which we shall call $J$.

Next we consider the case $p\neq q$. Two different cases arise, depending on whether $u_i$ and $u_j$ refer to the same value of the quantum number corresponding to the atomic quantum number $m$, or not. If they do, $u_i$ and $u_j$ are approximately equal to each other within the cell, and their product integrates to $1/N$ over the cell, so that the charge density $eu_i^*(1)u_j(2)$ is a charge of approximate amount $e/N$, distributed through the $p$th cell. Its potential at the $q$th cell will then be approximately $(e/N)(1/|\mathbf{R}_p-\mathbf{R}_q|)$, plus terms in higher inverse powers of $|\mathbf{R}_p-\mathbf{R}_q|$, arising from the fact that the charge distribution really has multipole components as well as a total charge. We shall see, however, that the whole effect is very small, and the multipole terms can consequently be neglected. On the other hand, if $u_i$ and $u_j$ refer to different $m$ values, the functions will be approximately orthogonal to each other, their product will integrate almost to zero, over the cell, the charge distribution will consist practically only of multipoles (beginning with a quadripole), and we may neglect its potential completely. We are left, then, only with the case of equal $m$ values, in which the contribution to the integral is the potential of a charge $e/N$ on an equal one at distance $|\mathbf{R}_p-\mathbf{R}_q|$. We may then convert the sum over $p$ and $q$ in (2) into a single sum in which the $p$th cell is at the origin, obtaining

$$I=J/N+N(e^2/N^2)\sum_q(\exp\left(i(\mathbf{k}_j-\mathbf{k}_i)\cdot\mathbf{R}_q\right))/R_q, \qquad (3)$$

if $u_i$ and $u_j$ refer to the same $m$ value, while

$I=J/N$ otherwise. It is to be noted that $J$ is different for different pairs of $m$ values of the two wave functions.

We shall not attempt to evaluate $I$ from (3) for each separate combination of functions $u_i$ and $u_j$, but only to find the average over all possible combinations, recognizing that this may involve us in certain errors in the final result. In reference 10 it was shown that the exchange integrals between two $d$ functions can be written in terms of two parameters, $F^2$ and $F^4$, which can be evaluated from atomic wave functions, or from observed atomic spectra. In the table of coefficients $b^k(lm_l;\ l'm_l')$ on p. 1312 of that reference, the necessary coefficients are given for different combinations of the $m$'s. When we average over the 25 combinations of the five $m$ values with each other, we find from that table that

$$\bar{J}=2/35(F^2+F^4). \tag{4}$$

For nickel, we can estimate the quantities $F^2$ and $F^4$ from the observed spectrum. The $(3d)^8(4s)^2$ configuration of Ni I involves energy separations determined by just these quantities. Taking the observed multiplet separations for this configuration, we can fit $F$ values to it. The fit is not very good, but to a rough approximation we have $F^2=80{,}000$ cm$^{-1}$, $F^4=50{,}000$ cm$^{-1}$. To indicate the order of accuracy, we give in Table I the energy differences between the multiplets, as obtained by taking the center of gravity of the observed multiplets, and we compare with the values determined from these parameters. Using these values of the $F$'s, we have $\bar{J}=7430$ cm$^{-1}$ approximately.

Next we wish to average the second term of (3) over all pairs of wave functions. We recall that this term is present only when $u_i$ and $u_j$ have the same $m$ values, which occurs only 1/5 of the time, so that we wish 1/5 of the average over $i$ and $j$ of this term. Strictly, the quantities $\mathbf{k}_i$ and $\mathbf{k}_j$ should be allowed to range over a polyhedral cell in the $k$ space, but it will make only a small error if instead we allow them to range over the interior of a sphere of the same volume. It is easy to show that the average of $\exp(i\mathbf{k}\cdot\mathbf{R})$ over the interior of a sphere of radius $K$ in $k$ space is $3(\sin KR-KR\cos KR)/(KR)^3$. Thus the average of the second term of (3) is

$$\frac{1}{5}(e^2/N)\sum_q\left\{\frac{3\sin KR_q-KR_q\cos KR_q}{(KR_q)^3}\right\}^2\Big/R_q. \tag{5}$$

Here $K$ is to be so chosen that $(4/3)\pi K^3$ is the volume of one cell in $k$ space. If $R$ is the distance from an atom to its nearest neighbors in a face centered lattice, it is not hard to show that this leads to $KR=6^{\frac{1}{2}}2^{\frac{1}{2}}\pi^{\frac{1}{2}}$. Inserting this value, the bracket above becomes 0.000352 for the case where $q$ is one of the nearest neighbors, and it is much less for more distant neighbors. The nearest ones are then the only ones which need be considered, and since there are 12 of them, the expression (5) becomes approximately

$$(12/5)(0.000352)(e^2/N)/R. \tag{6}$$

The distance $R$ from an atom to its nearest neighbor is about 4.67 atomic units in Ni. Inserting this value, and converting to cm$^{-1}$, the expression (6) becomes 36 cm$^{-1}/N$. It is thus evident that the terms for $p\neq q$ are almost negligible in finding the exchange integral, which arises almost entirely from the atomic integral. Adding our two expressions, we have $\bar{I}=7466$ cm$^{-1}/N$, and

Exchange energy of magnetic state − exchange energy of nonmagnetic state

$$=-(n^2/4)(7466)N$$
$$=-1866\,n^2 \text{ cm}^{-1} \text{ per atom.} \tag{7}$$

On account of the discrepancies between the observed multiplets and those calculated from our $F$ values, we may expect this value to be uncertain to between five and ten percent. We must recall, furthermore, that it represents only an average value, and that the exchange energy for particular pairs of wave functions can differ widely from the average.

TABLE I.

| | OBSERVED | COMPUTED |
|---|---|---|
| $^3F-{}^1D$ | 12,550 cm$^{-1}$ | 13,250 |
| $^3F-{}^3P$ | 14,750 | 15,950 |
| $^3F-{}^1G$ | 21,150 | 20,750 |
| $^3F-{}^1S$ | not obs. | 51,600 |

## CALCULATION OF CHANGE IN BINDING ENERGY

We must next find the change of binding energy involved in shifting $nN/2$ electrons from

the states of negative spin to those of positive spin, remembering that they must go into states previously unoccupied. Since the binding energy is known only in the form of numerical calculations, as summarized in Fig. 1, this calculation must be made numerically, not analytically. In terms of the function $f(E)$ plotted in Fig. 1, giving the number of states per unit energy range, the total energy of the electrons between two energy values, assuming them to fill all energy states between the limits, is $\int Ef(E)dE$ between these limits, or rather a corresponding summation, since $f(E)$ has been computed for discrete values of $E$. We must find the energy in two cases: (1) the state of no net spin, in which all states are filled from the bottom of the band to an energy such that there are $n/2$ states per atom of each spin vacant above this value; and (2) the state of maximum spin, in which all states of positive spin are filled, but in which states of negative spin are filled only to such an energy that there are $n$ states per atom of this spin vacant above this value. These energies have been computed, as a function of $n$, by obvious numerical methods, and their difference $E_2-E_1$ has been found, giving the increase in binding energy in going to the ferromagnetic state.

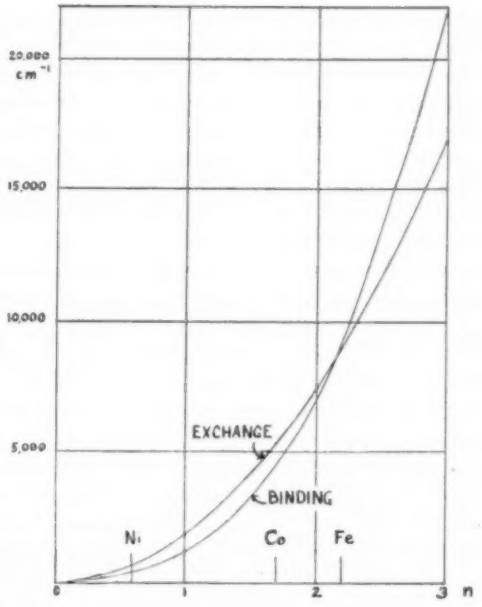


Fig. 2. Magnitudes of exchange and binding energy changes between ferromagnetic and nonferromagnetic states (in $cm^{-1}$ per atom), as function of $n$ (number of net electrons spins per atom). The condition for ferromagnetism is that the exchange energy term be greater numerically than the binding energy term.

## Net Energy Change from Nonmagnetic to Magnetic State

We have now found that on account of the exchange effect, as given in (7), the energy of the crystal decreases by $1866\ n^2\ cm^{-1}$ per atom when the electrons change from the state of no net spin to the state of maximum spin. On the other hand, the energy arising from binding increases by the amount $E_2-E_1$, as discussed in the last paragraph, when the same change is made. The absolute values of these two quantities, as functions of $n$, are plotted in Fig. 2. It is seen that, for small $n$'s, the increase in binding energy is less than the decrease in exchange energy, so that the net result is a decrease of energy, the ferromagnetic state is more stable than the nonmagnetic state, and the metal should be ferromagnetic. On the other hand, as $n$ increases, the two curves are seen to cross, so that for too large a value of $n$ (too small a total number of electrons in the $d$ shell, or in the atom), the increase in binding energy becomes greater than the compensating decrease in exchange energy, so that the state of zero spin is the most stable one. The question now is, in which part of the curve is nickel located? We have already pointed out that, according to our extrapolated copper energy bands, nickel should contain about 95 electrons per atom in the $3d$ bands, so that $n=0.5$. Mott[9] has shown that according to experiment $n$ is nearer 0.6. This is near enough our theoretical results so that the uncertainty in the extrapolation could easily account for the difference. In either case, Fig. 2 very definitely shows that nickel should lie in the ferromagnetic part of the curve. It is tempting, as we have remarked above, to extend the extrapolation further down the iron group, using these same curves for cobalt and iron, though of course they are really not accurate, since both the exchange energy (as computed from the spectrum) and the binding energy (as computed from the metallic energy bands) will really change as we go from atom to atom, and furthermore cobalt and iron have

different crystal structures from copper and nickel. We have seen that approximately $n=1.5$ for cobalt, 2.5 for iron. Mott[9] has shown that experimentally $n=1.7$ for cobalt, 2.2 for iron, approximately. These values of $n$ are all obtained from the observed saturation magnetic moments of the metals. From Fig. 2, on which the values 1.7, 2.2 are indicated, it is seen that the curves cross at approximately the $n$ value for iron, instead of between iron and manganese (that is, for $n>2.2$) as they should from the observed ferromagnetism of iron. But the error is one which we can easily attribute to the errors in our extrapolation. Both curves rise rapidly with $n$, and comparatively small changes in them would shift the intersection by the required amount. We may reasonably say, then, that our theory not only predicts the ferromagnetism of nickel, but also predicts that the phenomenon of ferromagnetism should persist for some distance down into the iron group of elements, approximately as far as it is observed experimentally, and then should cease.

## Magnetic Energy and Curie Point of Nickel

Let us adopt for nickel the value 0.6 for $n$, as indicated by experiment. Then we find the exchange energy to be 1866 $(0.6)^2$ cm$^{-1}$ = 672 cm$^{-1}$. The difference in binding energy between the two states is found to be 401 cm$^{-1}$. The net decrease in energy on going from the nonmagnetic to the ferromagnetic state is thus 271 cm$^{-1}$ per atom. This of course is at the absolute zero of temperature, for with both nonmagnetic and ferromagnetic states we have considered only the lowest possible energy level, all electrons being in the lowest state consistent with the given total spin. This quantity is not susceptible of experimental measurement, but it is closely related to the Curie point. For nickel, the Curie temperature $\theta$ is about 630° absolute, and the corresponding energy $k\theta$, where $k$ is Boltzmann's constant, is 440 cm$^{-1}$, when converted to spectroscopic units. This is obviously of the same order of magnitude as the quantity found theoretically. We can, however, make a more definite comparison, on the basis of available theories of ferromagnetism. For the present, we shall not try to replace these theories of the temperature variation of the magnetic moment by a more suitable theory based on the present model.

In the Weiss theory of ferromagnetism* in the absence of an external magnetic field, one writes the internal magnetic field in terms of the magnetic moment per unit volume as $\mathbf{H}=N\mathbf{I}$, where $N$ is an empirical constant, large compared with unity, and $\mathbf{I}$ is the magnetic moment per cc. The magnetic energy per unit volume is then $-\frac{1}{2}\mathbf{H}\cdot\mathbf{I}=-\frac{1}{2}NI^2$ in the magnetic case, as compared with a nonmagnetized state. The formula for the Curie point on this theory can be written $\theta=\sigma_{m0}^2N\rho/3mR$, where $\sigma_{m0}$ is the magnetic moment per gram molecular weight (equal to our $n$, times the Bohr magneton, times Avogadro's number), $\rho$ is the density, $m$ the molecular weight, $R$ the gas constant per gram molecular weight. In an obvious way $\sigma_{m0}$ can be written in terms of $I$, the magnetic moment per unit volume, so that $\theta$ is plainly proportional to the same quantity $NI^2$ appearing in the energy per unit volume. In fact, if we multiply this magnetic energy by the volume of an atom, to get the energy per atom, we have very simply

$$k\theta=\tfrac{2}{3}\text{ magnetic energy per atom (Weiss).} \quad (8)$$

We can proceed similarly in the Heisenberg theory.† The magnetic energy of the whole crystal is then written in terms of certain exchange integrals (not to be confused with our exchange integrals) denoted by $J$, a number of nearest neighbors $z$, and a total spin $S'$ of the crystal, equal to $NS$, where $S$ is the spin of one atom, $N$ the number of atoms in the crystal. It is then, as given by Van Vleck's formula (22) equal to $-zJS'^2/N$. The Curie point, on the other hand, is given by Van Vleck's formula (37) as $\theta=2zJS(S+1)/3k$. Thus we are led to the relation

$$k\theta=\tfrac{2}{3}S(S+1)/S^2\text{ times magnetic energy per atom (Heisenberg).} \quad (9)$$

It is observed that Heisenberg's result approaches Weiss's in the limit $S=\infty$, as it does in other respects. However, as Van Vleck

* See for example E. C. Stoner, *Magnetism and Atomic Structure*, p. 75.

† See for example Van Vleck, *Electric and Magnetic Susceptibilities*, p. 328.

points out, the experimental results for nickel are best represented by $S=1/2$, leading to $\frac{2}{3}S(S+1)/S^2=2$. Thus we may expect the Curie energy to be somewhere between $\frac{2}{3}$ and twice the energy of magnetization at the absolute zero, with the probabilities favoring the latter value. The experimental Curie energy 440 $cm^{-1}$ is 1.62 times the magnetization energy 271 $cm^{-1}$ which we have found. The agreement seems entirely satisfactory, considering the nature of the approximations which we have made.

### Electronic Specific Heat of Nickel at Low Temperature

It has been recently observed by Keesom[11] that the electronic contribution to the specific heat, which, being proportional to the temperature, outweighs the contribution of the lattice vibrations at low temperatures, is many times the normal amount in nickel. Both Keesom and Mott have suggested that this arises from the large concentration of energy levels in the neighborhood of the top of the Fermi distribution, on account of the 3*d* levels. We can easily test this hypothesis. Sommerfeld and Bethe (reference 2, p. 430) show that the specific heat per gram molecular weight on account of free electrons in a normal metal is $C_v=(2\pi^2/3)N(\zeta_0)k^2T$, where $N(E)dE$ represents the number of energy levels of one spin in $dE$, if we are dealing with a gram molecular weight, and $\zeta_0$ is the maximum energy occupied at the absolute zero. Thus his $N$ is half our distribution function $f$. For a ferromagnetic metal, however, at low temperatures all levels of positive spin are filled, so that they do not contribute to the specific heat, and we count only electrons of negative spin. This removes the factor 2 in the formula above. Furthermore, $\zeta_0$ must be taken to be the maximum energy of electrons with negative spin, when the electrons of positive spin occupy the whole band. In this case, from the numerical data from which Fig. 1 is drawn, we find that $N(E)$ is 26.15 times Avogadro's number, if energy is expressed in atomic units. Substituting this value, and appropriate constants, we find $C_v=0.0011T$ calories per mole per degree. Keesom's experimental value is $0.001744T$. The agreement is not very good, but still it is correct in order of magnitude. To get better agreement, the peak in Fig. 1 at energy $-0.45$ atomic unit would have to be about half again as high as it is, presumably being correspondingly more narrow. This does not seem impossible, though it is unlikely. In any case, the high specific heat is definitely connected with the high peak in the 3*d* distribution curve of Fig. 1, verifying again this general feature of our curve.

[11] Keesom and Clark, Physica **2**, 513 (1935); W. H. Keesom, Proc. Roy. Soc. **A152**, 12 (1935); N. F. Mott, Proc. Roy. Soc. **A152**, 42 (1935). I am much indebted to Mr. R. H. Fowler for calling my attention to these references.

APRIL 1, 1936 PHYSICAL REVIEW VOLUME 49

## A Note on Positron Theory and Proper Energies

Robert Serber,* *University of California, Berkeley*

(Received February 7, 1936)

The origin of the infinite light-quantum proper energy which follows, according to Heisenberg, from the creation of matter by the field of the photon, is examined in some detail. We are led to investigate the inconsistencies which appear on the incorporation of the Dirac positron theory into the formalism of the quantum theory. These inconsistencies make it impossible to regard with confidence any predictions of the theory for which a consideration of the singularities of the density matrix is essential. It is shown that when the off-diagonal distance in the density matrix is taken different from zero, the proper energy of a light quantum and the electromagnetic energy of an electron are, in order $e^2$, finite, and that the off-diagonal distance plays in these calculations the part of a generalized electron radius.

In a field free vacuum, the infinite distribution of electrons in negative energy states envisaged in Dirac's theory of the positron clearly should contribute nothing to the expectation values of observables of the system (charge and

* National Research Fellow.

current density, energy, electromagnetic fields). The contribution of this field free vacuum distribution has then to be subtracted from the expectation value of every observable. Since, however, the difference between the contributions of the vacuum distribution in the presence and absence of an electromagnetic field does not turn out to be finite,[1] the theory in this form cannot give sensible and determinate answers to questions involving the reaction of the electron distribution in varying fields. Dirac himself has now tried to modify the formalism in such a way that all expectation values would necessarily be finite.

Dirac's treatment of the problem[2] is based on a study of the density matrix

$$(x''k''\,|\,\Re\,|\,x'k')=\sum_{\text{occ}}\psi_n(x''k'')\psi_n{}^{+}(x'k').$$

Here $\psi_n(x''k'')$ is a one-electron wave function at a point $x_0''=ct''$, $x_1''$, $x_2''$, $x_3''$, and $k''$ is the spin variable. The summation is to be extended over all occupied states. Dirac has shown, by integration of the equation of motion for $\Re$, taking the $\psi_n$ as solutions of the ordinary Dirac equation, that $\Re$ is finite when the length of the four-vector $\mathbf{x}=\mathbf{x}'-\mathbf{x}''$ is different from zero, i.e., the density matrix is singular only when $x_\lambda x^\lambda=0$. The worst singularities in $\Re$ can be eliminated by symmetricizing the density matrix between positron and electron, that is, by replacing $\Re$ by

$$(x''k''\,|\,R\,|\,x'k')=\tfrac{1}{2}\Big[\sum_{\text{occ}}\psi_n(x''k'')\psi_n{}^{+}(x'k')-\sum_{\text{unocc}}\psi_n(x''k'')\psi_n{}^{+}(x'k')\Big].$$

Explicit expressions for the singular terms, $S$, which remain in $R$ have been given by Heisenberg.[3] These singular terms may be deleted by replacing $R$ by $r=R-S$. It is of course possible also to subtract finite terms. Heisenberg has included such a term in $S$; it is chosen to renormalize the polarization of vacuum for slowly varying and weak fields to zero. The expectation value of an operator $F$ at a point $\mathbf{X}=\frac{1}{2}(\mathbf{x}'+\mathbf{x}'')$ is now given by

$$\bar{F}(X)=\lim_{x\to 0}\sum_{k}(X-\tfrac{1}{2}x,\,k\,|\,Fr\,|\,X+\tfrac{1}{2}x,\,k),$$

and is guaranteed to be finite and determinate.

The electromagnetic field produced by the electron distribution is taken into account by including in the total current which appears in the Maxwell field equations the expectation value of the current calculated from the density matrix,

$$j_\lambda(X)=-e\lim_{x\to 0}\sum_{kk'}\alpha_{\lambda kk'}(X-\tfrac{1}{2}x,\,k'\,|\,r\,|\,X+\tfrac{1}{2}x,\,k).$$

Here $j_0=\rho$, $\alpha_0=1$. Heisenberg has shown that, despite the subtraction of the singular terms, the conservation law for the current still holds in the limit $\mathbf{x}\to 0$, as do also conservation laws for the energy and momentum of the entire system, material field plus electromagnetic field.

The passage from the density matrix treatment, based on the correspondence principle, to a quantized field theory can be made by regarding the equations of motion (the Dirac equation and the Maxwell equations) as matrix equations in the variables $\psi$, $\psi^+$, $E_i$, $A_i$, which satisfy the usual commutation laws. The consistency of such a procedure depends upon the compatibility of commutation laws and equations of motion: these equations must, namely, be such that the values of the commutators remain unchanged in the course of time. This condition is not satisfied by the system of equations with subtractative terms. Thus, with $\dot{A}_i=-E_i$ and $\mathbf{E}=\text{curl}\,\mathbf{H}+4\pi e\boldsymbol{\alpha}(R-S)$, $(d/dt)[E_i(X),\,A_i(X')]=-4\pi e[\alpha_i S(X),\,A_i(X')]\neq 0$. In fact the time rate of change of this commutator is singular.

A second scheme has also been proposed by Heisenberg. This consists in taking as a Hamiltonian function the energy expression of the density-matrix treatment, now regarded as a function of the $q$-numbers $\psi$, $\psi^+$, $E_i$, $A_i$. One takes as canonical conjugates $\psi$ and $\psi^+$, $A_i$ and $E_i$, as in the usual quantum electrodynamics. One sets the scalar potential $A_0=0$, and $x_0=0$. The Hamiltonian function is then[4]

[1] P. A. M. Dirac, Solvay Congress, 1933; W. H. Furry and J. R. Oppenheimer, Phys. Rev. **45**, 245 (1934); R. Peierls, Proc. Roy. Soc. **A146**, 420 (1934).

[2] P. A. M. Dirac, Proc. Camb. Phil. Soc. **30**, 150 (1934).

[3] W. Heisenberg, Zeits. f. Physik **90**, 209 (1934).

[4] We shall employ rational units, measuring length in terms of the Compton wave-length $\hbar/mc$, time in terms of $\hbar/mc^2$, and mass in terms of the electronic mass $m$. In these units $e^2=\alpha$.

$$H=\tfrac{1}{2}\int d\mathbf{X}\sum_{k'k''}[\alpha_{jk'k''}\{i\partial/\partial x_j+\tfrac{1}{2}e[A_j(X+\tfrac{1}{2}x)+A_j(X-\tfrac{1}{2}x)]\}+\beta_{k'k''}][\psi^+(X+\tfrac{1}{2}x,k')\psi(X-\tfrac{1}{2}x,k'')$$

$$-\psi(X-\tfrac{1}{2}x,k'')\psi^+(X+\tfrac{1}{2}x,k')]+\int d\mathbf{X}\sum_{k'}i\partial/\partial x_0(X-\tfrac{1}{2}x,k'|S|X+\tfrac{1}{2}x,k')+H_{EM},\quad(1)$$

where $H_{EM}=(1/8\pi)\int d\mathbf{X}(E^2+H^2)$. This Hamiltonian function can be formally treated as Hermitian, provided one understands that in taking the transpose of a matrix one is also to reverse the direction of $\mathbf{x}$. The interaction between electromagnetic field and matter is to be supposed a small perturbation and the usual perturbation theory, expanding in powers of the electronic charge $e$, is to be applied. In the result of any calculation one is to pass to the limit $\mathbf{x}\to 0$.

However, the Hamiltonian function carries with it its own equations of motion, and these are not the same as the equations of motion of the simple density matrix treatment. Thus the Hamiltonian equation for $\psi$ is

$$i\dot{\psi}(X)=[\alpha_j(-i\partial/\partial X_j+\tfrac{1}{2}e\{A_j(X)+A_j(X-x)\})+\beta]\psi(X-x),\quad(2)$$

which differs from the ordinary Dirac equation through the appearance of $\mathbf{x}$ on the right-hand side. Since the Heisenberg subtractative terms were determined on the supposition that $\psi$ obeys the Dirac equation, there is no warrant for believing them correct when, instead, $\psi$ obeys (2). The Hamiltonian equations for the electromagnetic field differ from the Maxwell equations even more radically, for the subtractative terms introduced into (1) are explicit functions of $E$ and $A$, and hence give rise to new terms in the equations of motion. Thus instead of the ordinary equation $-\dot{A}_i=E_i$, one finds, aside from terms of order $x$,

$$-\dot{A}_i=E_i-(e^2/3\pi)[x_ix_jE_j/x_\lambda x^\lambda-E_i\log(|x_\lambda x^\lambda|/c_1)].\quad(3)$$

The equations for $E_i$ can be written

$$-\dot{E}_i+\mathrm{curl}_i\,\mathbf{H}=4\pi[j_i(x)-e^2S_i(j)]+e^2\,(\text{singular terms}).\quad(4)$$

Here $\mathbf{j}(x)$ represents the contributions of the terms in (1) which are linear in $e$, and $-e^2\mathbf{S}(j)$ contains the subtractative terms necessary to cancel the singularities which appear in the expectation value of $\mathbf{j}(x)$ in order $e^2$. The appearance of singular terms in (3) and (4) is of course fatal to the theory, since $E_i$ and $A_i$ will evidently be singular as $\mathbf{x}\to 0$ and no provision has been made to remove such singularities. Moreover, in the derivation of the subtractative terms explicit use is made of the relation $-\dot{A}_i=E_i$. One would be just as badly off if one attempted to regard the subtractative terms in (1) as not being explicit functions of dynamical variables, since then the subtractative terms for the current would be lacking in the Hamiltonian equations for the field.

Heisenberg has applied the Hamiltonian function (1) to the calculation of the proper energy of a photon in order $e^2$ but he did not obtain a finite result. The reason for this is easily seen. Since $H$ is a function of $\mathbf{x}$ the transformation matrix which diagonalizes it will also depend on $\mathbf{x}$. The transformed Hamiltonian function is $\bar{H}(x)=S^{-1}(x)H(x)S(x)$. However Heisenberg set $\mathbf{x}=0$ in the transformation matrix, taking $\bar{H}(x)=S^{-1}(0)H(x)S(0)$, presumably in order to avoid any possible consequences of the change from the Dirac equation to (2). (2) of course reduces to the Dirac equation when $\mathbf{x}=0$. This precaution would be unnecessary if $S(0)$ led to a finite result, since in that circumstance it would be quite immaterial whether one used $S(0)$ or $S(x)$. Actually, if $S(0)$ is used, one term appears in $\bar{H}$, namely, $S^{-1}(0)H_{EM}S(0)$, which is completely independent of $\mathbf{x}$, and this term diverges.[5] Since the off-

[5] It would be of no aid to introduce $\mathbf{x}$ into $E^2+H^2$ in a way analogous to that in which it is introduced into $\psi^+\psi$. If the propagation vector of the photon is $\mathbf{k}$, such a modification would introduce into $H_{EM}$ a factor depending on $\mathbf{k}\cdot\mathbf{x}$. Such a factor does not help, since by the conservation laws $\mathbf{k}$ is equal to the sum of the momenta of the pair virtually created by the perturbation, whereas the singularities arise from integration over the difference of the momenta.

diagonal matrix elements of $\bar{\bar{H}}$, as well as the diagonal elements, approach no limit as $\mathbf{x}\to 0$, the artifice of setting $\mathbf{x}=0$ in the transformation matrix is clearly not permissible, nor can any conclusions regarding the characteristic values of $H$ be drawn from such a calculation.

If one carries out the calculation using $S(x)$ no difficulties are encountered as long as $\mathbf{x}\neq 0$, since now every term in $\bar{\bar{H}}$ involves $\mathbf{x}$. The photon proper energy in order $e^2$ is found to be

$$W=-(\alpha h\nu/3\pi)(z/R^2-2\log \tfrac{1}{2}CR+\mathrm{O}(R)), \qquad (\log C=0.577\cdots) \quad (5)$$

where $z$ is the component of $\mathbf{x}$ in the direction of the electric vector of the photon, and $R$ is the length of $\mathbf{x}$. But in the limit $\mathbf{x}\to 0$, the photon proper energy becomes infinite.

The entire contribution to (5) comes from $H_{EM}$, in fact (5) is just the expectation value of $H_{EM}-h\nu$. This seems paradoxical, since the unwanted singular terms in (3) and (4) do not affect the expectation value of $H_{EM}$ in order $e^2$, while from the remaining terms all singularities have presumably been removed. That the singular terms in (3) and (4) play no part may be seen most easily by inspection of the ordinary perturbation theory formula for $H_{EM}$. If we write $H=H^{(0)}+eH^{(1)}+e^2H^{(2)}$ we see that, since $H_{EM}$ is diagonal in the original representation, its expectation value in order $e^2$ is completely independent of $H^{(2)}$. However, the singular terms in (3) and (4) can be regarded as coming entirely from $H^{(2)}$.

Heisenberg has ascribed the photon proper energy difficulties to the point nature of the photon, that is, to the possibility of large fluctuations in the quantized electromagnetic field. That this is not the true explanation can be seen by thinking of the calculation as carried out by direct integration of the equations of motion in powers of $e$. One then sees that in order $e^2$ the energy contains no terms higher in degree than quadratic in the unperturbed value of the electromagnetic field variables, $b_{k\lambda}$ and $b_{k\lambda}^{+}$. For the photon proper energy, we require the terms in the energy proportional to $M_{k\lambda}$, the number of photons. Fluctuations in the field consequently contribute nothing: one must have terms at least quartic in $b_{k\lambda}$ and $b_{k\lambda}^{+}$ before fluctuation terms proportional to $M_{k\lambda}$ can appear.

The real source of the trouble lies in the fact that a Hamiltonian perturbation calculation in powers of $e$ is equivalent to integration of the equations of motion under the supposition that $e$ is a slowly varying function of the time, which increases from an initial value zero to its final value, $e$. But in the calculation of the subtractative terms it is explicitly assumed that $e$ is independent of time: all time dependences are to be included in the vector potential $\mathbf{A}$. If it were not for the subtractative terms it would be quite immaterial, in computing the current, which one supposed to vary, $e$ or the electromagnetic fields, since only the produce $e\mathbf{A}$ appears in the Dirac equation. However the subtractative terms in the current also involve $e\dot{\mathbf{A}}$, and hence will by no means be the same in the two cases. Suppose that the perturbation is applied over a time $T$. During this time transient terms of order $1/T$ will appear in the expression for the induced current, before inclusion of the subtractative terms. If one supposes $\mathbf{A}$ to vary with time, transient fields will also be present, which will contribute additional subtractative terms which at every instant just cancel the transient terms in the uncorrected current. However if $e$ is varied these additional subtractative terms will not appear. The transient terms which in consequence remain in the current vanish in the limit $T\to\infty$, but since they also act for a time $T$, their contribution to the electromagnetic fields will be of order unity as $T\to\infty$. If one calculates the contribution of these transient terms to $H_{EM}$, one obtains just the result (5). The photon proper energy calculation illustrates a further difficulty involved in the passage to a Hamiltonian theory: even though it is possible to give a rule by which non-singular solutions of the equations of motion may be obtained, these solutions will not, in general, correspond to stationary states of the Hamiltonian system.

The efficacy of the subtractative terms is in any event severely limited by the fact that they have been determined only in the approximation in which the density-matrix treatment is applicable, and so cannot be expected to give, in general, finite answers for problems in which fluctuations are involved.

The possibility of constructing a Hamiltonian theory, along the lines laid down by Heisenberg,

which would avoid the difficulties discussed above is very doubtful. Certainly no simple modification of the original scheme, such as the introduction of new subtractative terms in the Hamiltonian function, will give equations of motion and expectation values for energy which are both free of singularities. On the other hand formal arguments alone hardly provide an adequate basis for a more radical revision.

In the absence of any consistent theory, the simplest procedure which suggests itself is to dispense entirely with subtractative terms, to carry out all calculations with $\mathbf{x}$ different from zero, and in the result to pick out the term independent of $\mathbf{x}$ as the only one of significance. This scheme has the flaw that a classification of terms as depending on $\mathbf{x}$ or not depending on $\mathbf{x}$ is essentially ambiguous. It is of course possible to pick out terms which are singular or which vanish as $\mathbf{x}\rightarrow 0$, but since, unfortunately, $(x^2+y^2+z^2)/R^2=1$, an unambiguous separation into "determinate" and "indeterminate" terms is not possible. In this connection, it should be remembered that after the introduction of $\mathbf{x}$, an operator $F$ is in general no longer either Lorentz covariant or gauge invariant. This could lead to no inconsistencies provided the lack of the proper transformation properties manifested itself only in terms which were recognizably $x$-dependent. However, we have not succeeded in formulating a criterion for the seperation of determinate and indeterminate terms which, in any given problem, can be relied upon to lead to Lorentz covariant and gauge invariant results. Calculations made in this manner accordingly cannot lead to unequivocal results. But it may be hoped that they will give some indication of the sort of corrections which must be applied to present theory, and of the order of magnitude of the correction terms.

We shall introduce $\mathbf{x}$ into the theory in a somewhat different way than did Dirac and Heisenberg. The operators of the usual field theory will be left altogether unaltered, except for their symmetrization in electron and positron $(\psi^+(X)\psi(X)\rightarrow\frac{1}{2}[\psi^+(X)\psi(X)-\psi(X)\psi^+(X)])$. The commutation laws however, will be taken to involve $\mathbf{x}$:

$$[\psi^+(X),\ \psi(X')]^+=\delta(X-X'+x).$$

This formalism would correspond to the impossibility of making field measurements without mutual disturbance at two arbitrarily near points. It thus suggests a not unreasonable motive for the introduction of the off-diagonal distance $\mathbf{x}$.

As in the usual quantum electrodynamics, the wave equation associated with the Hamiltonian function is to be augmented by the auxiliary relation $\operatorname{div}\mathbf{E}-4\pi\rho=0$. This relation is, in fact, not compatible with the equations of motion, since the conservation law for the current holds only when $\mathbf{x}=0$. The inconsistency of the auxiliary relation with the equations of motion is only to be expected, for, with $\mathbf{x}\neq 0$, the Hamiltonian function is no longer gauge invariant. The same inconsistency appears if $\mathbf{x}$ is introduced into $\psi$ and $\psi^+$ instead of into the commutation relations. (Even in the density matrix treatment, it will be remembered, the conservation laws fail for $\mathbf{x}\neq 0$). Since the covariance of an inconsistent set of equations is in any event illusory, we have been content to introduce $\mathbf{x}$ into the theory in a patently noncovariant manner. As we shall see, this lack of covariance is much the same as that which appears in classical electrodynamics when one attempts to introduce the radius of the electron.

The formalism just described finds an interesting application in the calculation of proper energies of photon and electron in order $e^2$. The photon proper energy is found to be (in c.g.s. units)

$$W=-\frac{\alpha h\nu}{2\pi}\left\{\left(\frac{mc^2}{h\nu}\right)^2\left[8\frac{z^2}{R^4}+\left(\frac{4}{3}\right)\frac{x^2z^2}{R^4}-2\frac{z^2}{R^2}\right]+\frac{1}{3}\frac{x^2}{R^2}+O(R)\right\},$$

where $x$ is the component of $\mathbf{x}$ in the direction of propogation of the photon, $z$ is the component in the direction of the photon's electric vector, and $R$ is the length of $\mathbf{x}$. This result may reasonably be interpreted as indicating a null photon proper energy in order $e^2$.

If we carry out the elimination of the electrostatic field variables in the usual way, overlooking, of course, the inconsistency of the auxiliary relation, we obtain in the energy a term

$$\tfrac{1}{4}\sum_{nmst}(a_n^+a_m-a_ma_n^+)(a_s^+a_t-a_ta_s^+)Q_{nm;\,st}, \tag{6}$$

where

$$Q_{nm;\,st}=\tfrac{1}{2}e^2\int d\mathbf{X}\int d\mathbf{X}'\frac{v_n^+(X)v_m(X)v_s^+(X')v_t(X')}{|\mathbf{X}-\mathbf{X}'|}\exp\,-\tfrac{1}{2}i(\mathbf{k}_n+\mathbf{k}_m+\mathbf{k}_s+\mathbf{k}_t)\cdot\mathbf{x},$$

and $\psi$ and $\psi^+$ have been expanded in electronic plane wave functions $v_n$, of momentum $\mathbf{k}_n$: $\psi=\sum_n a_nv_n$ $\exp-\tfrac{1}{2}i\mathbf{k}_n\cdot\mathbf{x}$, $\psi^+=\sum_n a_n^+v_n^+\exp-\tfrac{1}{2}i\mathbf{k}_n\cdot\mathbf{x}$. The factors $\exp-\tfrac{1}{2}i\mathbf{k}_n\cdot\mathbf{x}$ are inserted so that the $a_n$ and $a_n^+$ will obey the usual commutation relations. The diagonal matrix elements of (6) give the ordinary Coulomb and exchange terms, and in addition, terms which represent the electrostatic proper energies of electrons and positrons. The proper energy of an electron in a state $r$ is

$$W_{ES}=\sum_{r'}Q_{rr';\,r'r}-\sum_{\rho}Q_{r\rho;\,\rho r}. \tag{7}$$

Here $r$ and $r'$ refer to positive energy states, $\rho$ to negative energy states. Evaluating (7) in a Lorentz frame in which the electron is at rest, we find

$$W_{ES}=(e^2/16\pi^3)\int d\mathbf{r}/|\mathbf{r}+\mathbf{x}|\int d\mathbf{k}(1+k^2)^{-1}\exp(i\mathbf{k}\cdot\mathbf{r})=(e^2/4\pi^2)\int d\mathbf{r}K_1(r)/r|\mathbf{r}+\mathbf{x}|,$$

where $K_1(r)$ is the Bessel function defined in Whittaker and Watson, *Modern Analysis*, §17.71. The angular integration gives

$$W_{ES}=(e^2/\pi)\left[R^{-1}\int_0^R rK_1(r)dr+\int_R^\infty K_1(r)dr\right],$$

which can be reduced, by use of the recurrence relation $K_1(r)=(d/dr)K_0(r)$, to

$$W_{ES}=(e^2/\pi R)\int_0^R K_0(r)dr=-(2e^2/\pi)[\log\tfrac{1}{2}CR-1+O(R)].$$

The electromagnetic proper energy in order $e^2$ can also be shown to be finite when $\mathbf{x}\neq 0$. Thus the artifice introduced to eliminate the singularities due to the sea of negative energy electrons has a very natural extension to the treatment of the electronic proper energy difficulties.

It will be observed that the filling of the negative energy states results in the summations over positive and negative states appearing in the electrostatic proper energy with opposite sign. If the negative energy states were left empty, the proper energy would instead be $\sum_{r'}Q_{rr';\,r'r}$ $+\sum_{\rho}Q_{r\rho;\,\rho r}$. This gives $W_{ES}=e^2/2R$, which is just the electrostatic energy of an electron of radius $R$. The off-diagonal distance $\mathbf{x}$ thus appears to find a classical analogue in the electron radius.

Our method of calculation, too, is strongly reminiscent of that employed in classical electrodynamics, which can likewise be described as the introduction of a parameter, the electron radius, and the final abandonment of all terms except those independent of this parameter. The aim, of course, is to separate, insofar as possible, those terms which obviously depend on the particular model employed or on the way in which calculations are carried out, from those which seem to be independent of these factors, and which may be hoped therefore to have some significance, despite the unquestionable inadequacy of the theory.

I wish to express my deepest thanks to Professor J. R. Oppenheimer, to whom I am indebted for many illuminating discussions of this subject.

# LETTERS TO THE EDITOR

*Prompt publication of brief reports of important discoveries in physics may be secured by addressing them to this department. Closing dates for this department are, for the first issue of the month, the twentieth of the preceding month; for the second issue, the fifth of the month. The Board of Editors does not hold itself responsible for the opinions expressed by the correspondents.*

**Communications should not in general exceed 600 words in length.**

## Note on Neutron-Proton Exchange Interaction

The matrix elements of the interaction between a proton with coordinates $\mathbf{x}_1$ and a neutron with coordinates $\mathbf{x}_2$ as proposed by Majorana[1] may be written as

$$(\mathbf{x}_1\mathbf{x}_2|\ V|\mathbf{x}_1'\mathbf{x}_2') = -J(|\mathbf{x}_1-\mathbf{x}_2|)\delta(\mathbf{x}_1-\mathbf{x}_2')\delta(\mathbf{x}_2-\mathbf{x}_1'). \quad (1)$$

This interaction assumption corresponds to an interchange of the positional coordinates $(\mathbf{x}_1, \mathbf{x}_2)$ of the two particles; clearly this interchange will entail a shift in the center of mass if the mass of the proton, $m_1$, is not the same as the mass of the neutron, $m_2$. A similar effect on the center of mass is also characteristic of the Heisenberg interaction assumption[2] in which both spin and positional coordinates are interchanged, and of any "mixed" Heisenberg-Majorana interaction. While the difference between the masses of the proton and neutron according to present values is small, the difficulty introduced by the shift in the center of mass has perhaps a theoretical interest and has been discussed by Breit and Wigner.[3]

This center of mass difficulty is made at once evident by considering the matrix elements of the exchange interaction in terms of momentum variables. Thus, the transformation of (1) gives

$$(\mathbf{p}_1\mathbf{p}_2|\ V|\mathbf{p}_1'\mathbf{p}_2') = f(|\mathbf{p}_2'-\mathbf{p}_1|)\delta(\mathbf{p}_1'-\mathbf{p}_1+\mathbf{p}_2'-\mathbf{p}_2), \quad (2)$$

in which $\mathbf{p}_1$ is a momentum of the proton, and $\mathbf{p}_2$ a neutron momentum and the form of $f$ depends on the particular form assumed for $J$ in (1). If the matrix elements (2) are now written as functions of the total momentum $\mathbf{P}=\mathbf{p}_1+\mathbf{p}_2$ and the relative momentum $\mathbf{p}=\mu(\mathbf{p}_2/m_2-\mathbf{p}_1/m_1)$, where $\mu=m_1m_2/(m_1+m_2)$, (2) becomes

$$(\mathbf{pP}|\ V|\mathbf{p}'\mathbf{P}') = f(|\mathbf{p}+\mathbf{p}'+\mathbf{P}(m_2-m_1)/(m_1+m_2)|)\delta(\mathbf{P}-\mathbf{P}'), \quad (3)$$

in which form the flaw in the exchange interaction assumption is obvious: the matrix elements of the interaction are explicit functions of the momentum $\mathbf{P}$ of the center of mass so that it is not possible to separate the energy or the wave function into parts characteristic, respectively, of the internal motion and the motion as a whole. (3) is to be regarded as a consequent interaction law only insofar as one may put $m_1=m_2$, for which case

$$(\mathbf{pP}|\ V|\mathbf{p}'\mathbf{P}') = f(|\mathbf{p}+\mathbf{p}'|)\delta(\mathbf{P}-\mathbf{P}'), \quad (3')$$

and the difficulty mentioned above disappears.

There are many possible ways of modifying the interaction assumption (1) or (2) without losing the essential feature of the exchange, and without introducing at the same time any error due to a difference in masses. One simple possibility is to take instead of (2) the following

$$(\mathbf{p}_1\mathbf{p}_2|\ V|\mathbf{p}_1'\mathbf{p}_2') = f\left(\frac{\mu}{m_1m_2}|m_1(\mathbf{p}_2'+\mathbf{p}_2) - m_2(\mathbf{p}_1'+\mathbf{p}_1)|\right)\delta(\mathbf{p}_1'-\mathbf{p}_1+\mathbf{p}_2'-\mathbf{p}_2). \quad (4)$$

Then,
$$(\mathbf{pP}|\ V|\mathbf{p}'\mathbf{P}') = f(|\mathbf{p}+\mathbf{p}'|)\delta(\mathbf{P}-\mathbf{P}'). \quad (5)$$

The identity of (5) and (3′) proves the interesting result that the wave functions $\psi(p)$ and the energy values $E(P)$ found by using the Majorana interaction under the assumption $m_1=m_2$ are exactly the same as the corresponding wave functions and energy values deduced from the modified interaction which is valid regardless of the values of $m_1$ and $m_2$.

The same conclusions as given above should of course follow from consideration of the interaction in a coordinate representation. In fact, the coordinate representation of (4) is

$$(\mathbf{x}_1\mathbf{x}_2|\ V|\mathbf{x}_1'\mathbf{x}_2') = -J(|\mathbf{x}_1-\mathbf{x}_2|) \times\delta\left[\mathbf{x}_1-\mathbf{x}_2'+\frac{m_1-m_2}{m_1+m_2}(\mathbf{x}_1-\mathbf{x}_2)\right] \times\delta\left[\mathbf{x}_2-\mathbf{x}_1'+\frac{m_1-m_2}{m_1+m_2}(\mathbf{x}_1-\mathbf{x}_2)\right], \quad (6)$$

which is the same interaction as has been proposed by Breit and Wigner. If the wave function for a neutron and a proton is written as $\psi=u(\mathbf{X})g(\xi)$ where $\mathbf{X}=(m_1\mathbf{x}_1+m_2\mathbf{x}_2)/(m_1+m_2)$ and $\xi=\mathbf{x}_1-\mathbf{x}_2$, and if $V$ is the operator defined by (6), $V\cdot u(\mathbf{X}')g(\xi')=-J(|\xi|)u(\mathbf{X})g(-\xi)$, while the operator defined by (1) is such that $V\cdot u(\mathbf{X}')g(\xi')=-J(|\xi|)u(\mathbf{X}+(m_2-m_1)\xi/(m_2+m_1))g(-\xi)$.

It is clear that it is possible to extend the exchange interaction law so as to include the case of two particles of different masses without adding any essential complication. The greater complexity of (6) as compared with (1) is only apparent and should be regarded as characteristic of the particular coordinate system used. Although there may be other reasons for supposing that the exchange interaction is accurate only insofar as $(m_1-m_2)/(m_1+m_2)$ can be neglected in comparison with unity, it does not appear that such a limitation[3] can be found by examining the exchange hypothesis itself for consistency and simplicity.

MILTON S. PLESSET

University of Rochester,
Rochester, N. Y.,
March 11, 1936.

[1] E. Majorana, Zeits. f. Physik **82**, 137 (1933).
[2] W. Heisenberg, Zeits. f. Physik **77**, 1 (1932); **78**, 150 (1932).
[3] G. Breit and E. Wigner, Phys. Rev. **48**, 918 (1935).

### The *F* Terms of Ce IV

Following the publication by the author of a partial analysis[1] of the spectrum of Ce IV considerable interest appeared concerning the position of the *F* terms. These terms have now been located and this opportunity is taken to give a brief note concerning them. A rather complete analysis of the spectrum is now nearing completion and details will be published elsewhere.

The 5*F* terms are quite regular as compared with neighboring ions of similar electronic structure and are given by the following lines:

$5D_{1\frac{1}{2}}-5F_{2\frac{1}{2}}$ 741.79 (40) 134,809
$5D_{2\frac{1}{2}}-5F_{3\frac{1}{2}}$ 754.60 (30) 132,520
$5D_{2\frac{1}{2}}-5F_{2\frac{1}{2}}$ 755.75 (12) 132,319.

The question whether the 4*F* or the 5*D* terms are the deepest in the spectrum is a very interesting one and seems now to be definitely settled in favor of the former possibility. The lines involved are:

$4F_{2\frac{1}{2}}-5D_{1\frac{1}{2}}$ 2009.94 (100) 49,737
$4F_{3\frac{1}{2}}-5D_{2\frac{1}{2}}$ 2000.42 (100) 49,973
$4F_{2\frac{1}{2}}-5D_{2\frac{1}{2}}$ 1914.75 (35) 52,226.

The following term values are based upon three *S* terms using a Ritz formula.

| | |
|---|---|
| $4F_{2\frac{1}{2}}$ 296,197 | $5F_{2\frac{1}{2}}$ 111,652 |
| $4F_{3\frac{1}{2}}$ 293,944 | $5F_{3\frac{1}{2}}$ 111,451. |

The reality of these terms is confirmed by the 5*G* combinations and also by the fact that the 4*F* interval corresponds sufficiently well with the proper intervals in the low terms of Ce III.

R. J. LANG

University of Alberta,
Edmonton, Alberta, Canada,
March 10, 1936.

[1] R. J. Lang, Can. J. Research **A13**, 1 (1935).

---

### Magnetic Moment of the $Li^7$ Nucleus

The value of the magnetic moment of the $Li^7$ nucleus has been determined in two different ways. Breit and Doermann[1] calculated it to be 3.28 nuclear magnetons, on the basis of hyperfine structure measurements of the $^3P_0-^3S_1$ group of $Li^+$. Fox and Rabi,[2] by the molecular beam method, found the hfs separation of the ground state ($^2S_{\frac{1}{2}}$) of the normal Li atom to be $\Delta(s)=0.0267\pm0.0003$ cm$^{-1}$. The resulting value of the nuclear magnetic moment, estimated from the Goudsmit-Fermi-Segrè formulae, was found to be 3.20 nuclear magnetons. However, even apart from other objections[3] to the GFS formulae, it is not to be expected that a statistical theory will yield correct results for an atom as light as lithium. Therefore, a more accurate calculation is desirable.

Recently, Fock and Petrashen[4] have published values of wave functions (self-consistent with exchange) for lithium. For the 2*s* electron, the value of $\chi=(f_{20}/r)$ at the origin is 1.44. The value of the nuclear magnetic moment, in terms of nuclear magnetons, is[3] $g=949\ \Delta(s)[I/(2I+1)]\times[1/\chi^2(0)=4.58$. This is in disagreement with the above value of 3.28 as found by Breit and Doermann.

Fock and Petrashen have also calculated the transition probabilities for some members of the principal series of lithium. The agreement with observation[5] is mostly qualitative, and not quantitative. This work indicates, then, that the Fock functions are inadequate for transition probability calculations. Our work shows that the same is true for nuclear moment calculations, if the theory be supposed to be correct.

It may be possible, with more accurate wave functions, to resolve the above discrepancy between 4.58 and 3.28. This is being investigated.

JAMES H. BARTLETT, JR.
J. J. GIBBONS, JR.

Department of Physics,
University of Illinois,
March 6, 1936.

[1] Breit and Doermann, Phys. Rev. **36**, 1262 (1930).
[2] Fox and Rabi, Phys. Rev. **48**, 746 (1935).
[3] Gibbons and Bartlett, Phys. Rev. **47**, 692 (1935).
[4] Fock and Petrashen, Physik. Zeits. Sowjetunion **8**, 547 (1935).
[5] A. Filippov, Zeits. f. Physik **69**, 526 (1931). The disagreement between these observations and Fock's theory seems to be quite outside the experimental error.

---

### A New Form of Crystalline Quartz at −183.5°C

When *X*, *Y* and specially oriented *Y* cuts,[1] encased in an air-tight brass crystal holder (Fig. 1), were subjected to low temperatures, they ceased abruptly to oscillate piezoelectrically near the boiling point of liquid air. In one set of experiments these cuts of quartz were driven by a Hartley oscillator. Resonance responses of the plates were noted by listening for the corresponding characteristic disturbances produced in the horn of an amplifier which was connected across a portion of the Hartley plate circuit. This method is perhaps the most sensitive test[2] for the piezoelectric property. In another set of experiments specially oriented *Y* cuts were placed in the usual nonregenerative crystal oscillator circuits. These circuits ceased abruptly to oscillate near the boiling point of liquid air. Piezoelectric activity increased steadily from room temperature to approximately −175°C. By immersing the crystal holder in liquid oxygen boiled under reduced pressure, the temperature at which alpha quartz is transformed to the nonpiezoelectric form, called $\delta$ quartz, was found to be −183.5°C. The temperature of the $\delta\rightarrow\alpha$ transition occurs above the boiling point of liquid oxygen at atmospheric pressure. The range permitted by our

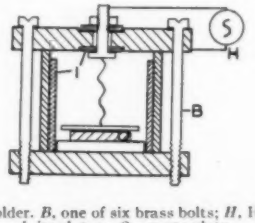


FIG. 1. Crystal holder. *B*, one of six brass bolts; *H*, Hartley oscillator; *I*, insulators; *Q*, quartz plate.

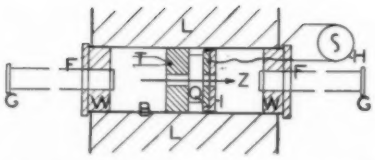


FIG. 2. Polarimeter crystal holder. *Q*, quartz plate; *Z*, optic axis; *T*, thermocouple; *I*, insulator for mounting one of the brass electrodes; *W*, wooden spools; *F*, iron tubes; *G*, glass windows; *L*, liquid air; *B*, brass tubing; *H*, Hartley oscillator.

apparatus showed that this transition must occur above −182.4°C. The existence of two separate transition temperatures is perhaps due to the tendency of either state to persist.

In the most satisfactory arrangement for studying the discontinuity in the optical rotatory power at the $\alpha \longleftrightarrow \delta$ transition the quartz plate was mounted in a holder which[1] is incompletely described in Fig. 2. This holder was mounted in a Lippich three-prism polarimeter.[3] For the 5461A line of Hg the optical rotatory power of both right and left-handed quartz decreased from 25.59°/mm at room temperature to a minimum of 24.89°/mm at the $\alpha \longleftrightarrow \delta$ transition. Here, optically right or left-handed quartz remained optically right or left handed, respectively. Below the transition point the rotatory power of $\delta$ quartz increased to 24.95°/mm at the lowest temperature (perhaps −190°C). In calculating these rotatory powers the $z$ dimensions of the plates were assumed to remain constant. Changes in the rotatory power were more abrupt at the $\alpha \rightarrow \delta$ transition than at the $\delta \rightarrow \alpha$ transition. This was also true as regards the piezoelectric property, but the changes in rotatory power were sluggish as compared to the rapid piezoelectric changes. Both of these changes occurred together. Corresponding changes in volume must be small since quartz can be plunged into liquid air without the slightest damage.

Upon the assumption that $\delta$ quartz is a member of the hexagonal system, the loss of the piezoelectric property is interpreted to mean that it falls among classes 9, 12, 21 or 24 (Voigt) or 24, 25, 30 or 32 (Schoenflies). Of the four types ($\alpha$, $\beta$, $\gamma$[4] and $\delta$) of crystalline quartz $\gamma$ and $\delta$ quartz are nonpiezoelectric.

Time was lacking for determining the $\delta \rightarrow \alpha$ transition temperature and measuring the optical rotatory power of $\delta$ quartz as a function of temperature.

My thanks are due to Robert E. Adams for his assistance in this work and to Professor J. R. Roebuck for helpful discussions.

HAROLD OSTERBERG

University of Wisconsin,
March 10, 1936.

[1] Lack, Willard and Fair, Bell Sys. Tech. J. **13**, 453 (1934).
[2] Giebe and Scheibe, Zeits. f. Physik **33**, 760 (1925).
[3] R. H. Houstoun, *A Treatise on Light* (1927), p. 216.
[4] Osterberg and Cookson, J. Frank. Inst. **220**, 370 (1935).

---

## Errata: Continuation of Work on Scattering of Slow Neutrons

ALLAN C. G. MITCHELL, EDGAR J. MURPHY AND LAWRENCE M. LANGER, *New York University*
(Phys. Rev. **49**, 400 (1936))

AND

## Selective Scattering of Slow Neutrons

ALLAN C. G. MITCHELL, EDGAR J. MURPHY AND MARTIN D. WHITAKER, *New York University*
(Phys. Rev. **49**, 401 (1936))

Through an inadvertence Fig. 1 of the first letter appears with the caption and text of the second letter on page 401 and Fig. 1 of the second letter appears with the caption and text of the first letter on page 400. An interchange of these two figures should be made to rectify the error.